

# Hydrothermal synthesis of perfectly shaped micro- and nanosized carbonated apatite

Ilya E. Nifant'ev,<sup>\*a,b,c</sup> Alexander V. Tavtorkin,<sup>a</sup> Sergey A. Legkov,<sup>a</sup> Sofia A. Korchagina,<sup>a</sup> Georgiy A. Shandryuk,<sup>a</sup> Egor A. Kretov,<sup>a,c</sup> Artem O. Dmitrienko<sup>b,d</sup> and Pavel V. Ivchenko<sup>a,b</sup>

<sup>a</sup> A. V. Topchiev Institute of Petrochemical Synthesis, Russian Academy of Sciences, Moscow, Russian Federation. E-mail: ilnif@yahoo.com

<sup>b</sup> M. V. Lomonosov Moscow State University, Department of Chemistry, Moscow, Russian Federation. E-mail: inif@org.chem.msu.ru

<sup>c</sup> National Research University Higher School of Economics, Faculty of Chemistry, Moscow, Russian Federation.

<sup>d</sup> G. V. Plekhanov Russian University of Economics, Moscow, Russian Federation

\*Corresponding autor. E-mail: inif@org.chem.msu.ru; ilnif@yahoo.com

## Supplementary Information

S1. SEM images of CAp samples	S2–S22
S2. XRD studies of CAp samples	S23–S29
S3. FT-IR spectra of CAp samples	S30–S36
S4. Thermal studies of CAp samples	S37–S51
S5. UV calibration data for vancomycin solutions	S52

## S1. SEM images of CAp samples

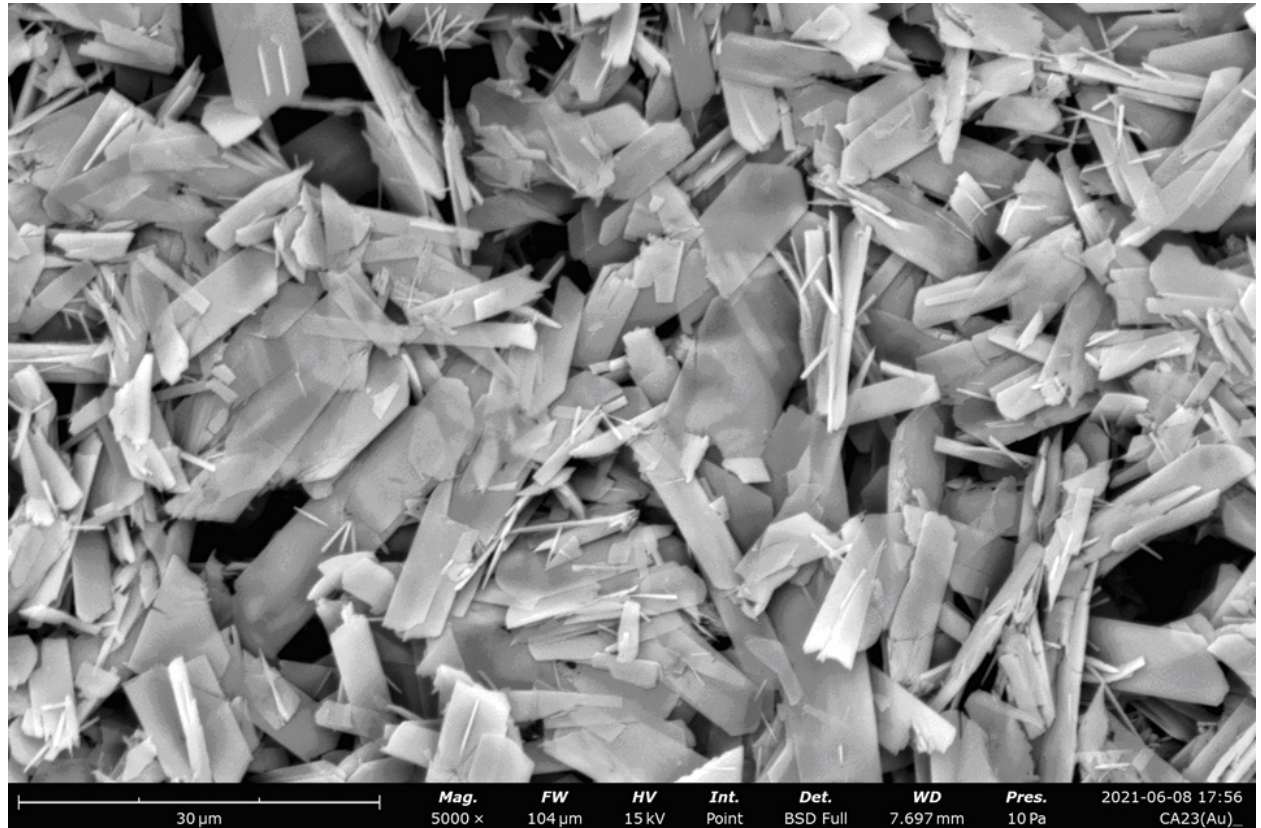
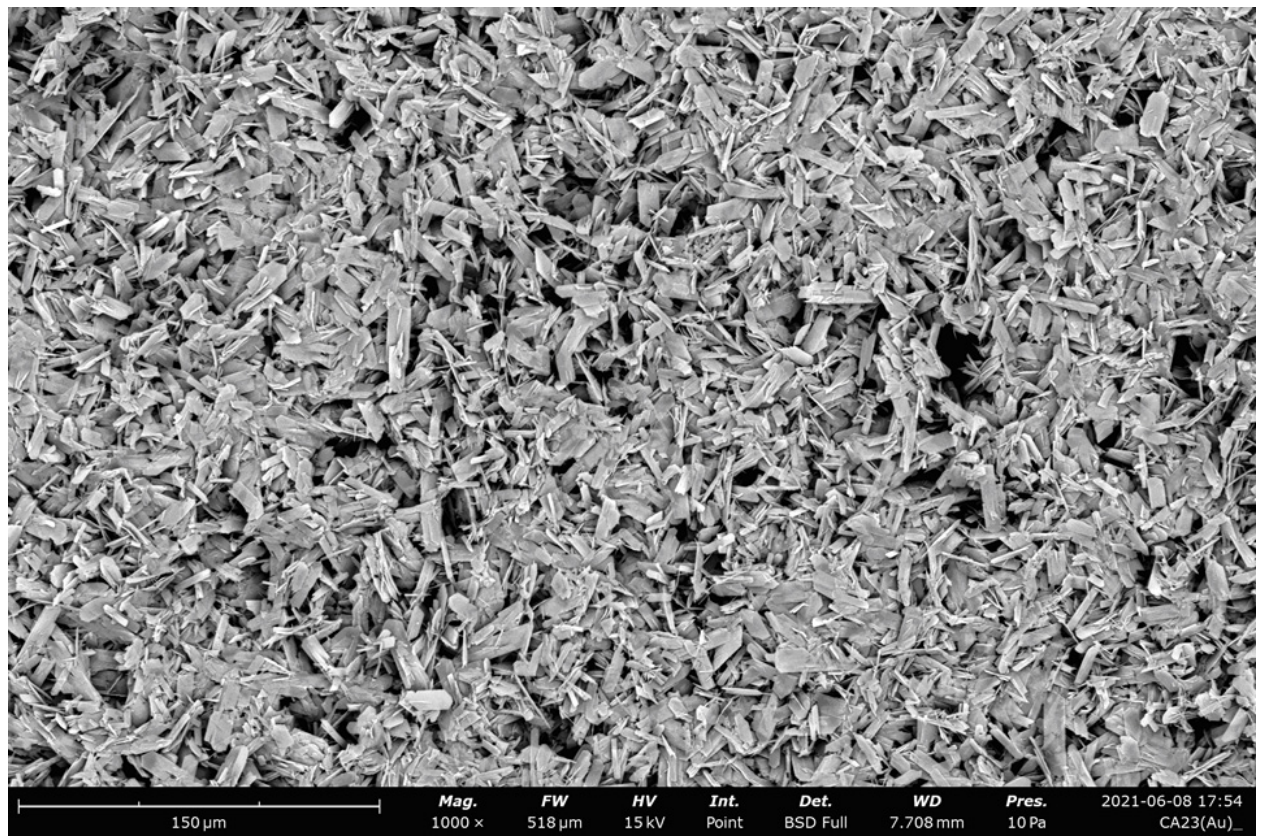


**Fig. S1** SEM images of CAp microcrystals (Table 1, Entry 1).

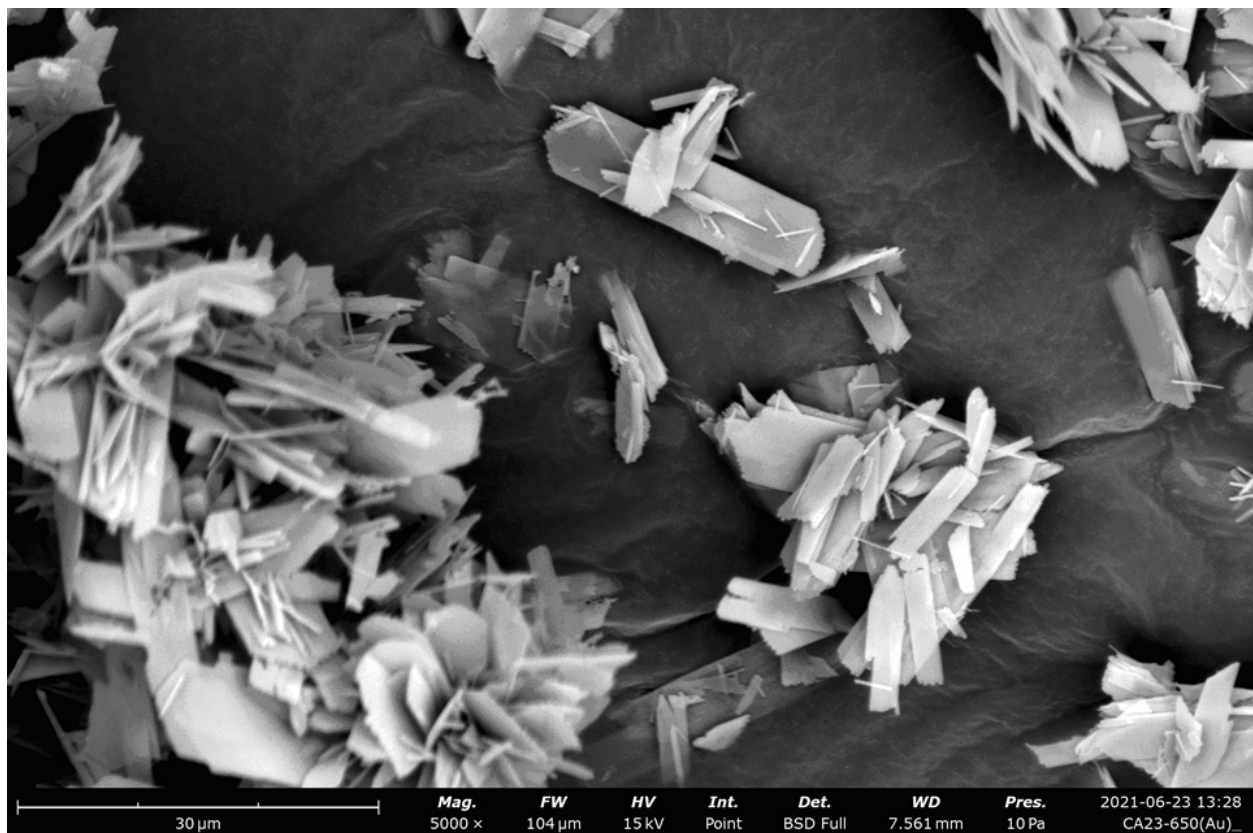
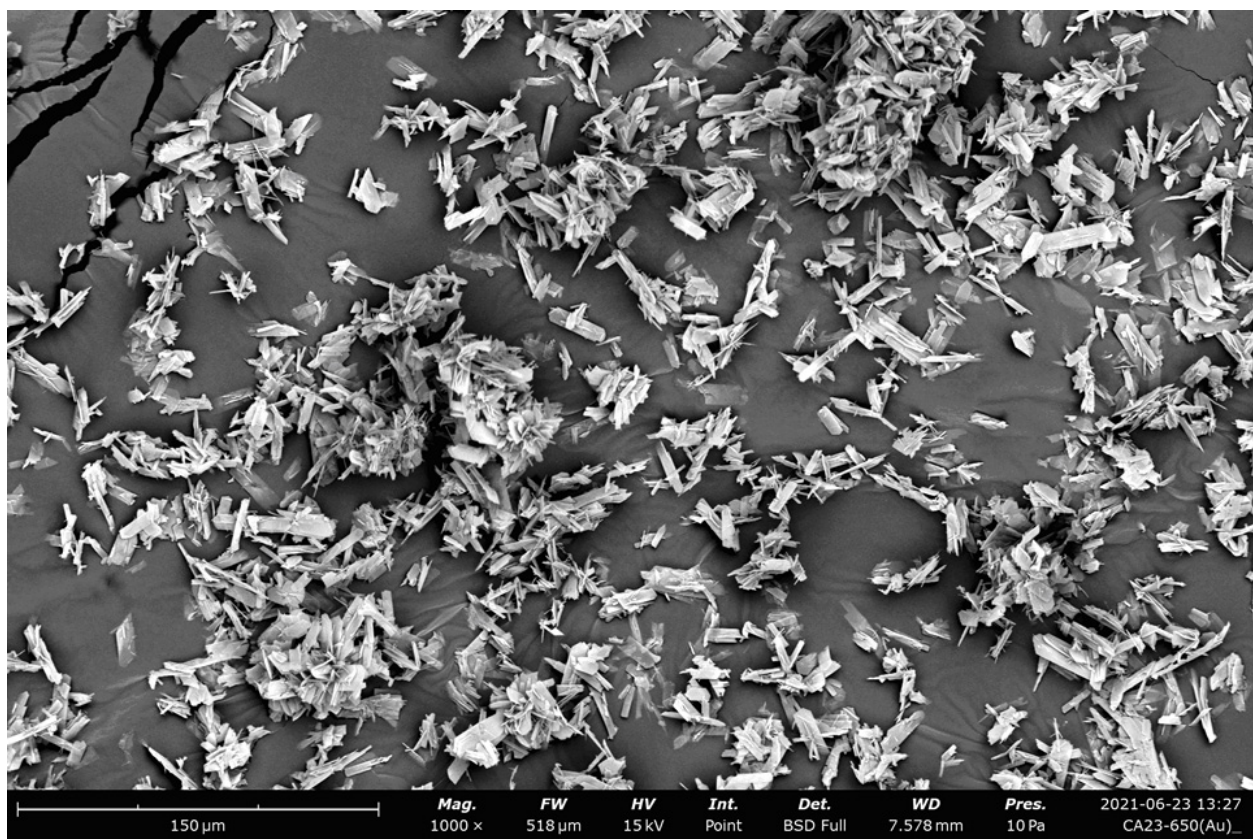


**Fig. S2** SEM images of CAp microcrystals (Table 1, Entry 1), sintered at 650 °C.

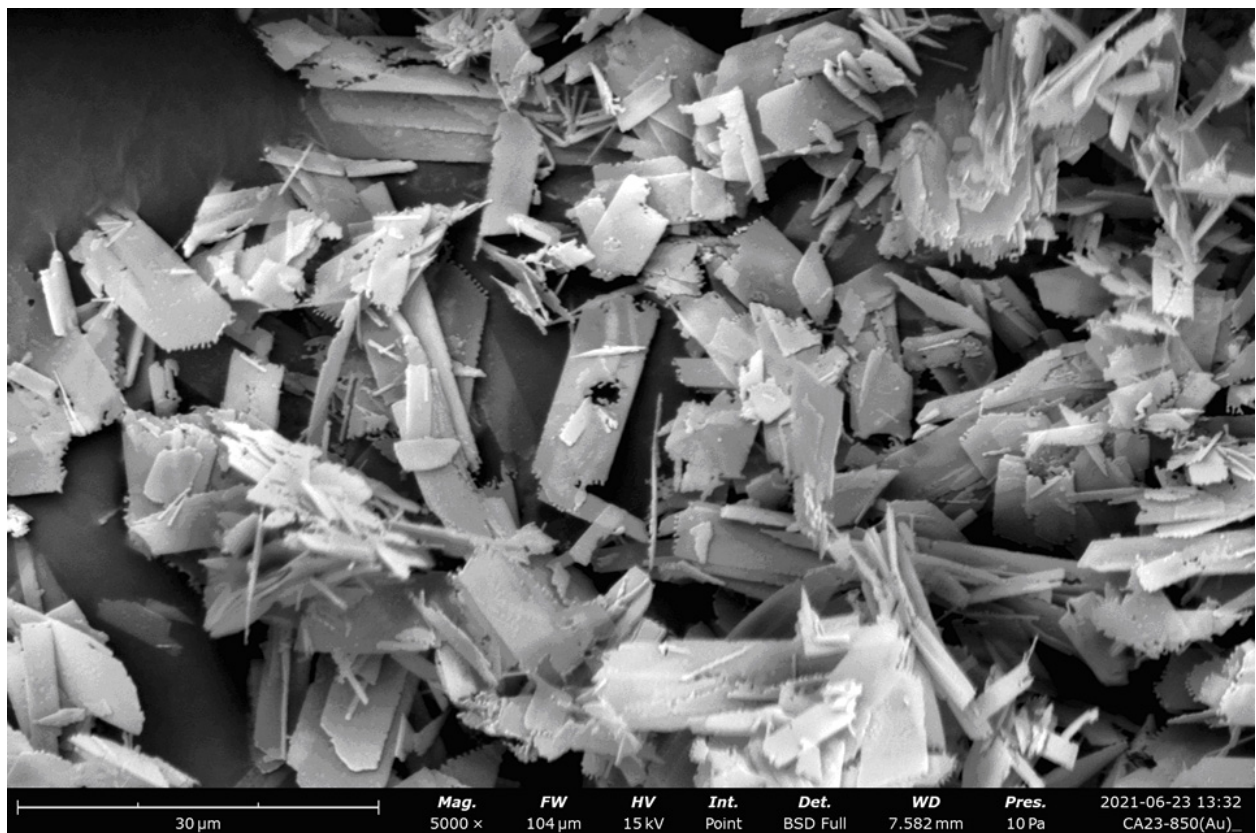
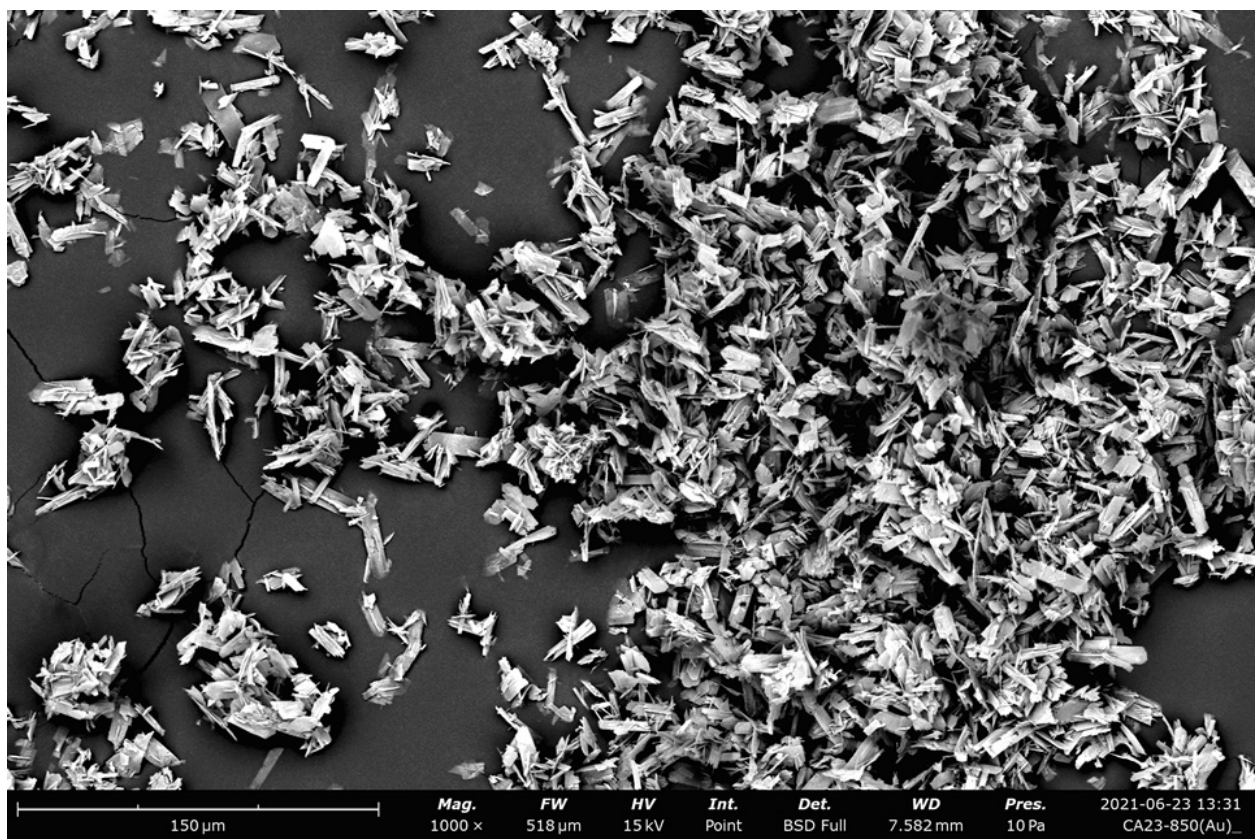


**Fig. S3** SEM images of CAp microcrystals (Table 1, Entry 1), sintered at 850 °C.

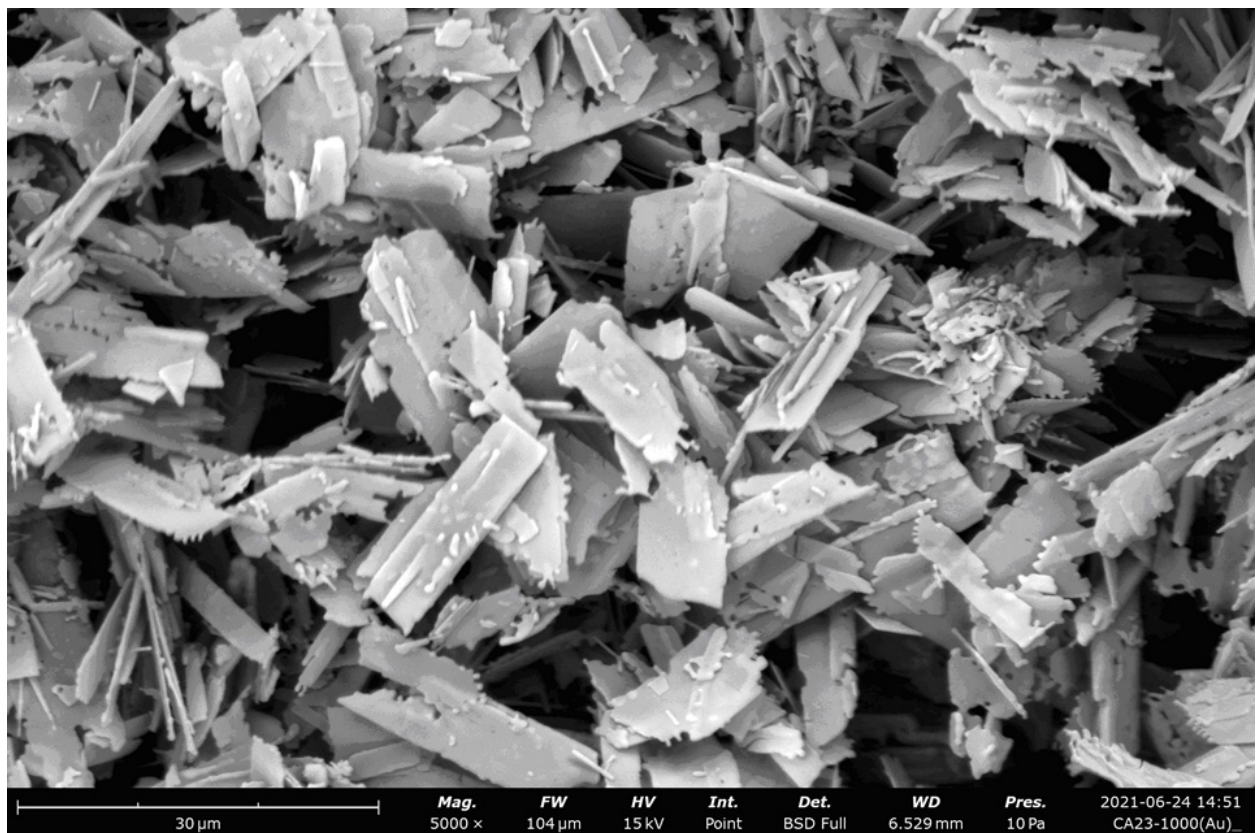
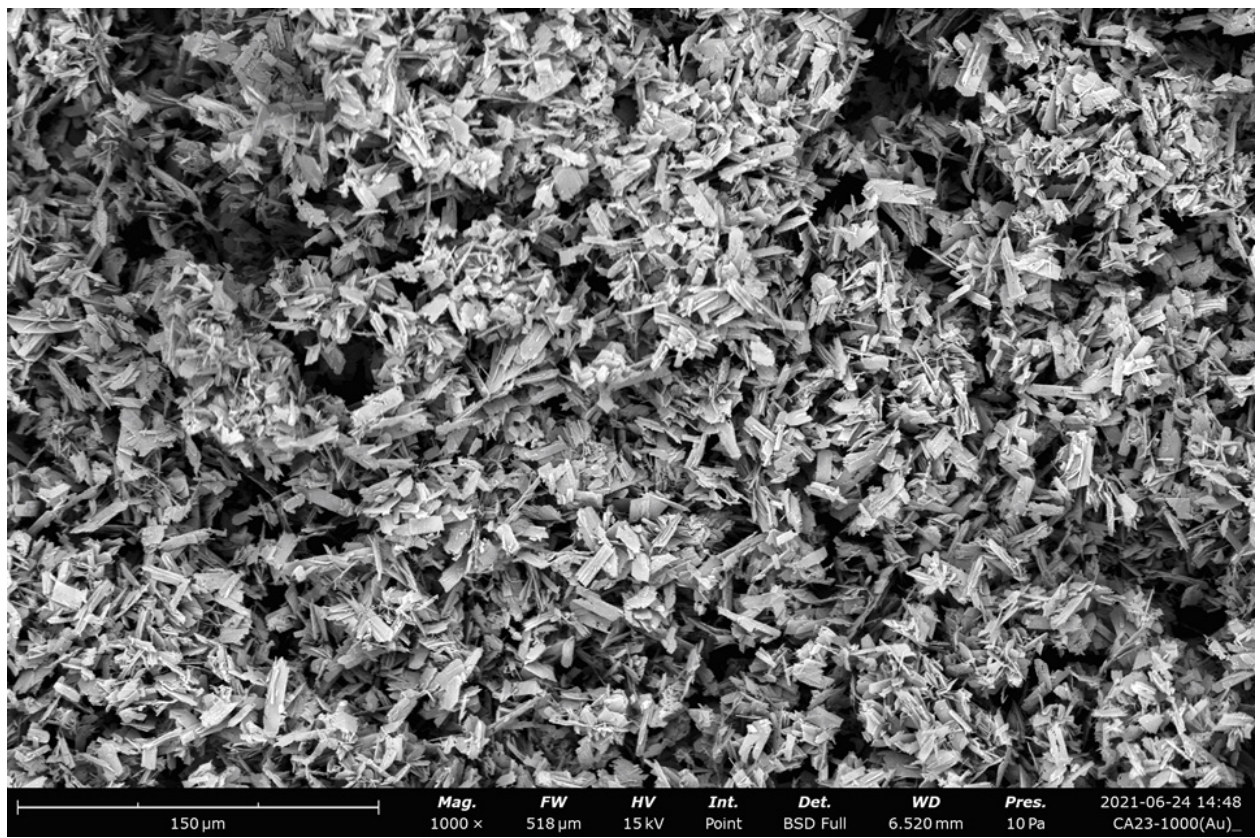


**Fig. S4** SEM images of CAp microcrystals (Table 1, Entry 1), sintered at 1000 °C.

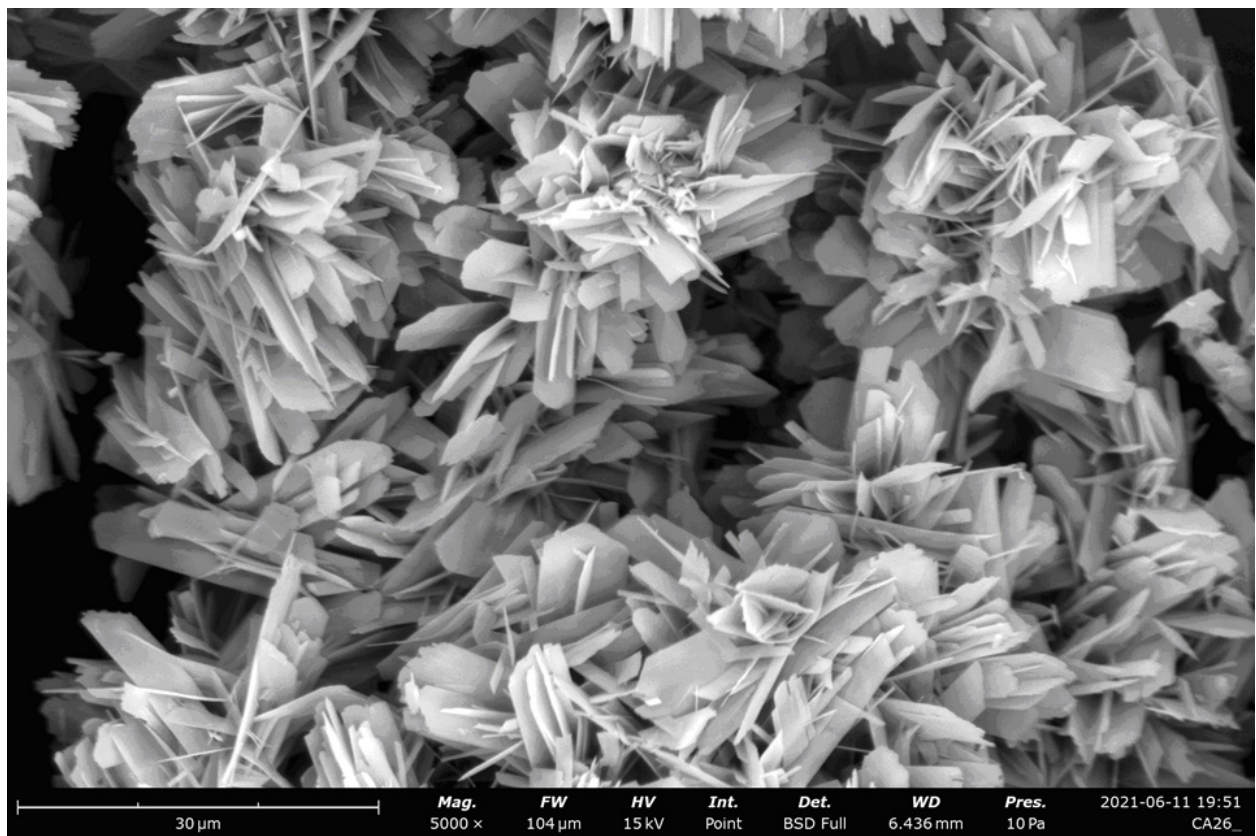
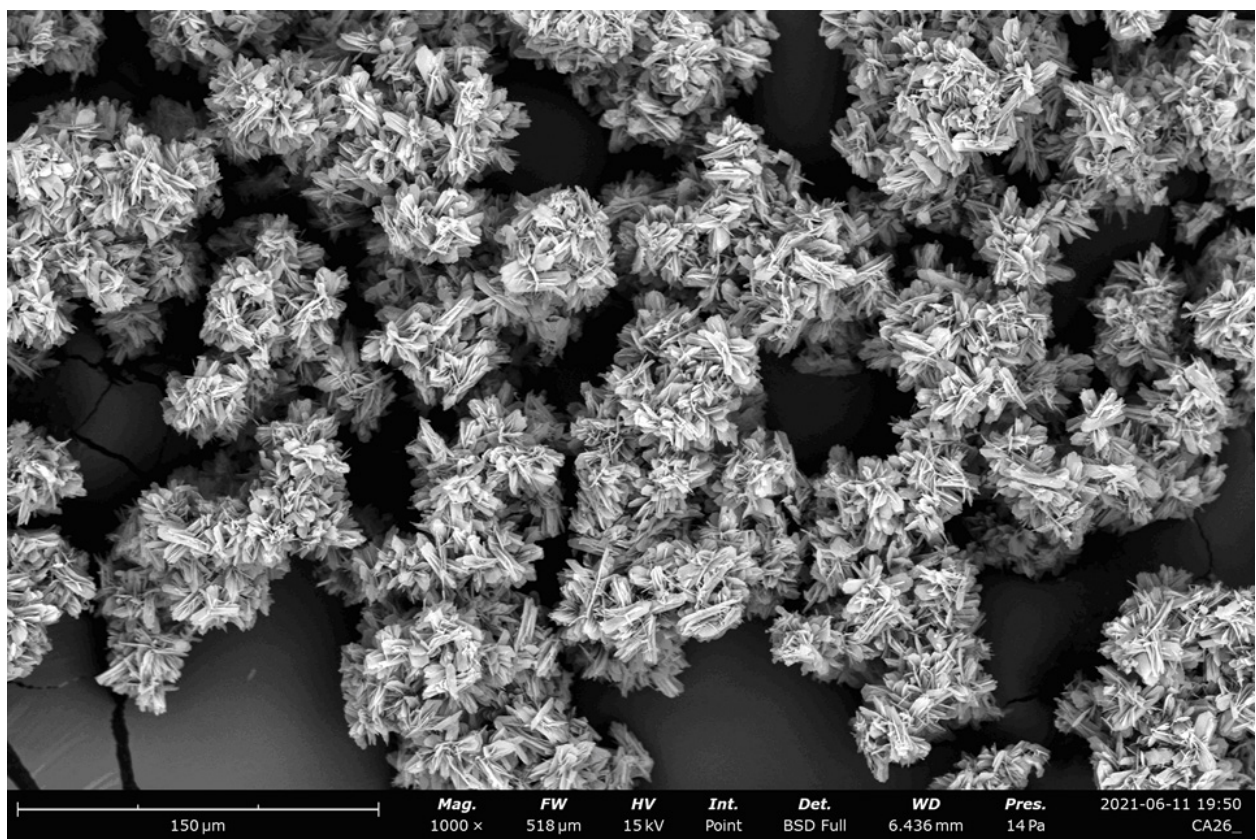


**Fig. S5** SEM images of CAp microcrystals (Table 1, Entry 2).

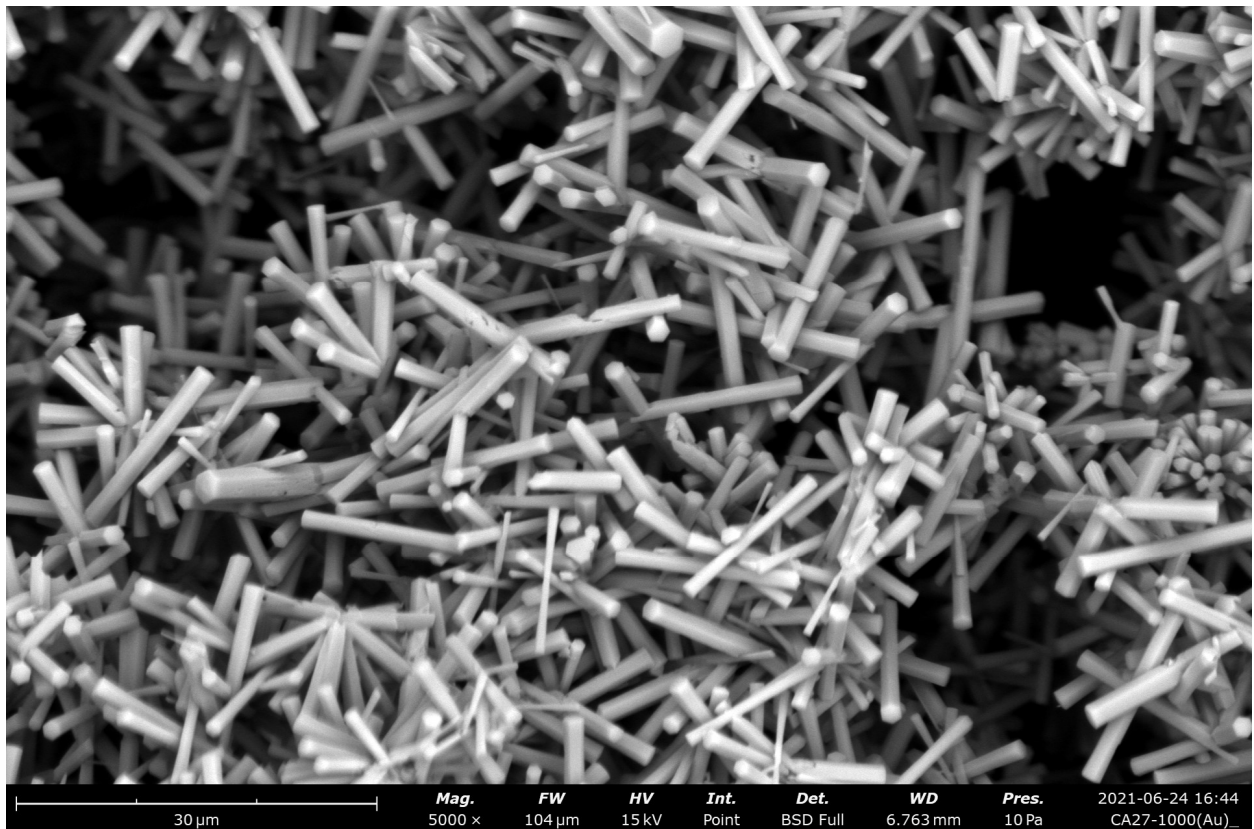
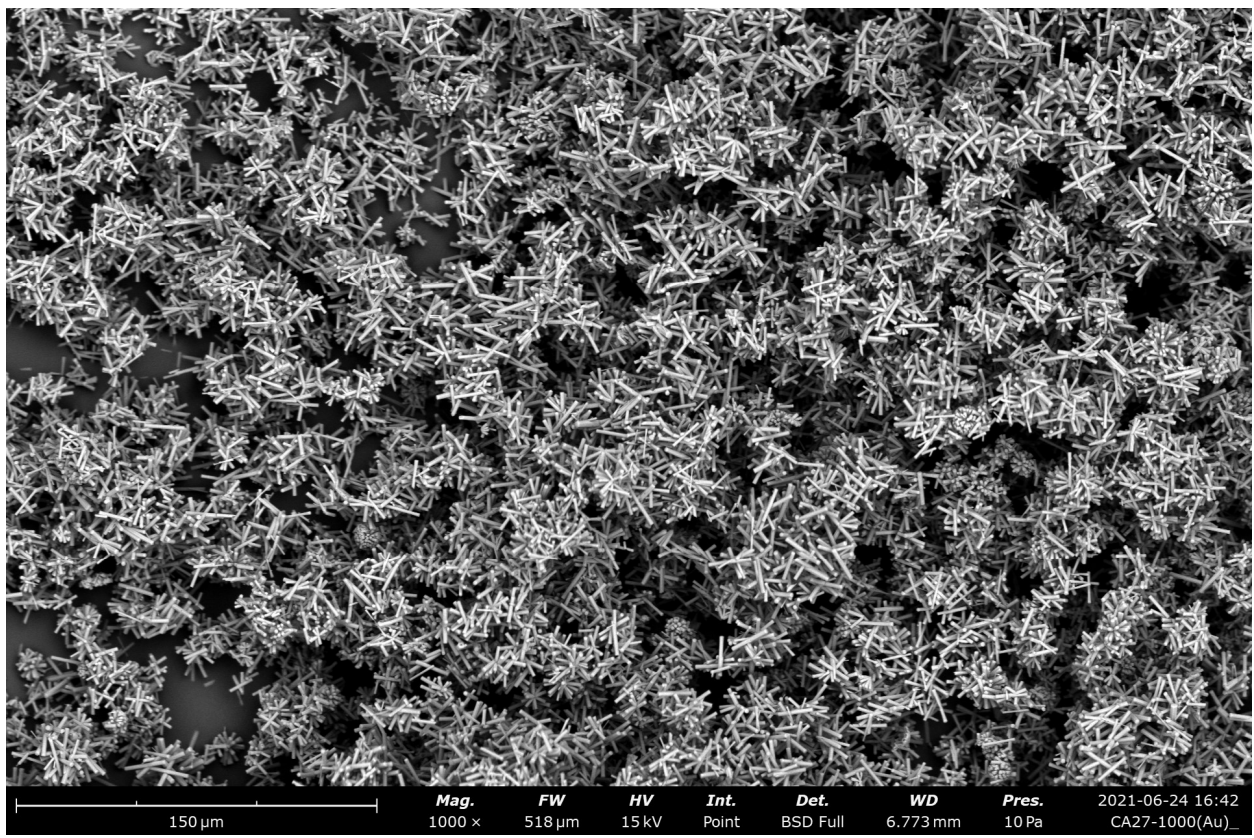


**Fig. S6** SEM images of CAp microcrystals (Table 1, Entry 3).

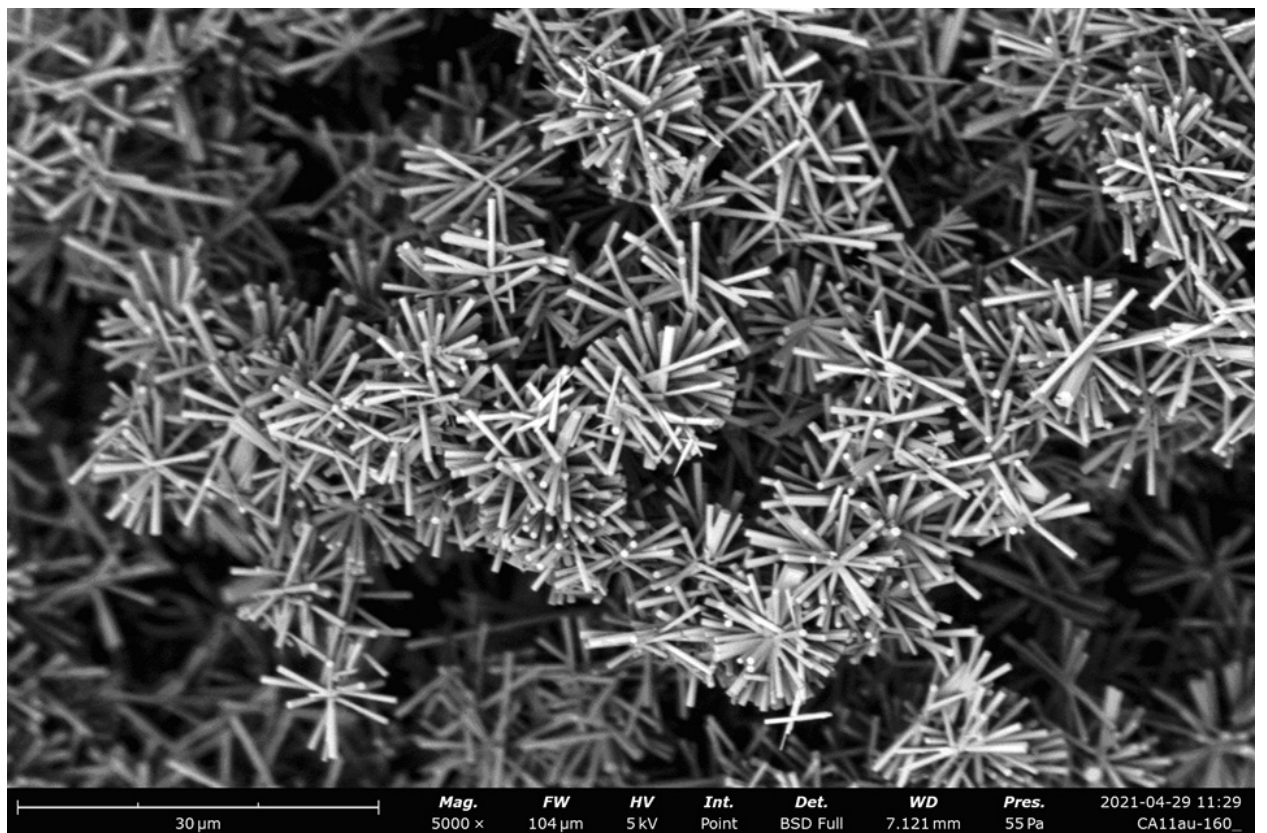
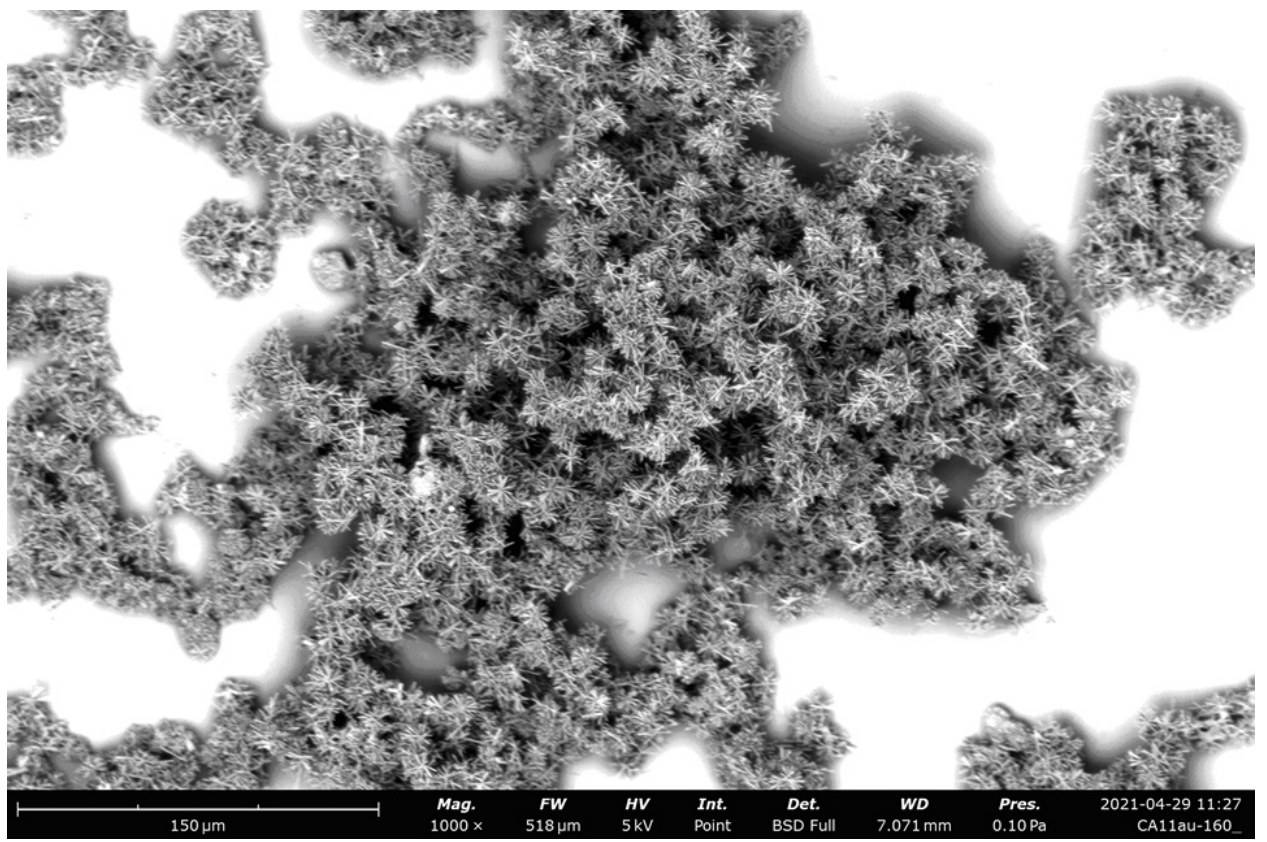


**Fig. S7** SEM images of CAp microcrystals (Table 1, Entry 4).

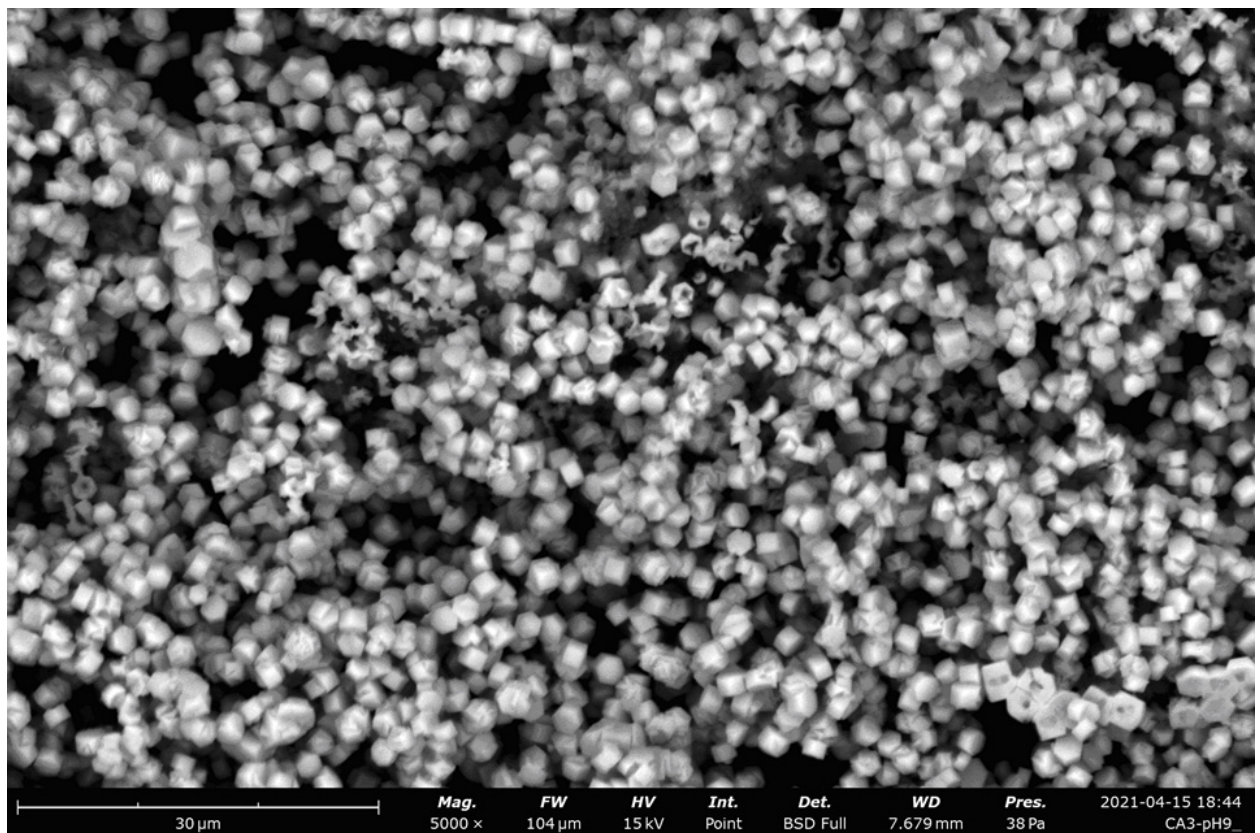
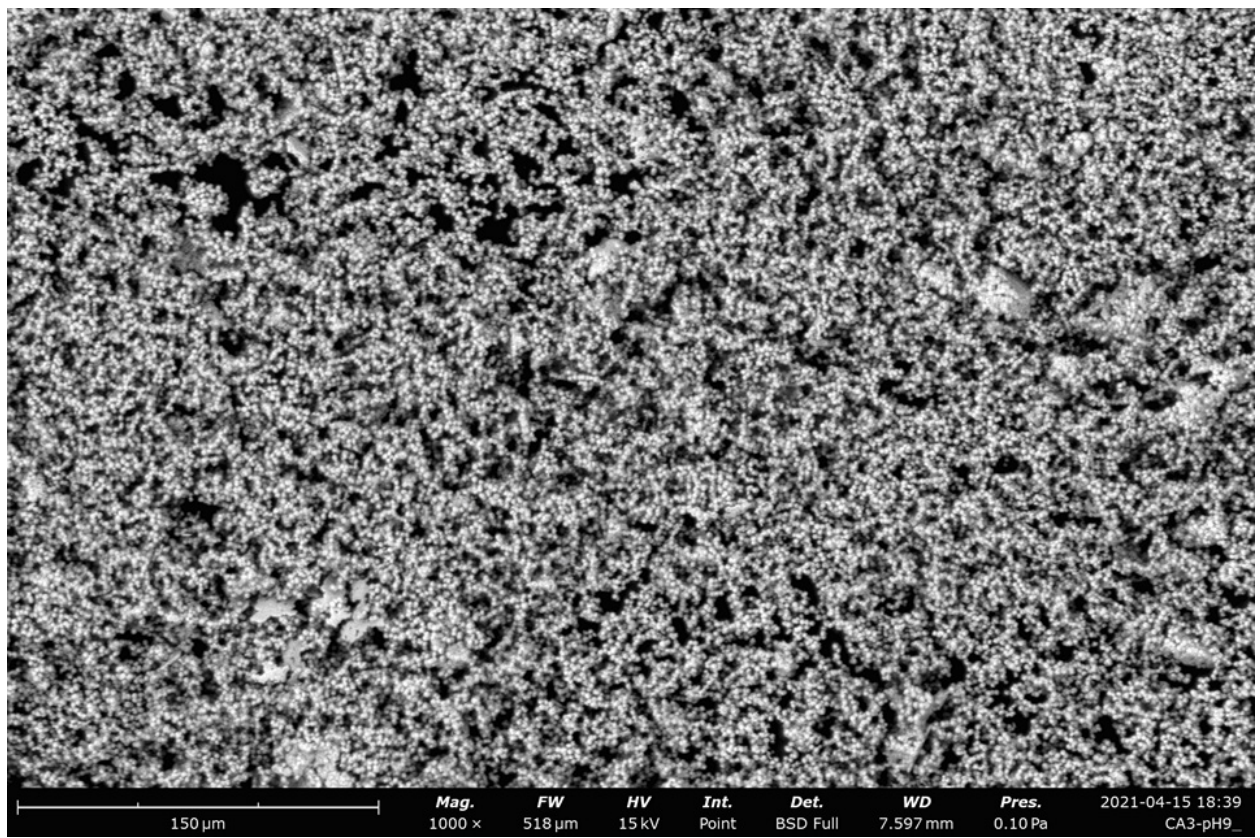


**Fig. S8** SEM images of CAp microcrystals (Table 1, Entry 5).

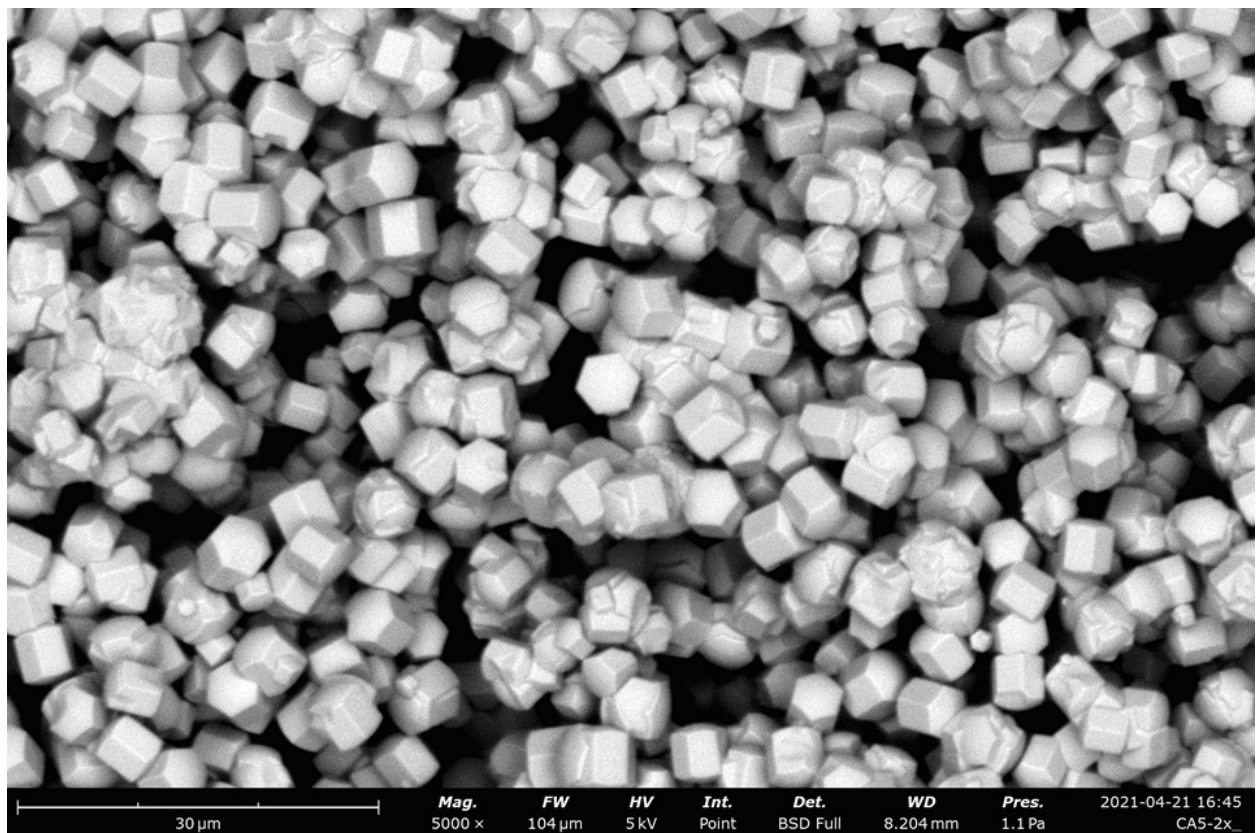
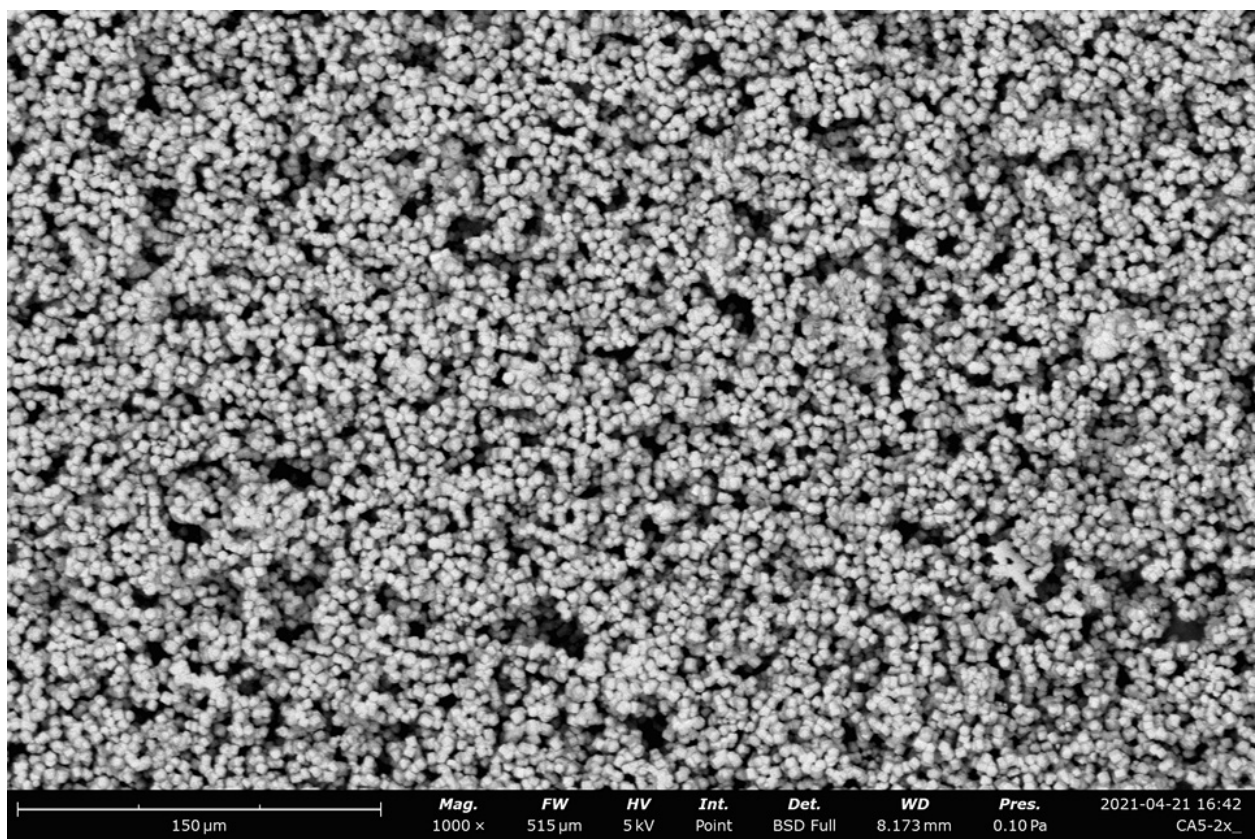


**Fig. S9** SEM images of CAp microcrystals (Table 1, Entry 7).

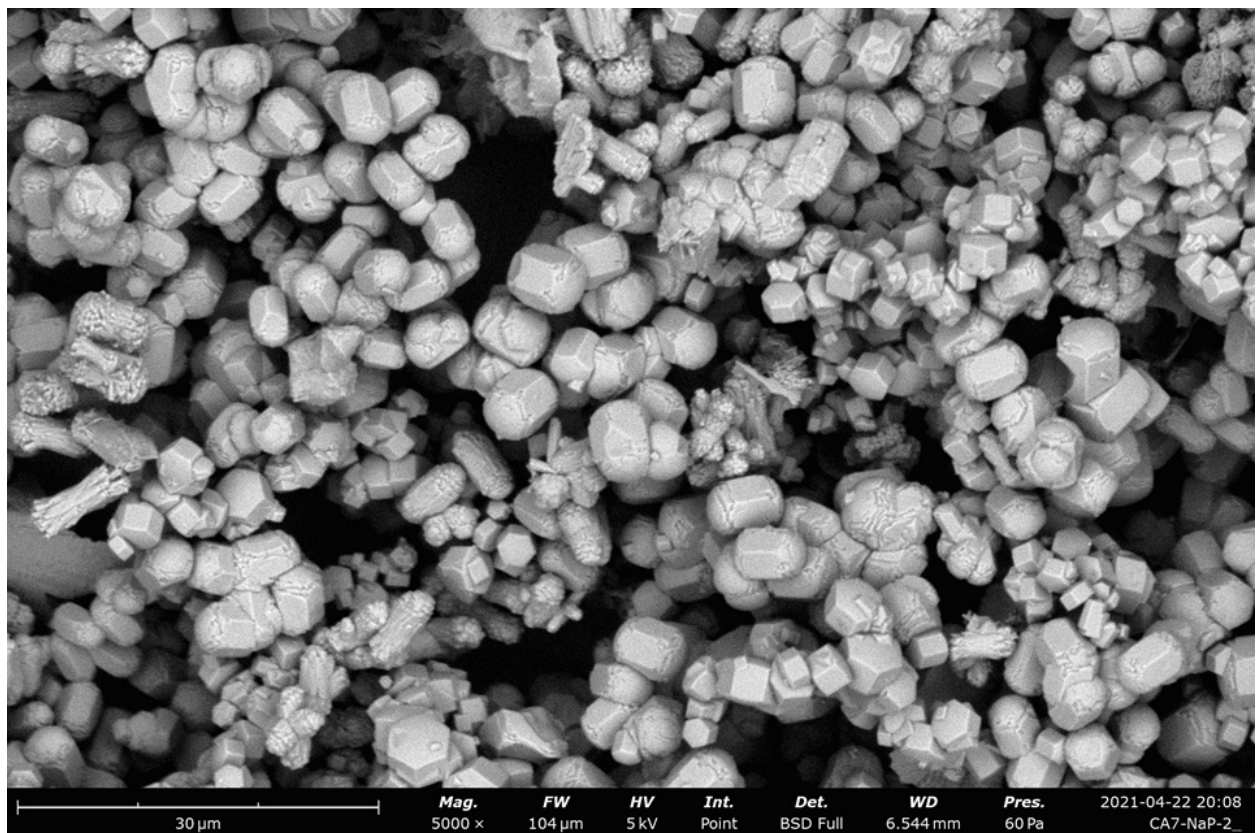
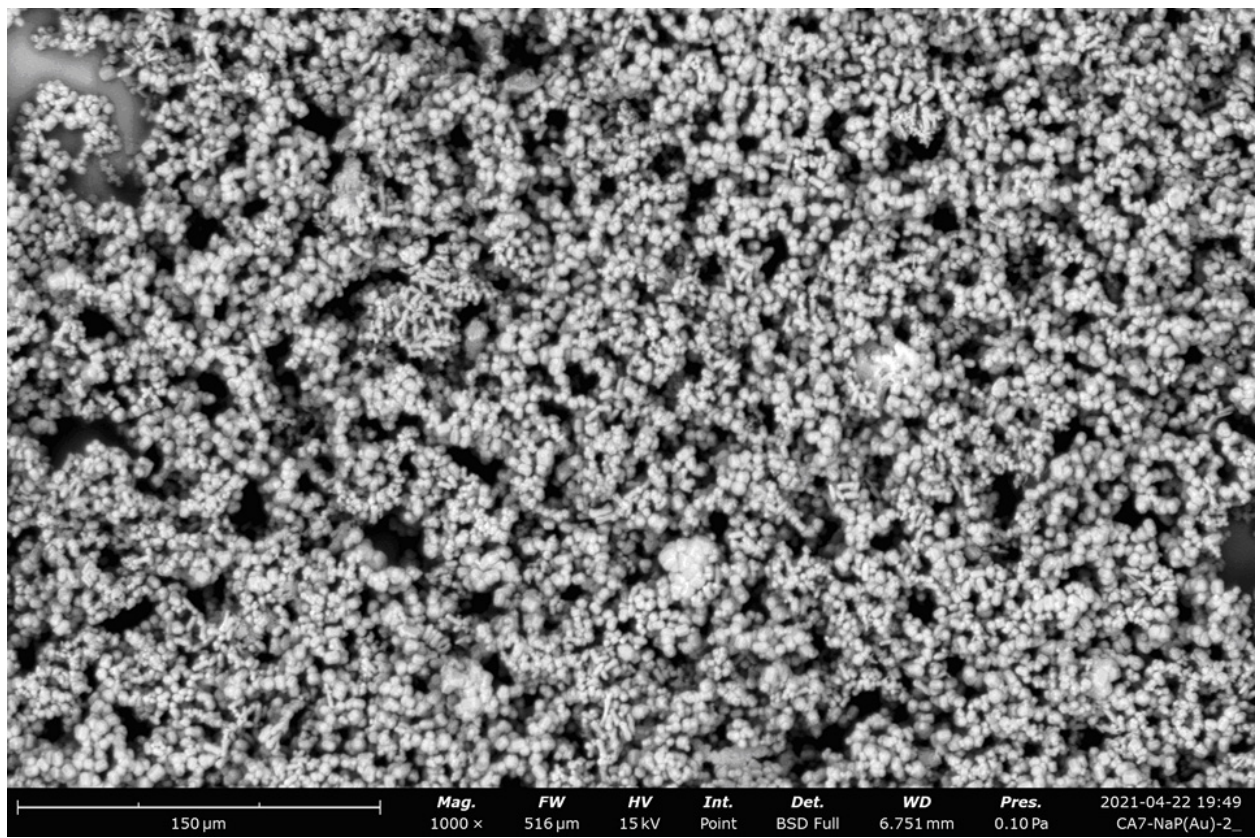


**Fig. S10** SEM images of CAp microcrystals (Table 1, Entry 8).

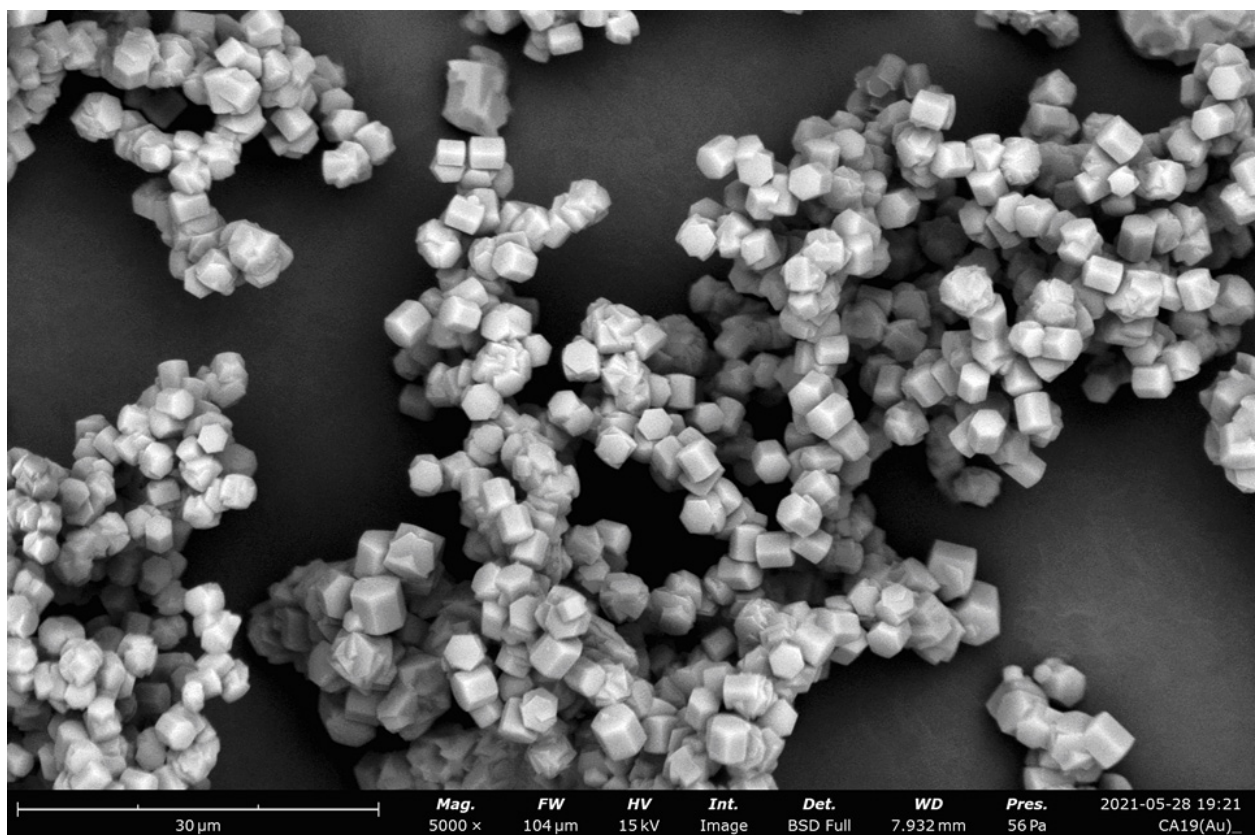
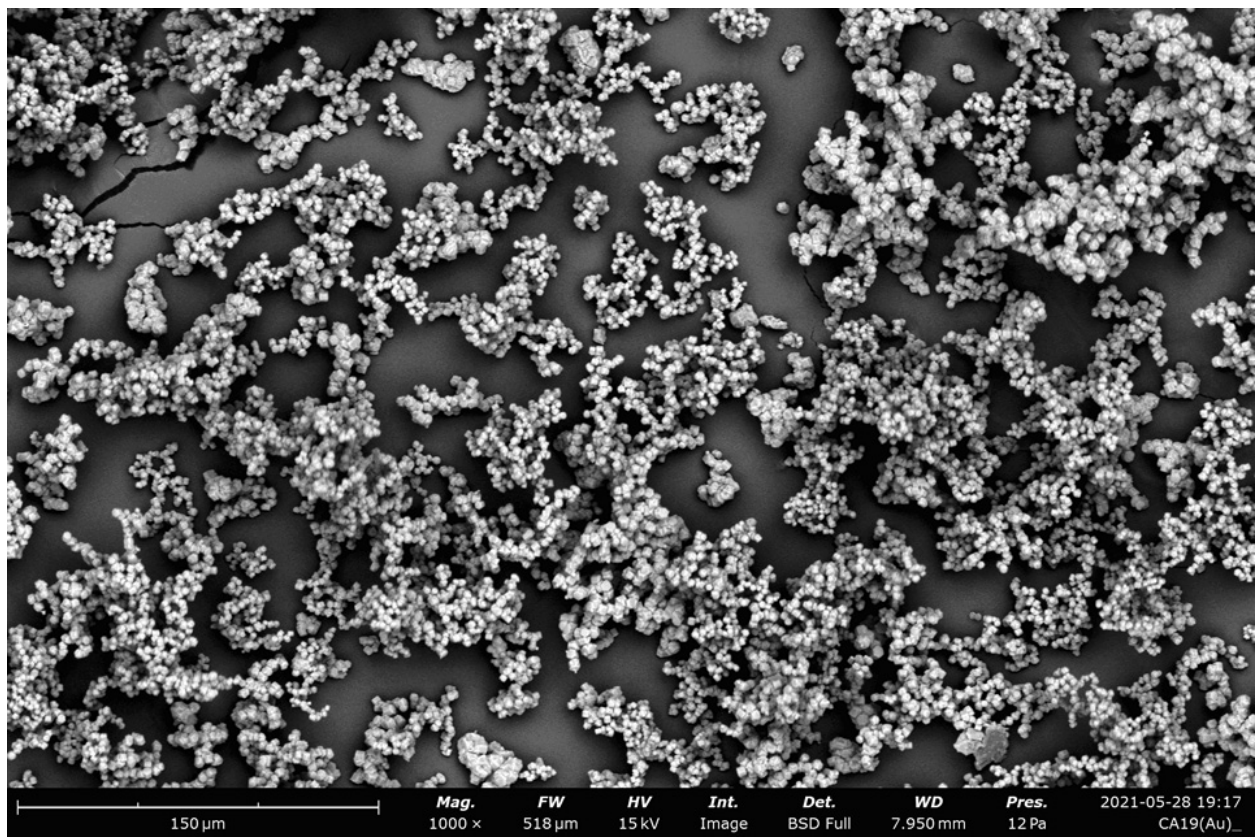


**Fig. S11** SEM images of CAp microcrystals (Table 1, Entry 9).

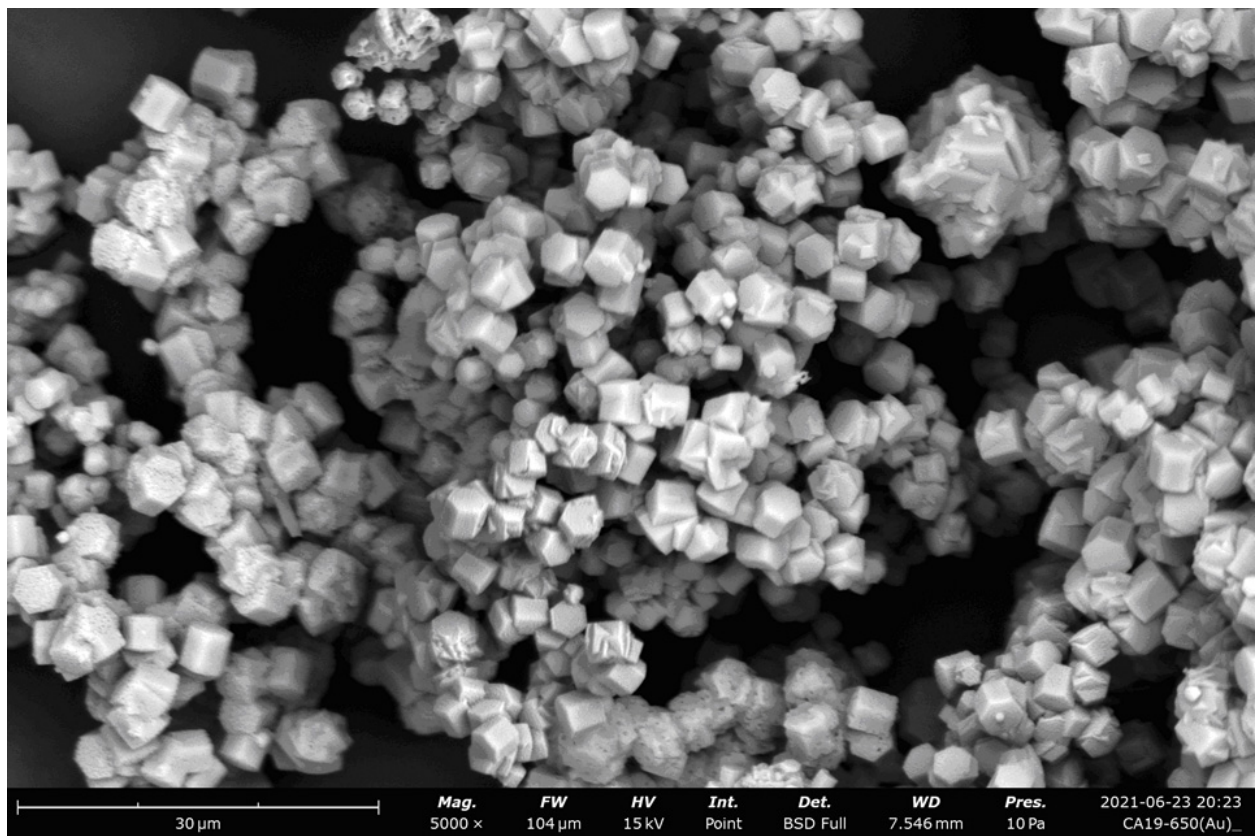
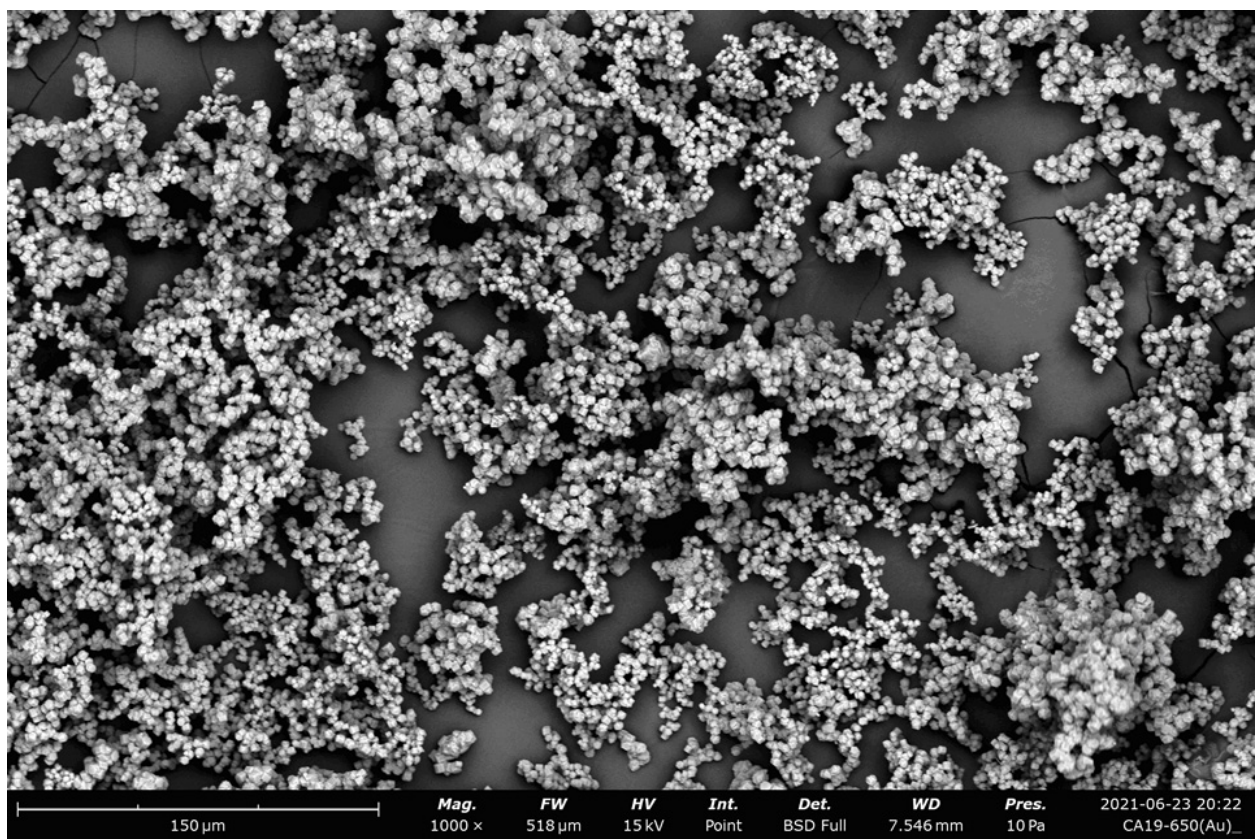


**Fig. S12** SEM images of CAp microcrystals (Table 1, Entry 9), sintered at 650 °C.

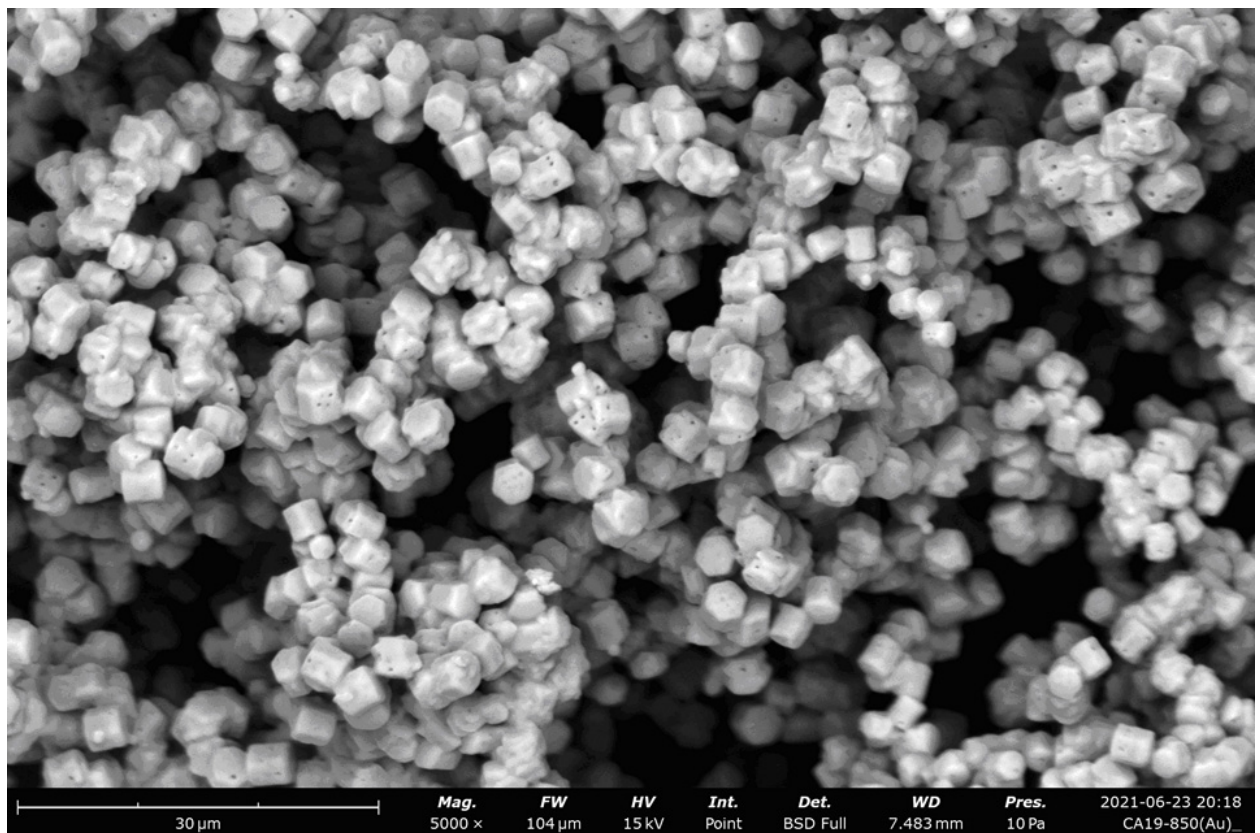
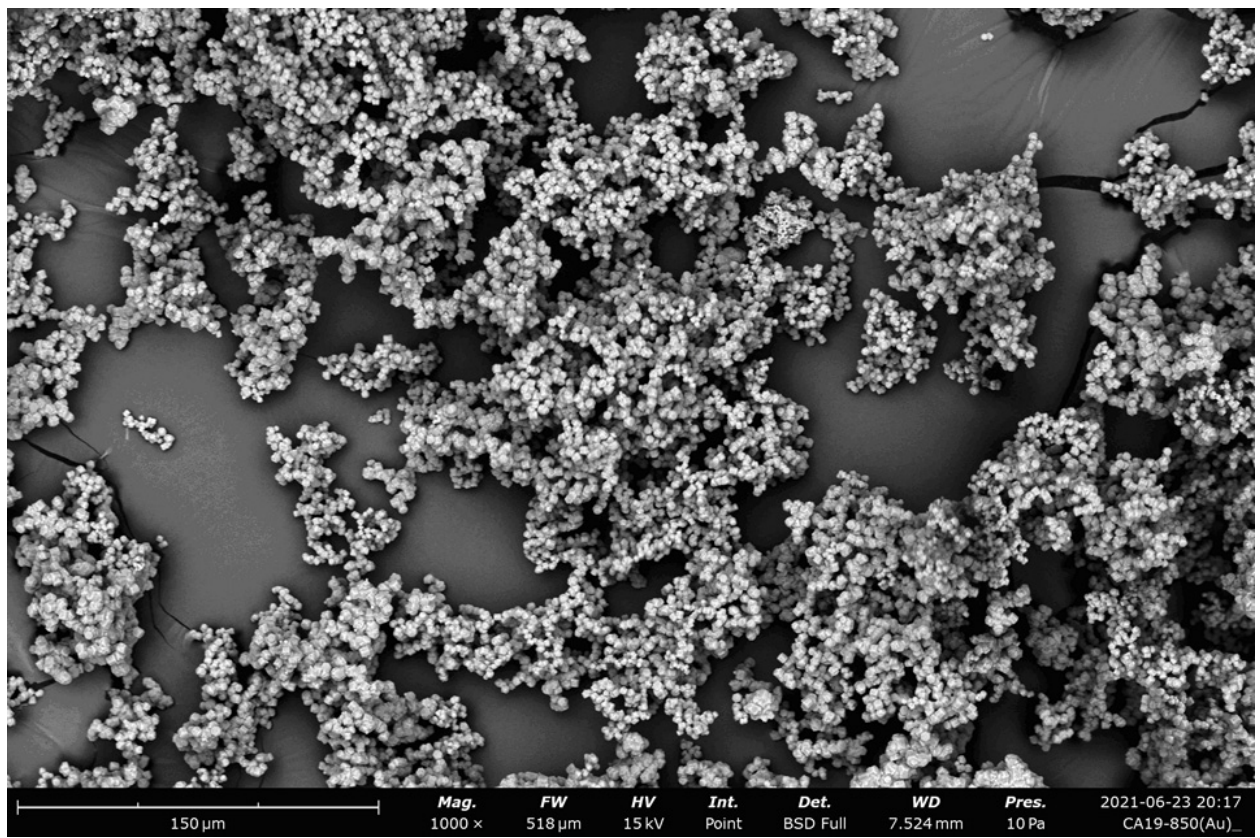


**Fig. S13** SEM images of CAp microcrystals (Table 1, Entry 9), sintered at 850 °C.

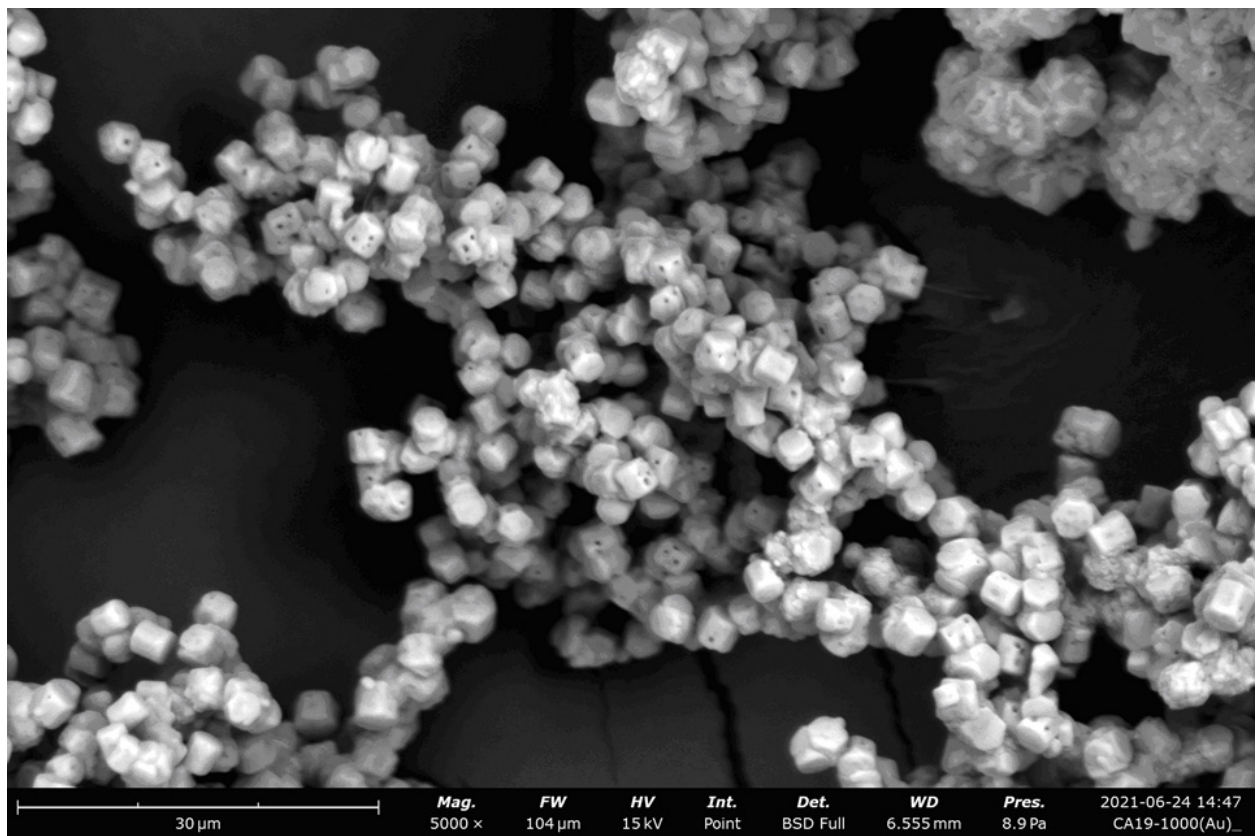
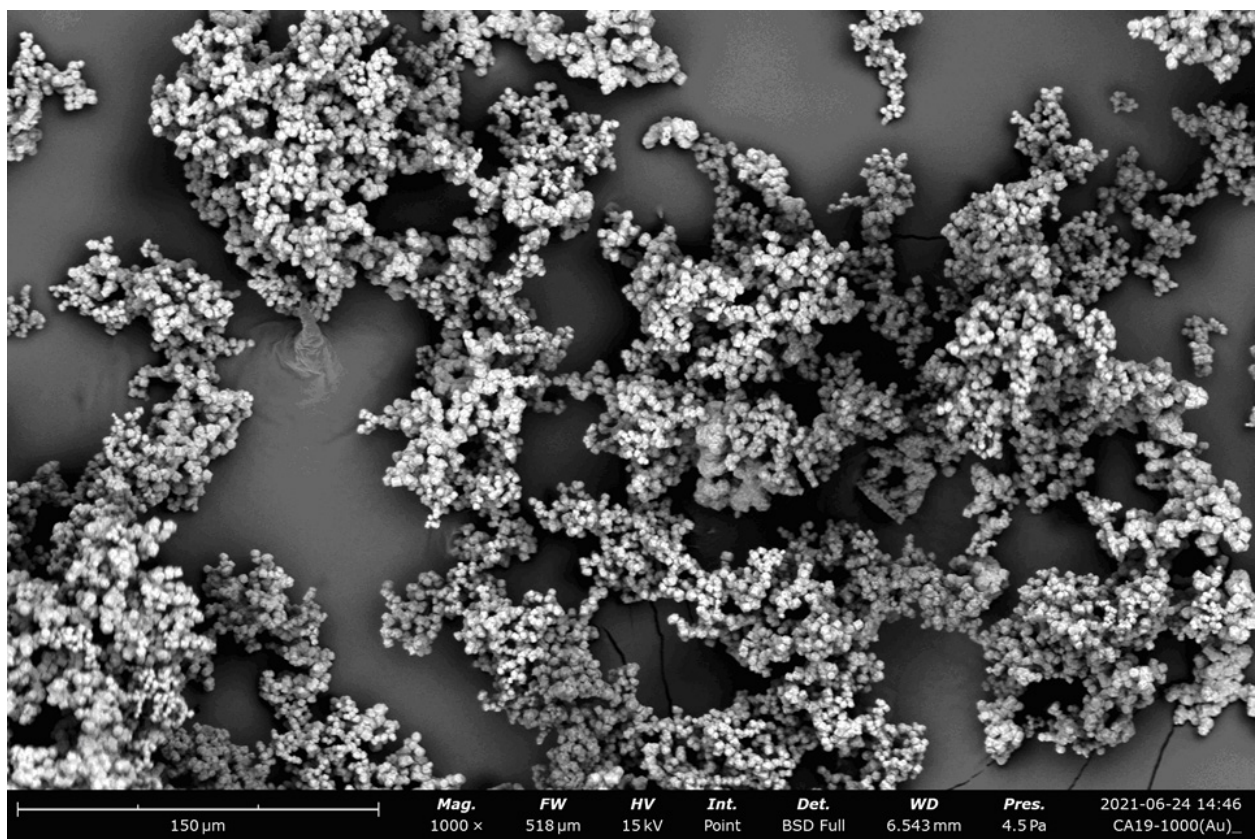


**Fig. S14** SEM images of CAp microcrystals (Table 1, Entry 9), sintered at 1000 °C.

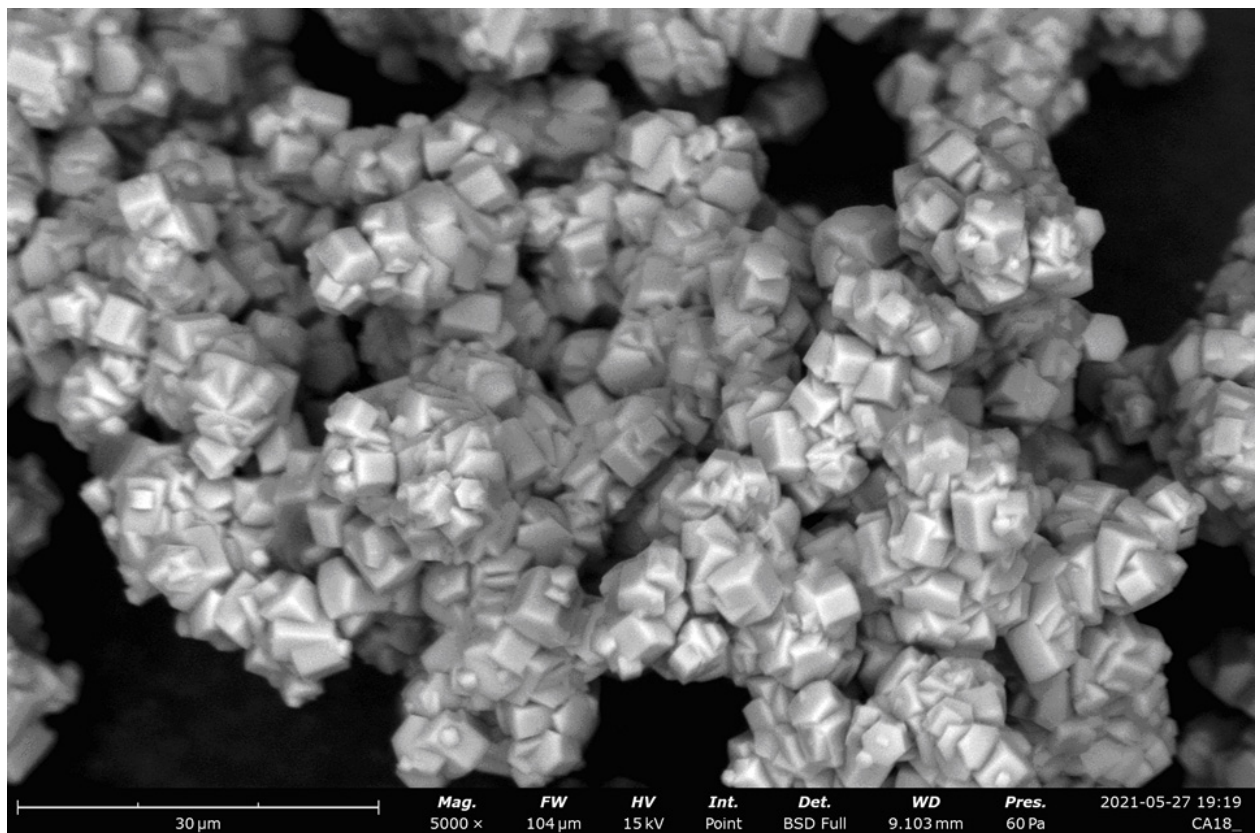
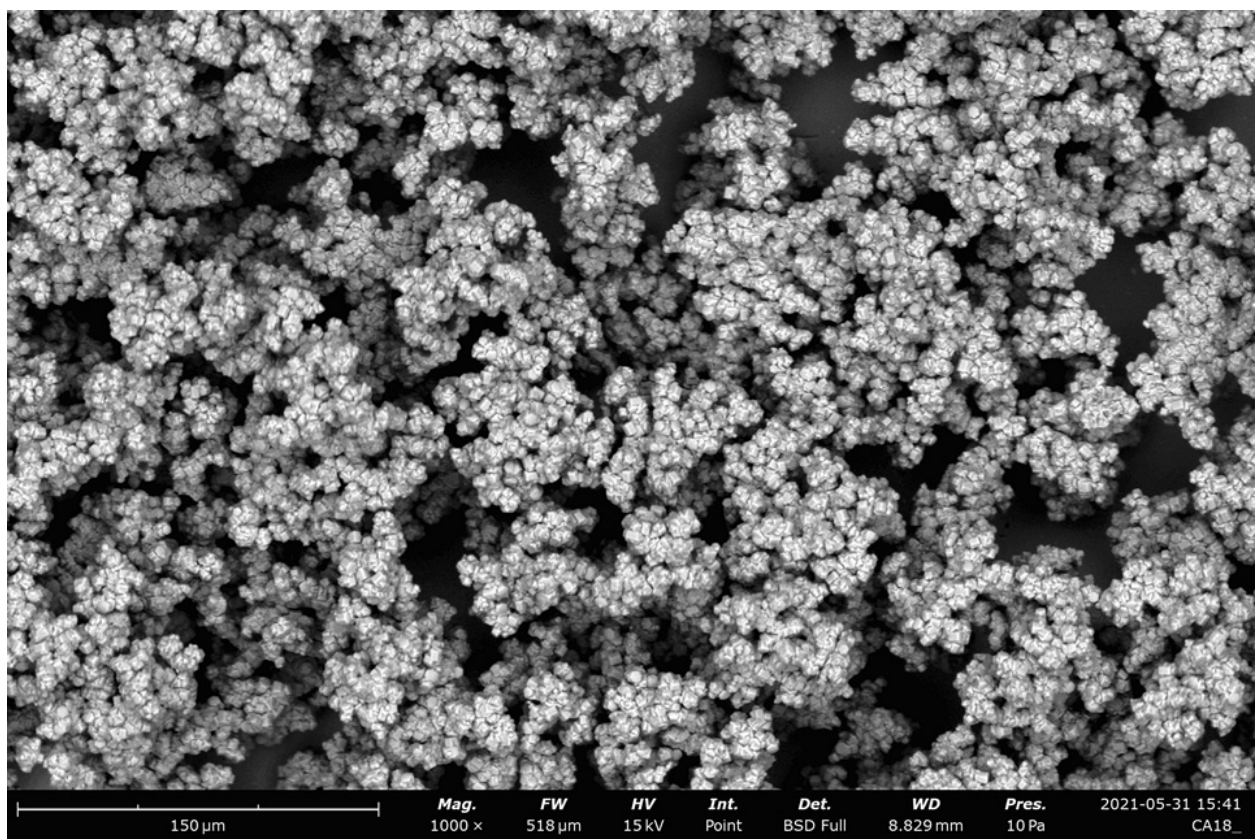


**Fig. S15** SEM images of CAp microcrystals (Table 1, Entry 10).

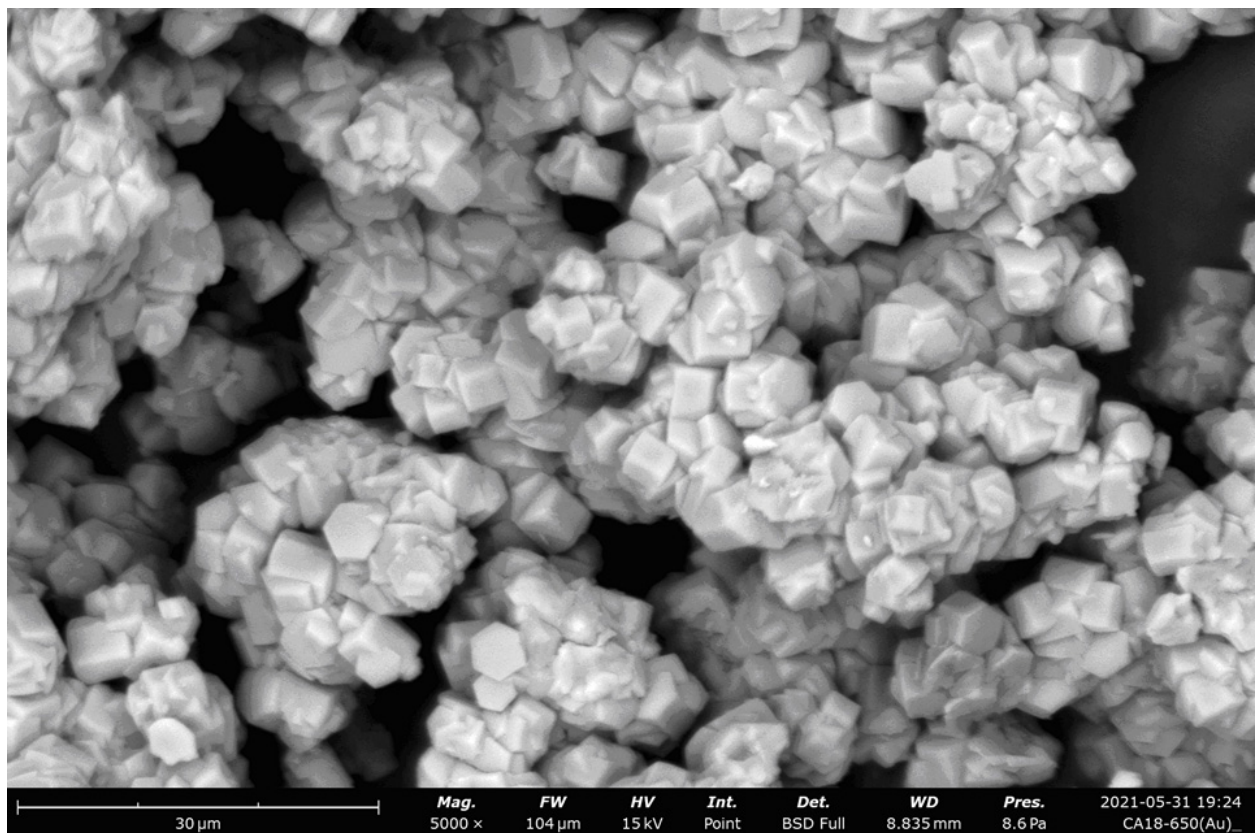
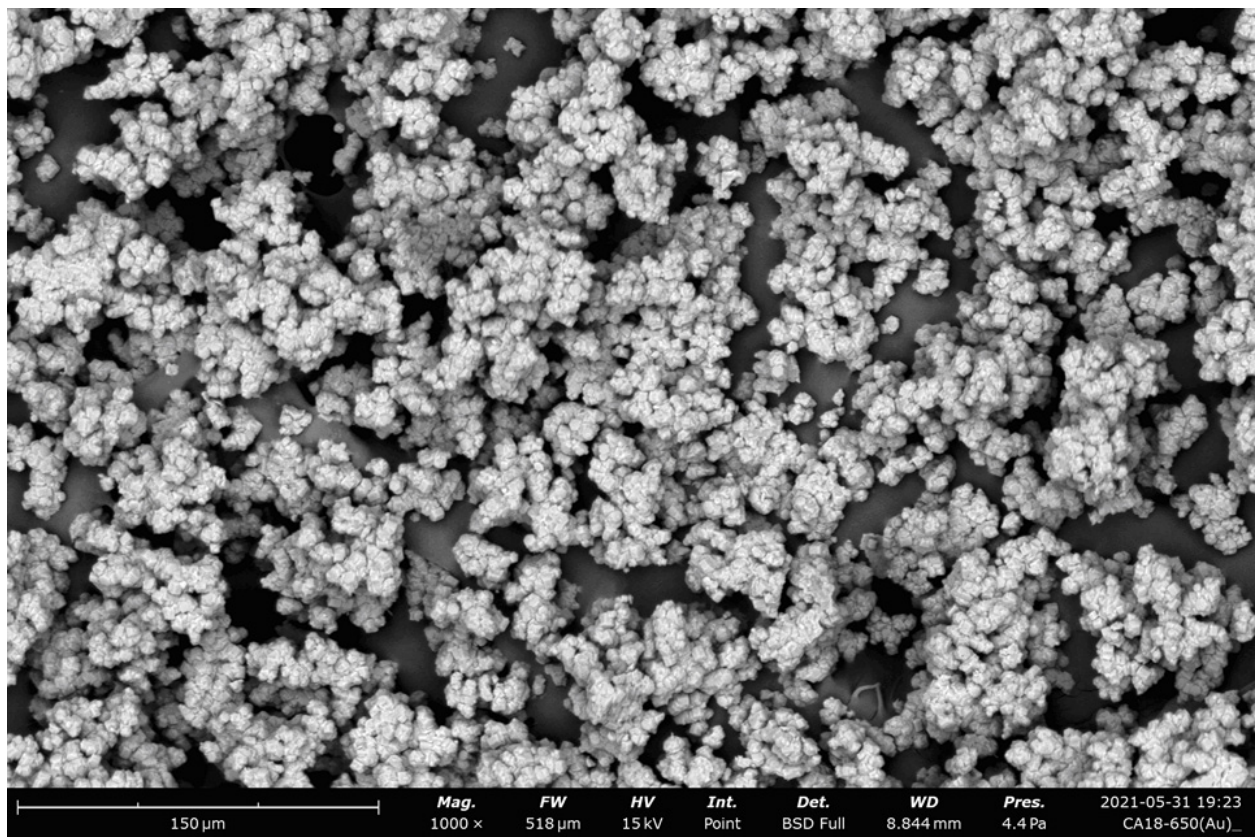


**Fig. S16** SEM images of CAp microcrystals (Table 1, Entry 10), sintered at 650 °C.

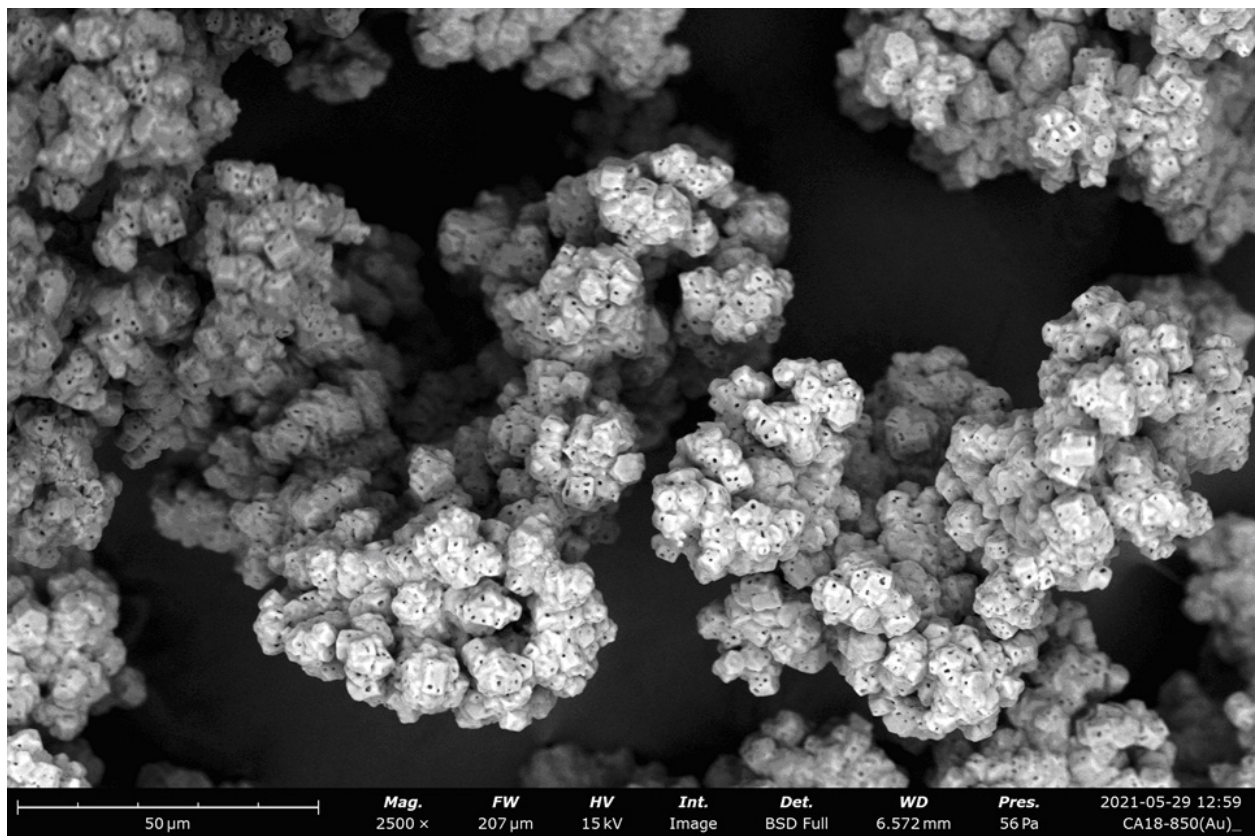
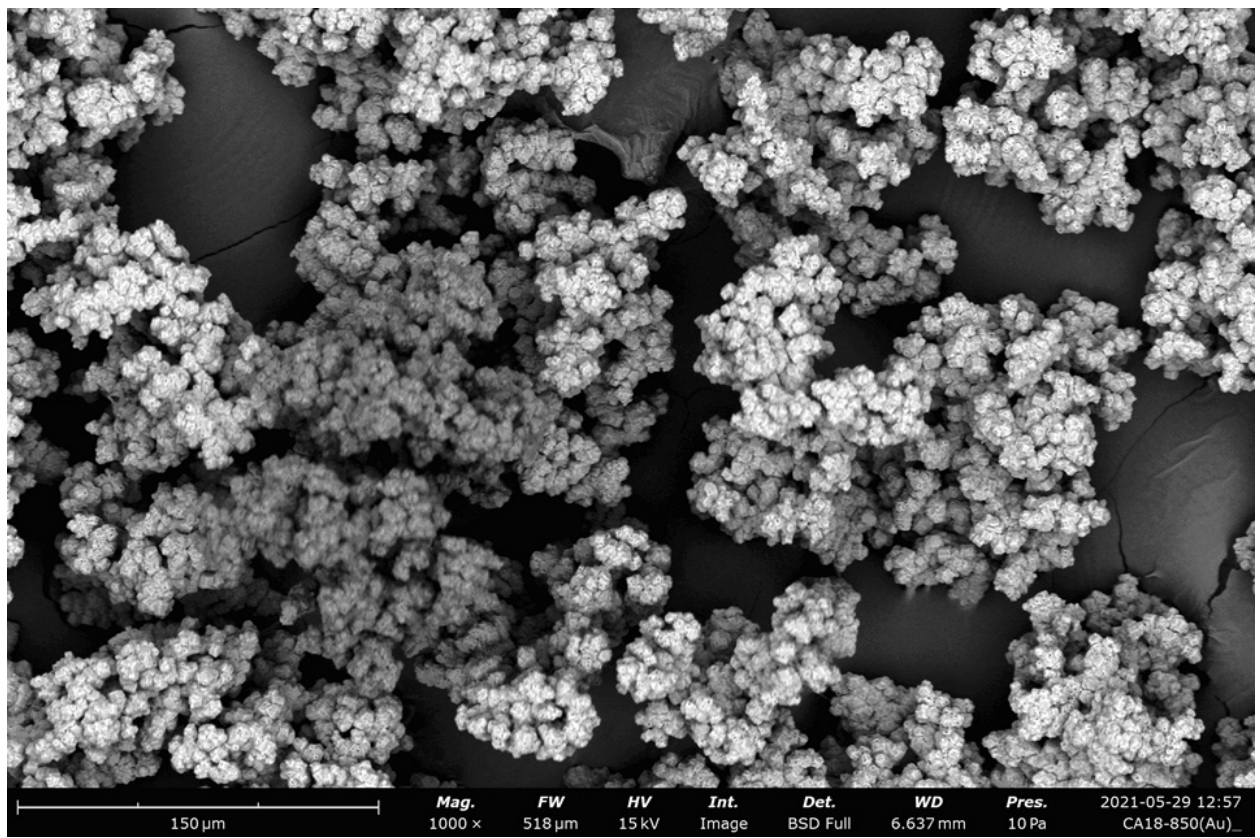


**Fig. S17** SEM images of CAp microcrystals (Table 1, Entry 10), sintered at 850 °C.

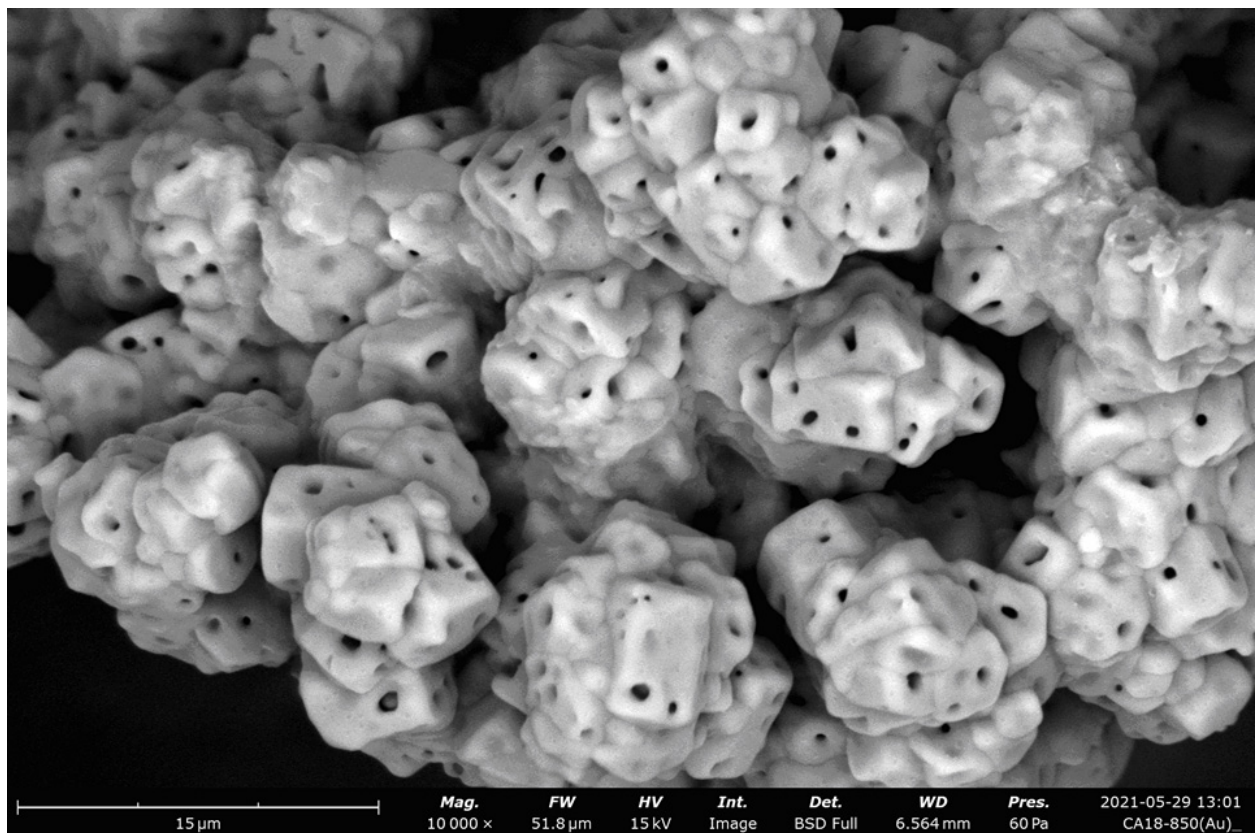
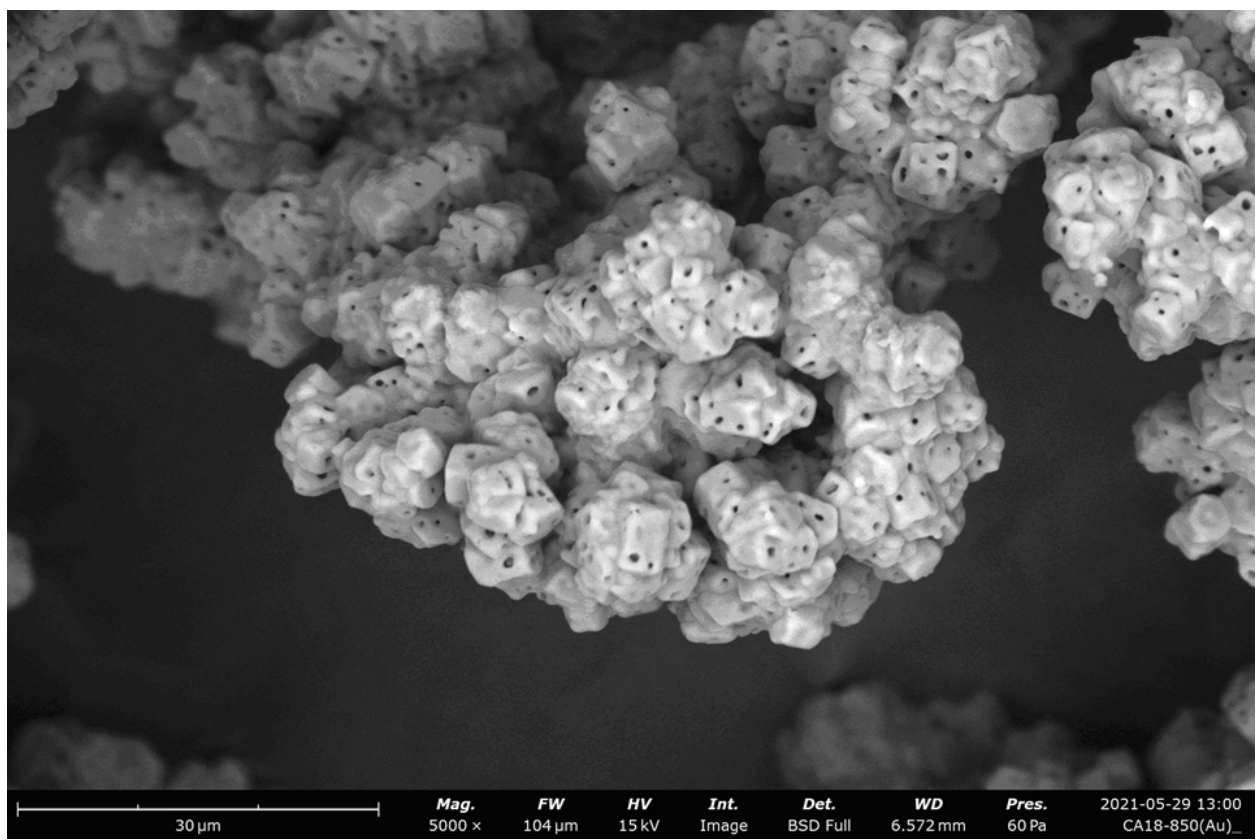


**Fig. S17 (continued)** SEM images of CAp microcrystals (Table 1, Entry 10), sintered at 850 °C.

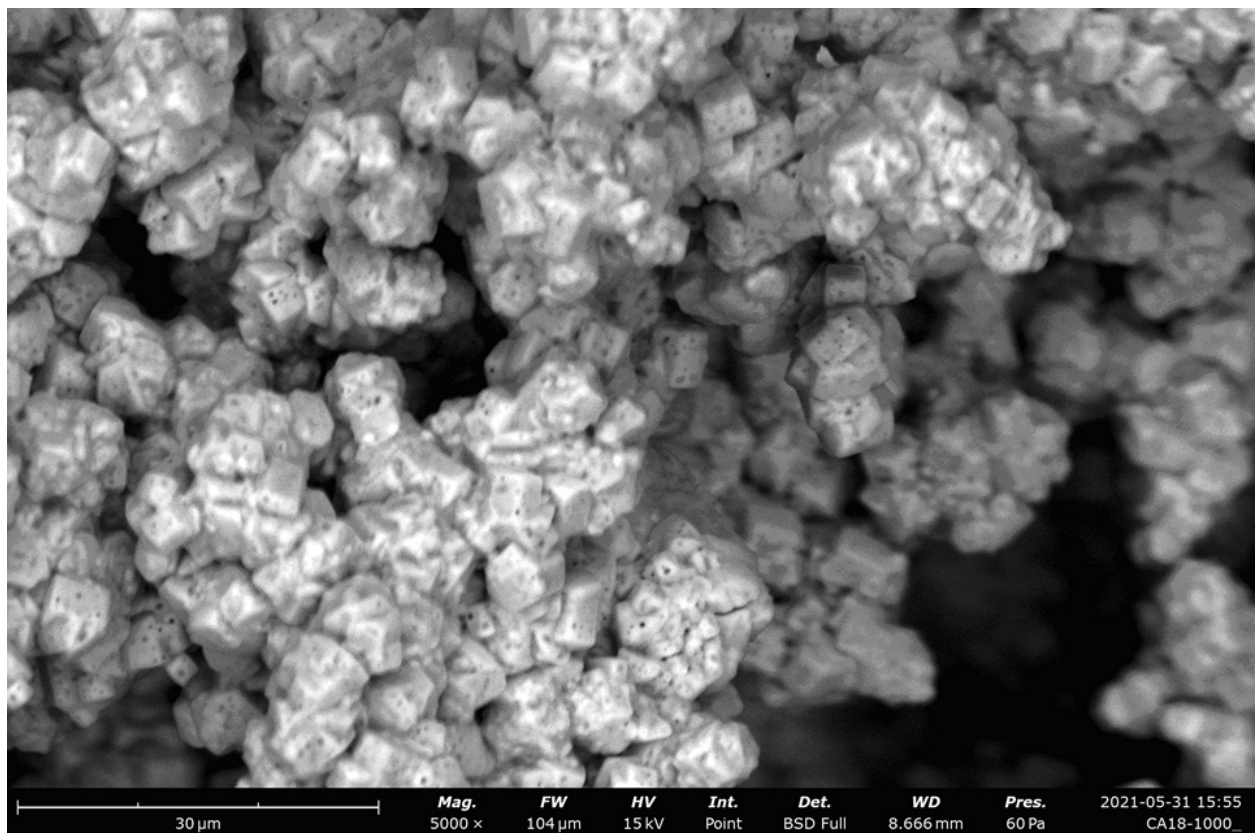
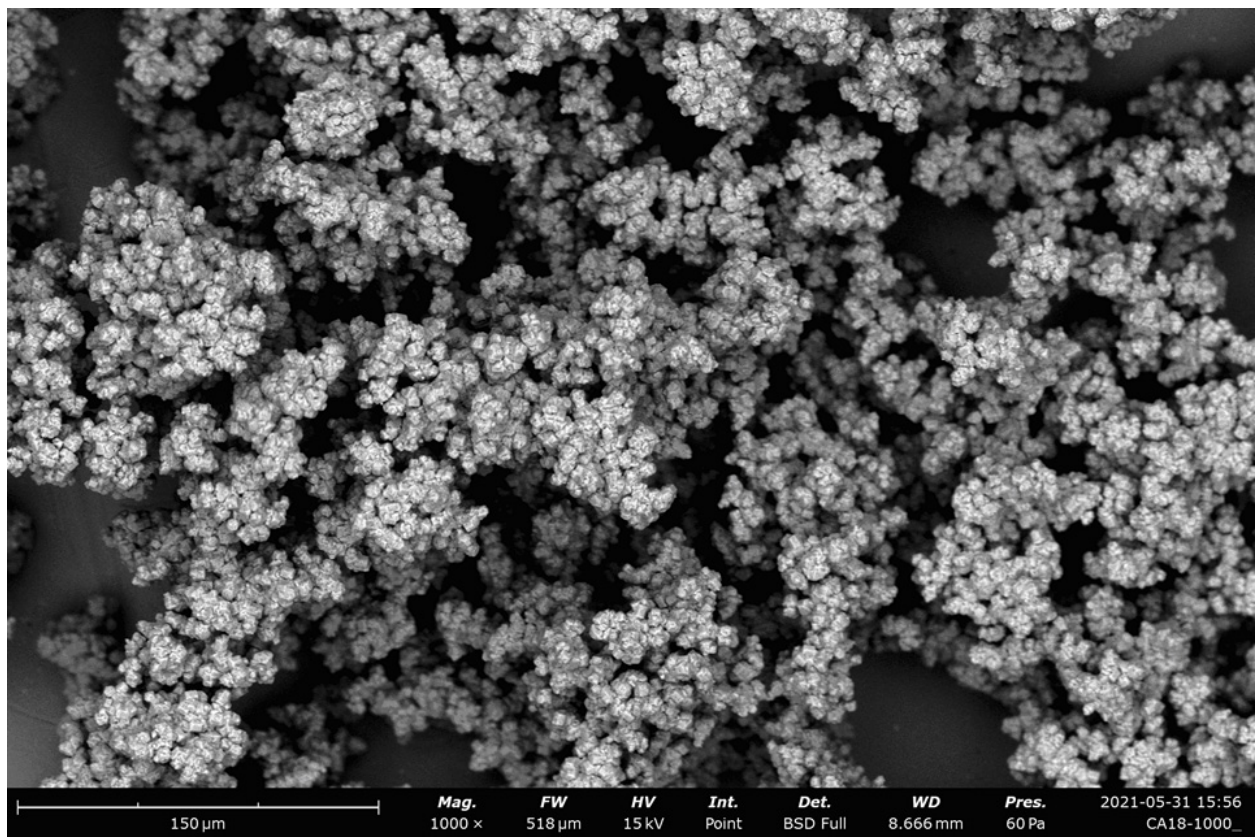


**Fig. S18** SEM images of CAp microcrystals (Table 1, Entry 10), sintered at 1000 °C.

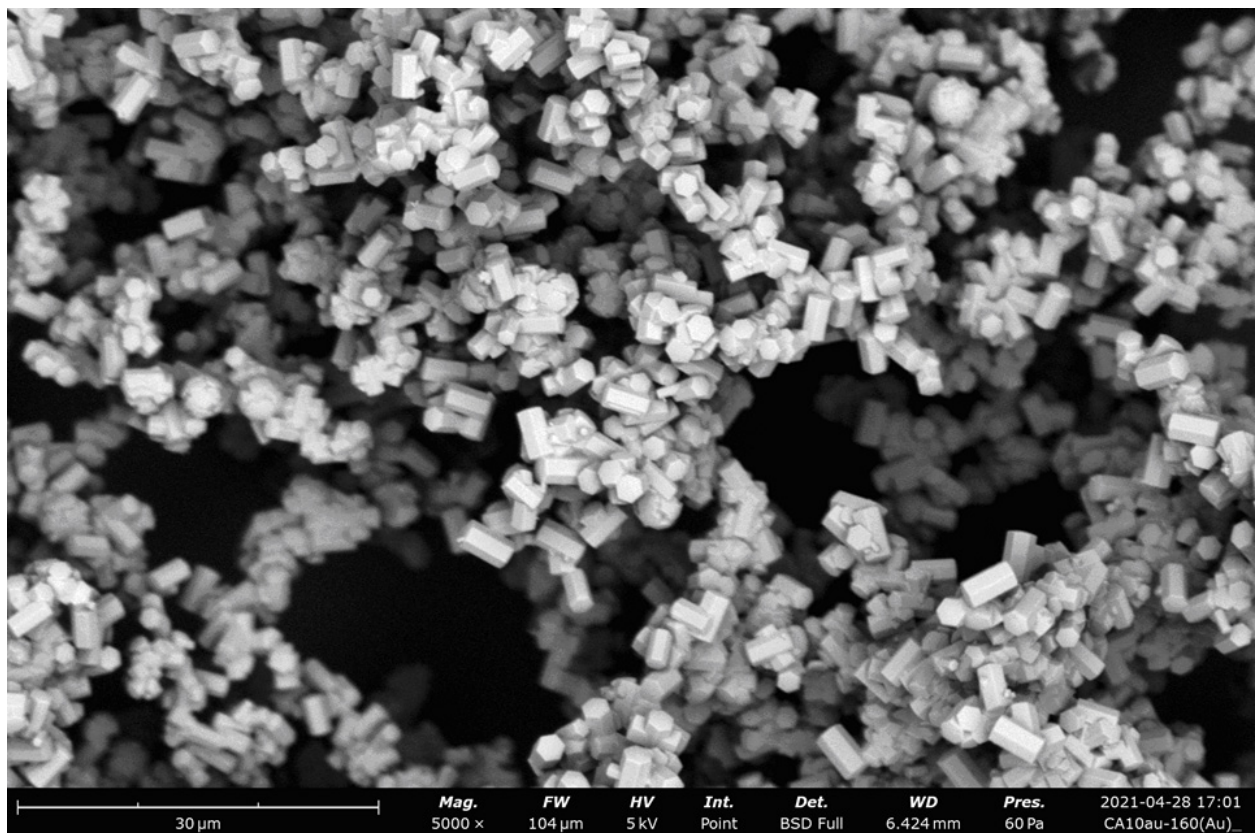
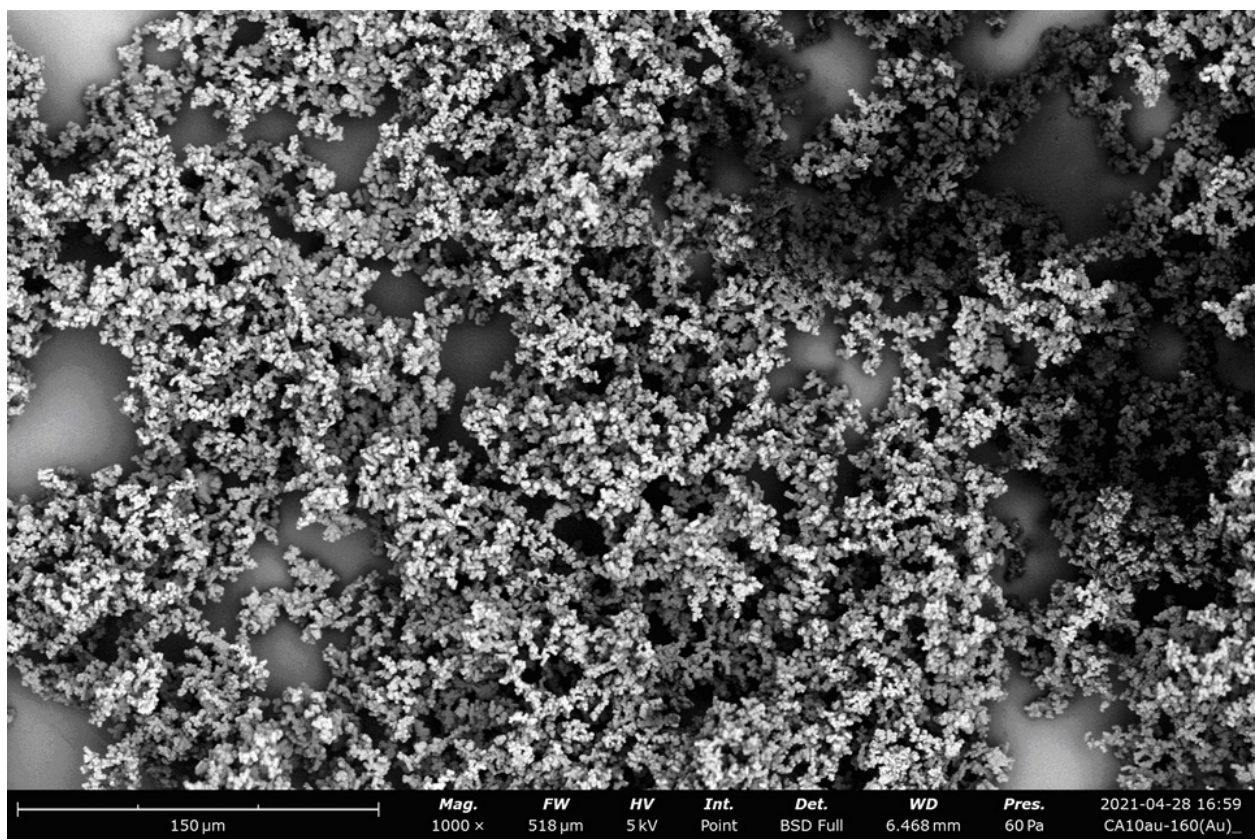


**Fig. S19** SEM images of CAp microcrystals (Table 1, Entry 11).

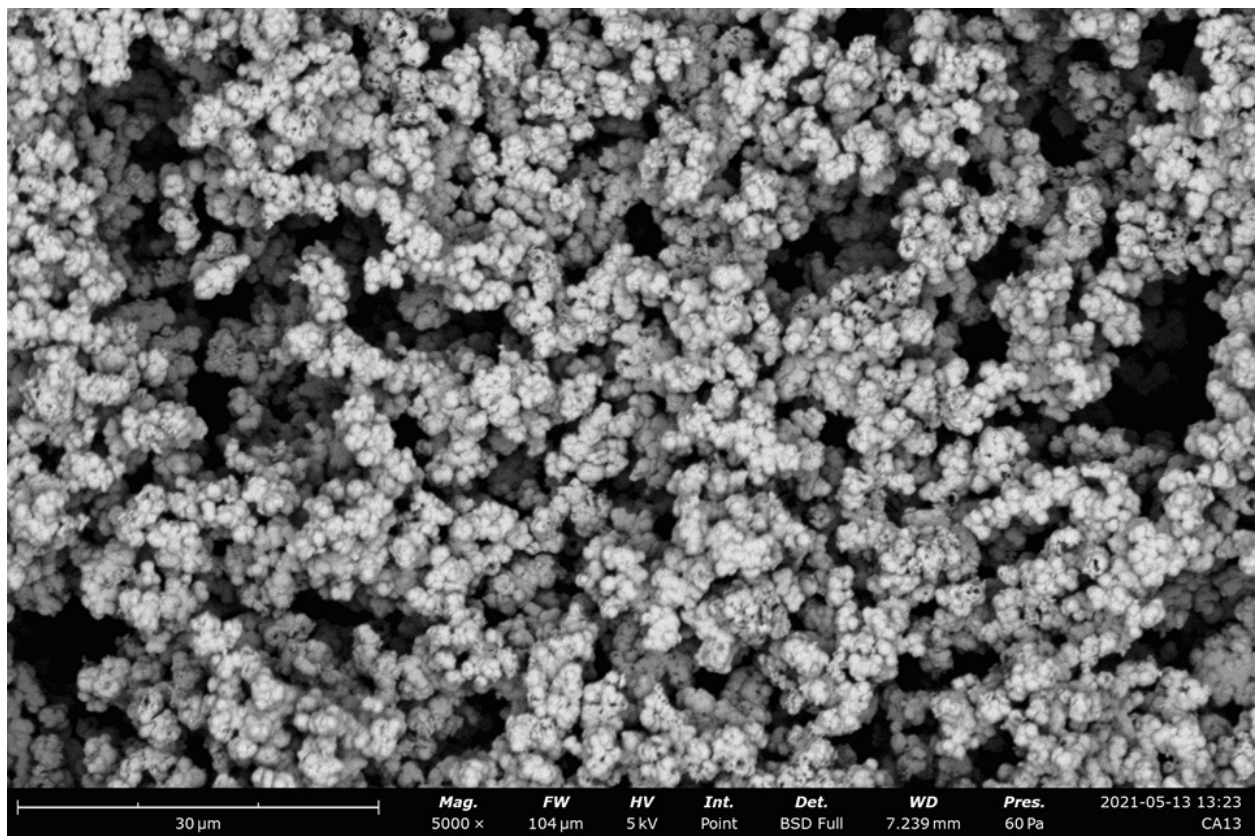
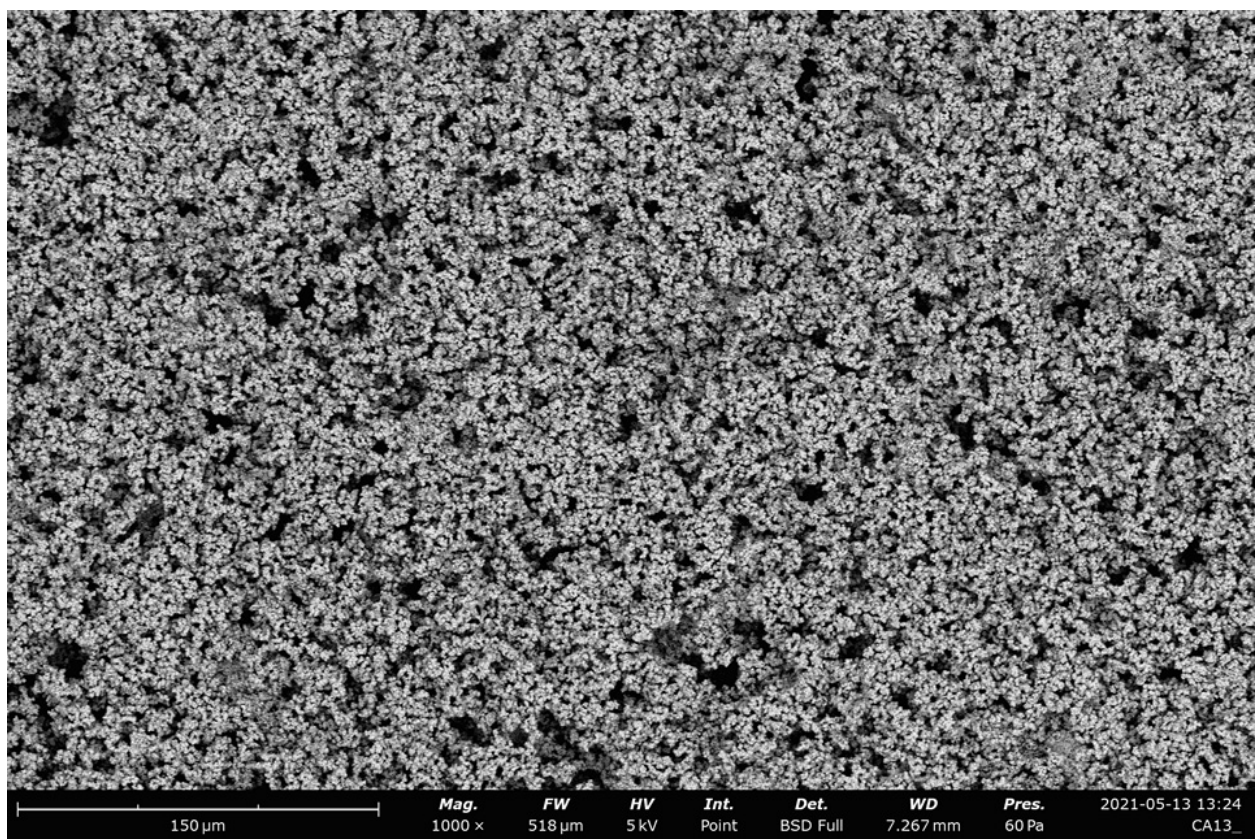


**Fig. S20** SEM images of CAp microcrystals (Table 1, Entry 12).

## S2. XRD studies of CAp samples

Cell parameters were determined by Pawley refinement.

Experimental (blue) and calculated (red) diffractograms, difference curves (gray) and impurity peaks (vertical lines) are presented in figures below.

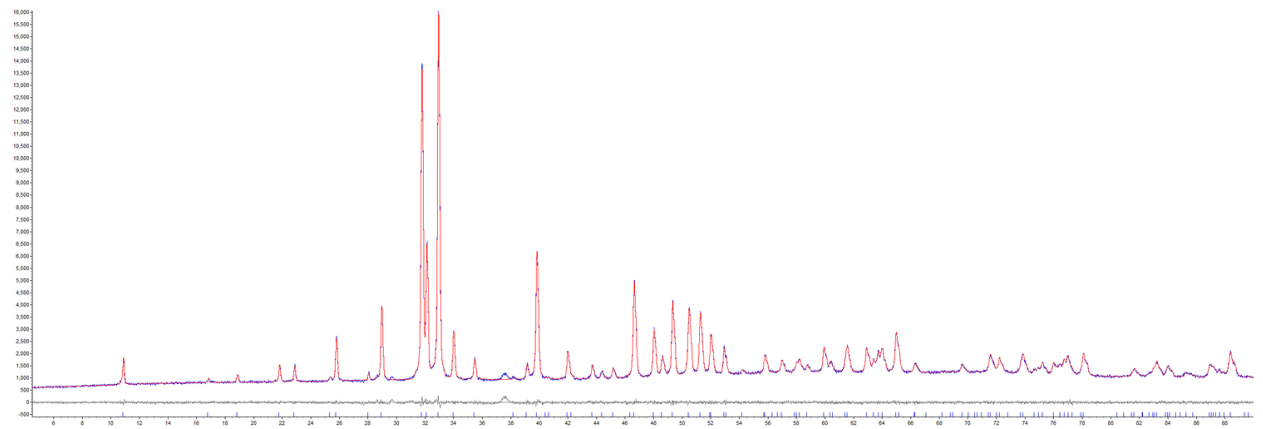


Fig. S21 XRD patterns of CAp (Table 1, Entry 1).

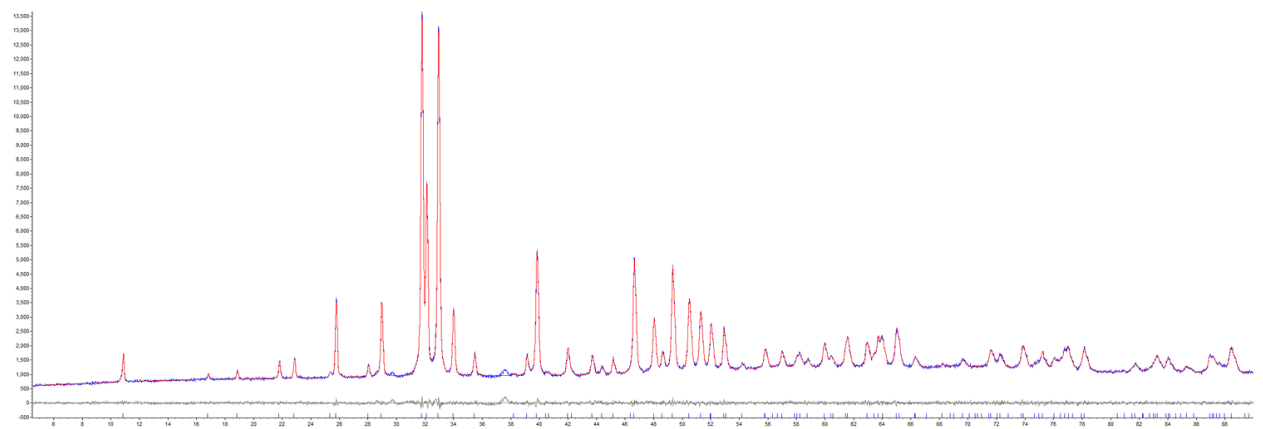


Fig. S22 XRD patterns of CAp (Table 1, Entry 2).

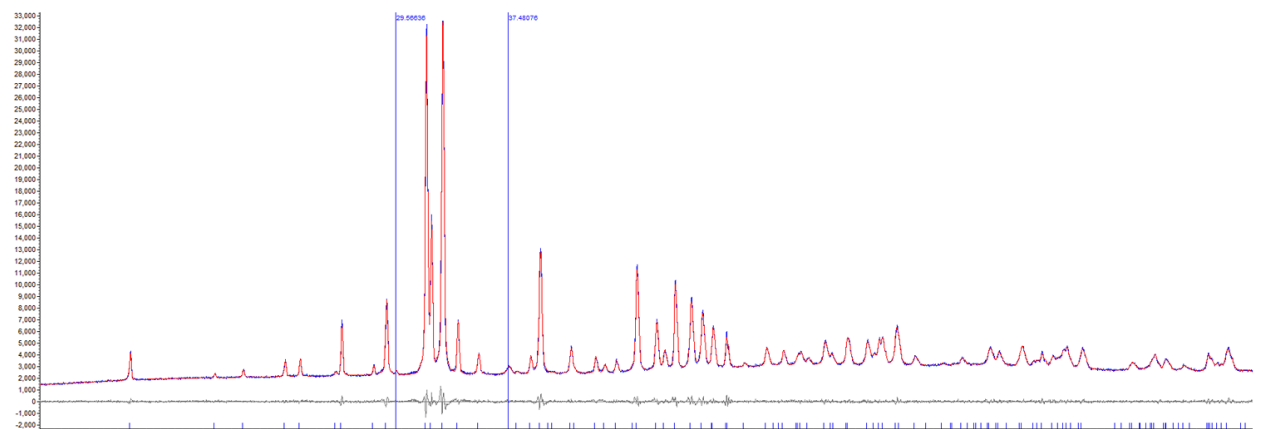
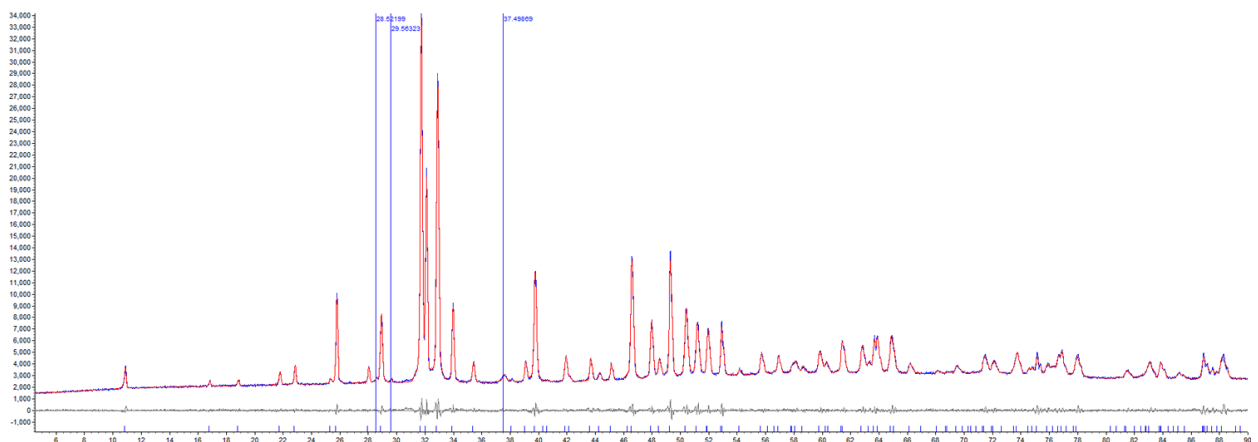
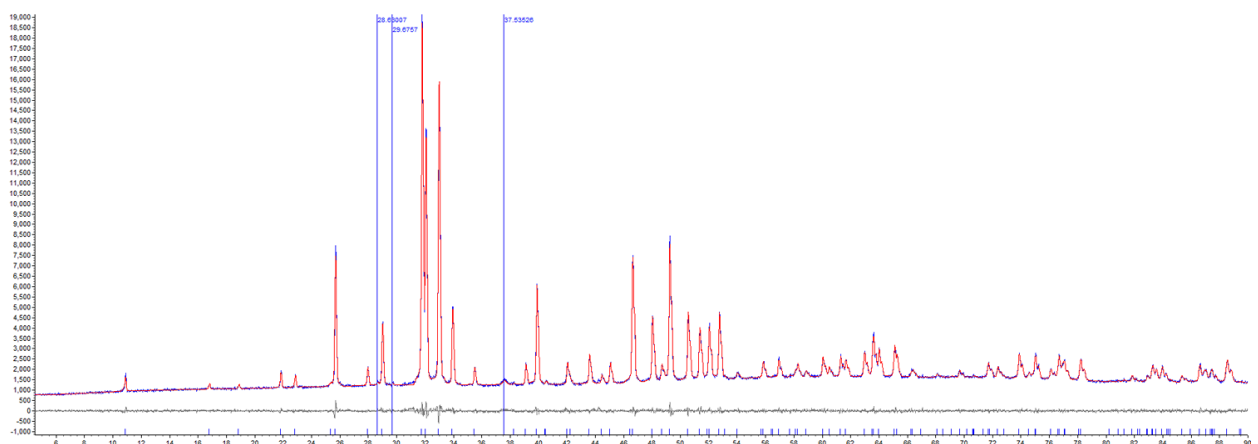


Fig. S23 XRD patterns of CAp (Table 1, Entry 3).



**Fig. S24** XRD patterns of CAp (Table 1, Entry 4).



**Fig. S25** XRD patterns of CAp (Table 1, Entry 5).

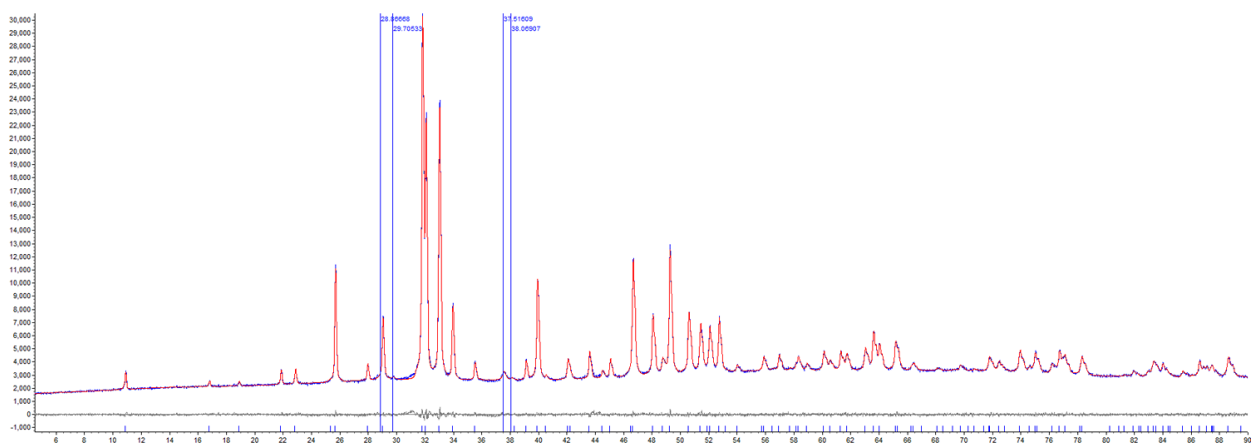


**Fig. S26** XRD patterns of CAp (Table 1, Entry 7).

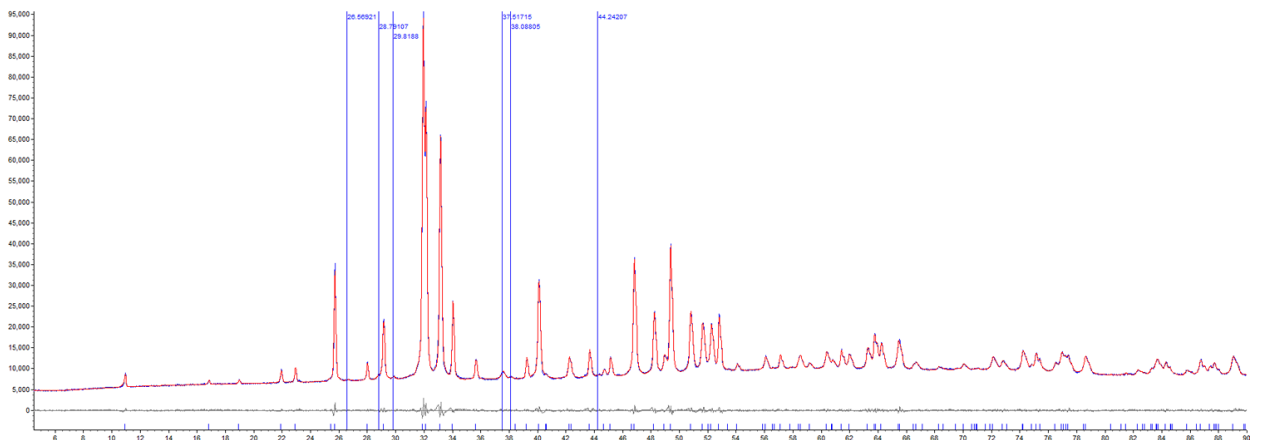


**Fig. S27** XRD patterns of CAp (Table 1, Entry 8).

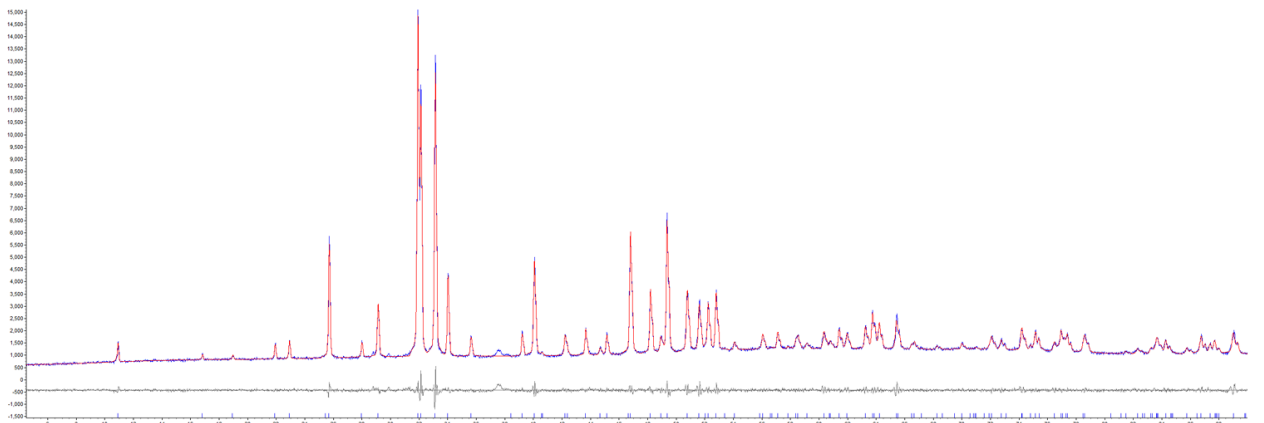


**Fig. S28** XRD patterns of CAp (Table 1, Entry 9).

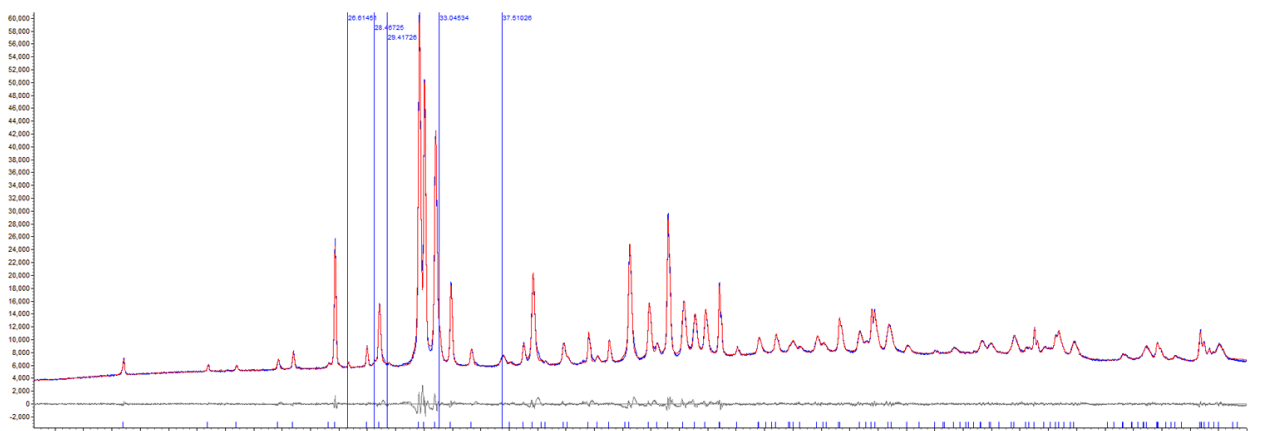


**Fig. S29** XRD patterns of CAp (Table 1, Entry 10).

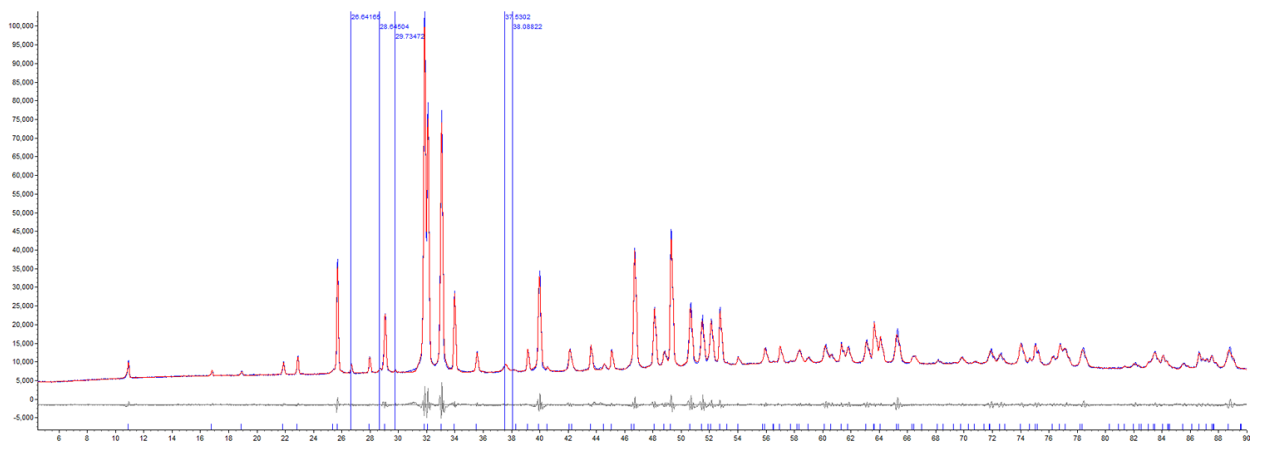


**Fig. S30** XRD patterns of CAp (Table 1, Entry 11).

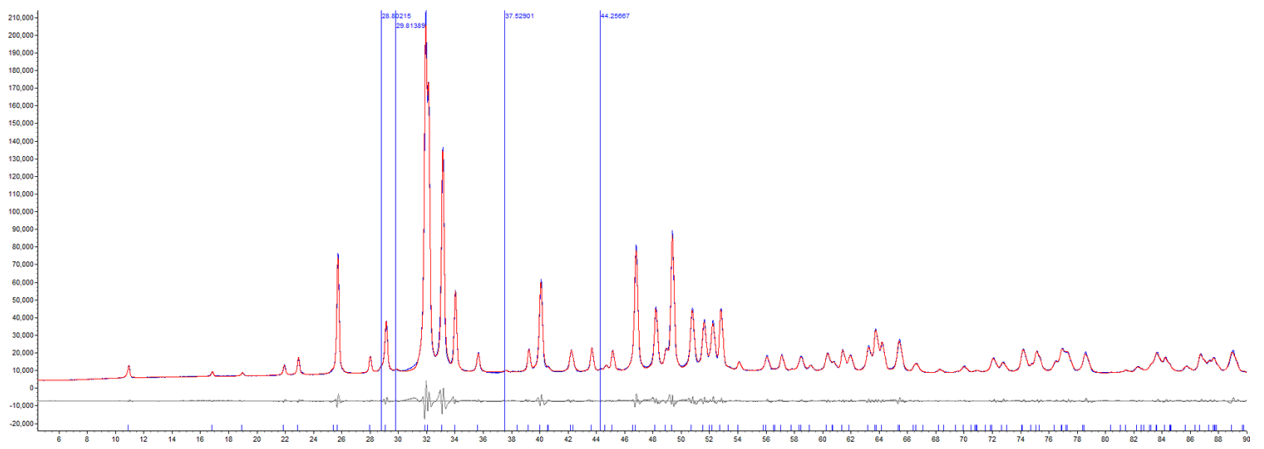


**Fig. S31** XRD patterns of CCap (Table 1, Entry 12).

The XRD data of sample 1 and sintered samples (1-650, 1-850 and 1-1000) are presented in Table S1. XRD patterns of the sintered samples are presented in Figs. S32–S34

**Table S1.** XRD parameters of sintered CAp samples 1

Sample	Phase	$a$ , Å	$b$ , Å	$c$ , Å	CSR, nm
1-650	Buchwaldite	20.518(10)	5.4147(7)	9.1539(10)	63(3)
	HAp	9.4170(3)	–	6.9101(2)	10000
1-850	Buchwaldite	20.388(3)	5.4082(5)	9.1582(7)	10000
	HAp	9.4423(3)	–	6.8982(2)	10000
1-1000	Buchwaldite	20.3940(17)	5.4075(3)	9.1617(4)	10000
	HAp	9.42312(13)	–	6.89531(13)	10000

The sample 1 is single-phase; the compositions of the sintered samples:

1-650: HAp 79.3(5)%; buchwaldite 20.7(5)%

1-850: HAp 81.7(8)%; buchwaldite 18.3(8)%

1-1000: HAp 80(2)%; buchwaldite 20(2)%

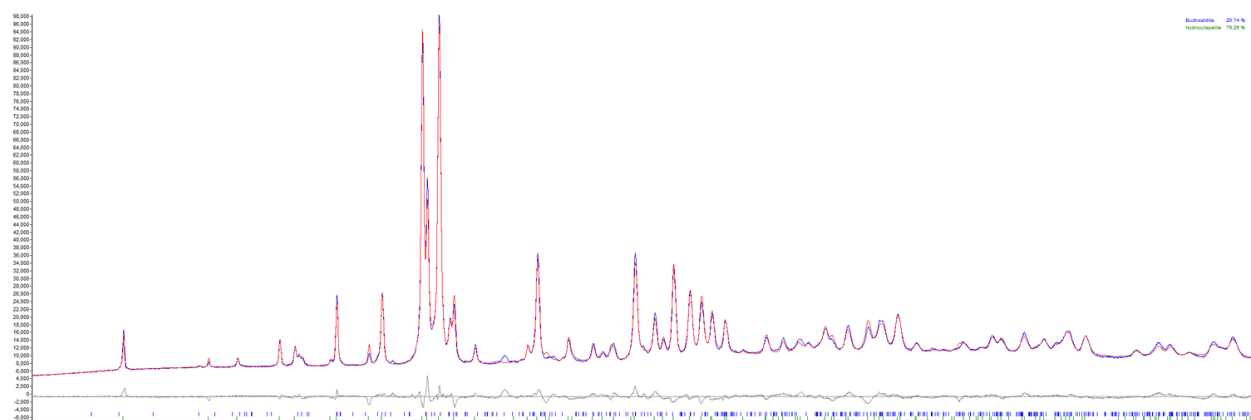


**Fig. S32** XRD patterns of CAp (Table 1, Entry 1), sintered at 650 °C.

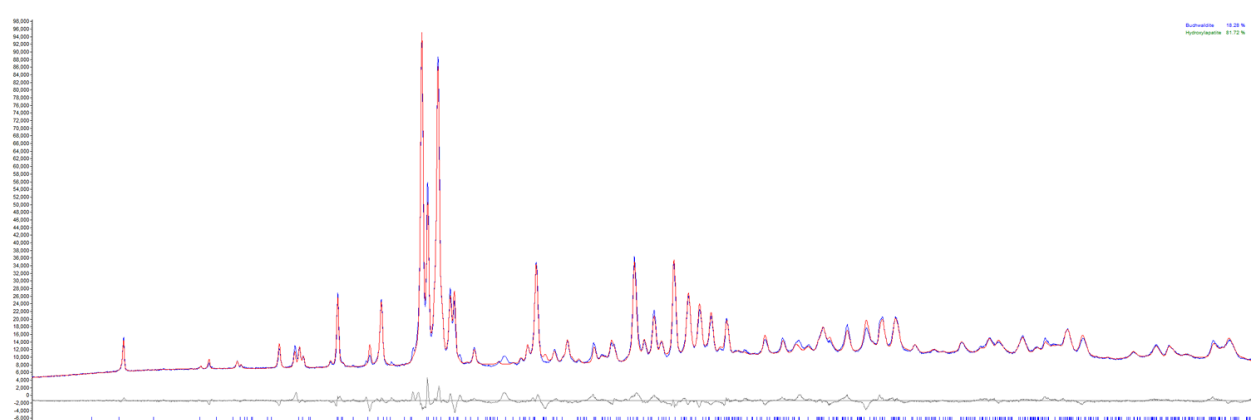


**Fig. S33** XRD patterns of CAp (Table 1, Entry 1), sintered at 850 °C.

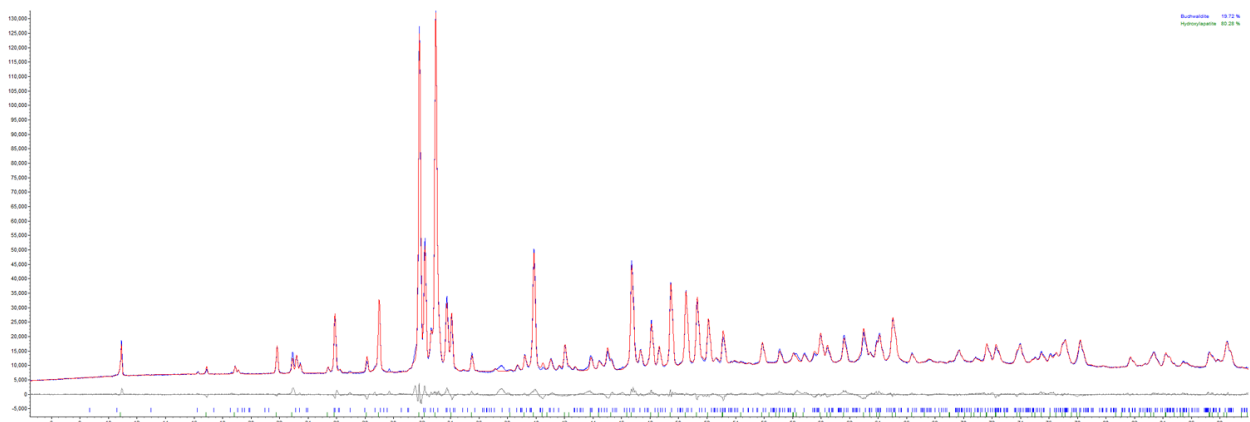


**Fig. S34** XRD patterns of CAp (Table 1, Entry 1), sintered at 1000 °C.

The XRD data of sample 9w and sintered samples (9w-650, 9w-850 and 9w-1000) are presented in Table S2. Corresponding XRD patterns of the sintered samples are presented in Figs. S35–S37

**Table S2.** XRD parameters of CAp sample 12w and sintered samples

Sample	Phase	<i>a</i> , Å	<i>b</i> , Å	<i>c</i> , Å	CSR, nm
12w	HAp	9.36588(4)	–	6.93218(9)	10000
12w-650	HAp	9.37839(8)	–	6.91916(19)	1200(500)
12w-850	Buchwaldite	21.235(4)	5.2834(5)	9.136(3)	10000
	HAp	9.4102(2)	–	6.89218(17)	10000
	CaO	4.8081(2)	–	–	79(4)
12w-1000	Buchwaldite	20.5615(15)	5.3830(4)	9.1425(6)	10000
	HAp	9.41161(15)	–	6.89087(11)	10000
	CaO	4.8080(2)	–	–	89(6)

The sample 9-650 contains minimal amount of buchwaldite; the compositions of the samples, sintered at higher temperatures:

9-850: HAp 78.7(4)%; buchwaldite 17.4(4)%; CaO 3.86(10)%

9-1000: HAp 65.6(5)%; buchwaldite 31.3(5)%; CaO 3.05(8)%

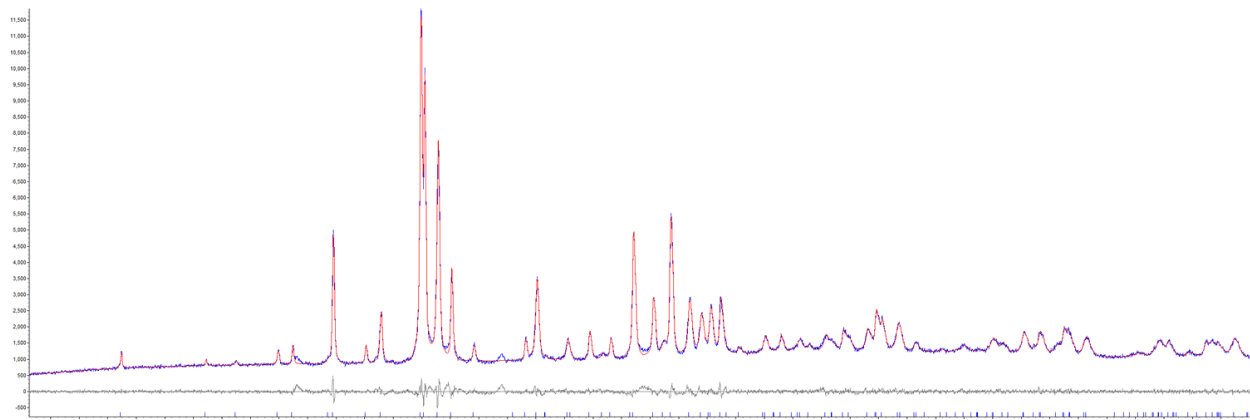


**Fig. S35** XRD patterns of CAp (Table 1, Entry 9w), sintered at 650 °C.

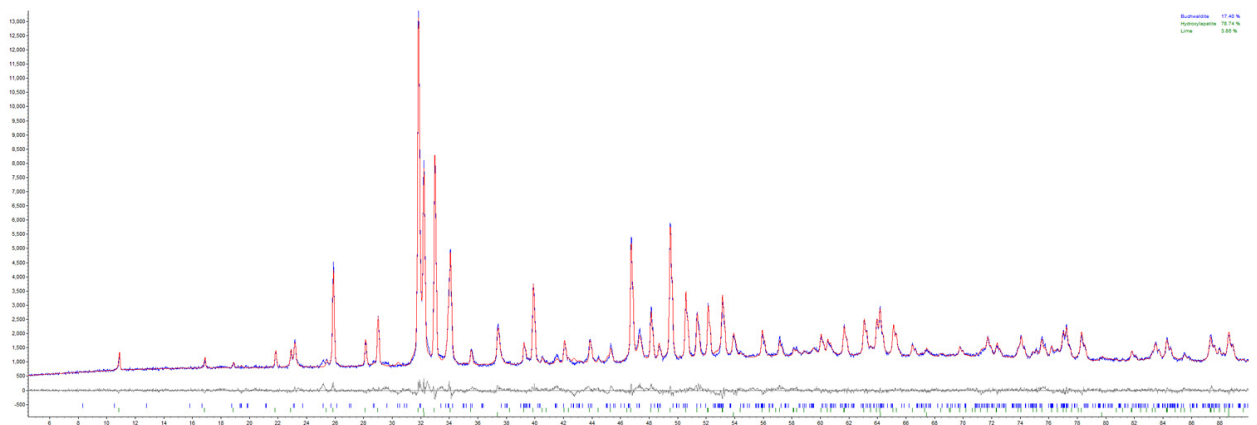


**Fig. S36** XRD patterns of CAp (Table 1, Entry 9), sintered at 850 °C.

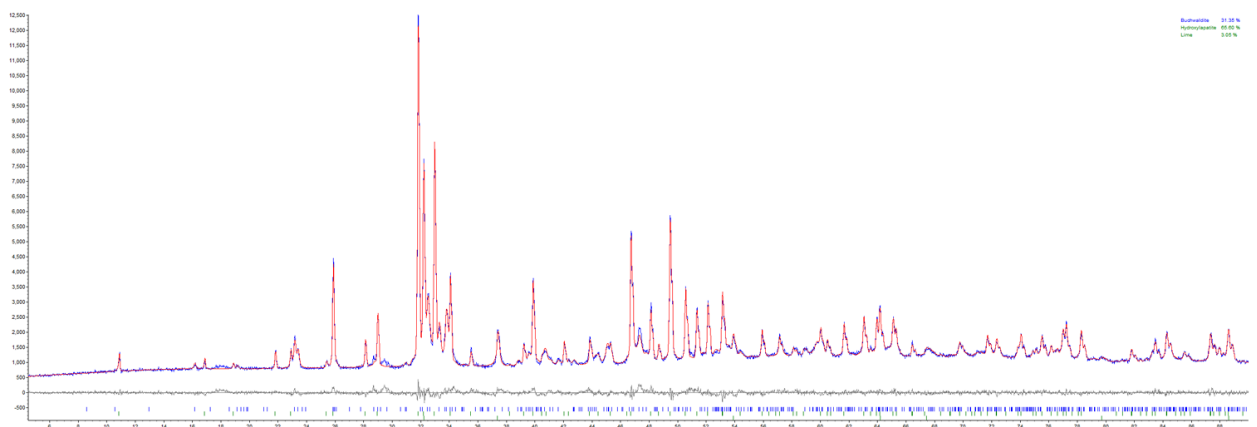


**Fig. S37** XRD patterns of CAp (Table 1, Entry 9), sintered at 1000 °C.

### S3. FT-IR spectra of CAp samples

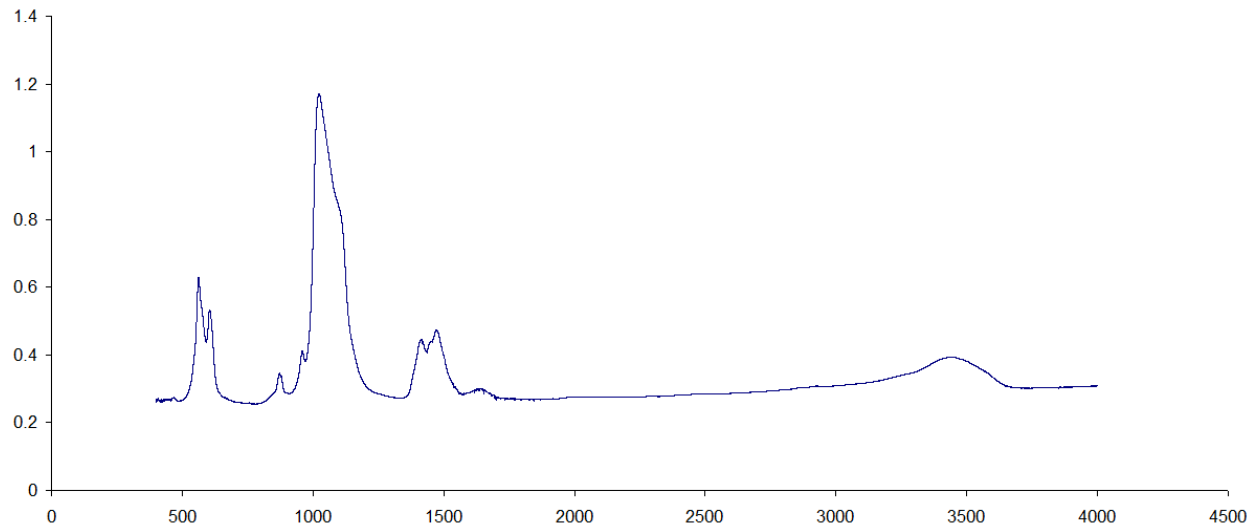


**Fig. S38** FT-IR spectrum of CAp (Table 1, Entry 1).

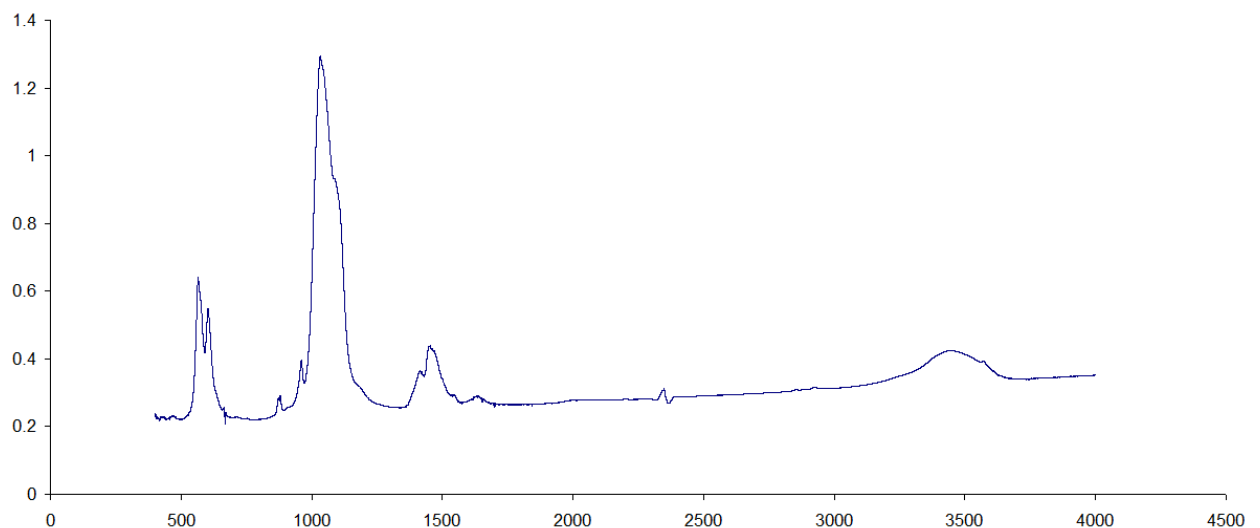


**Fig. S39** FT-IR spectrum of CAp (Table 1, Entry 1), sintered at 650 °C.

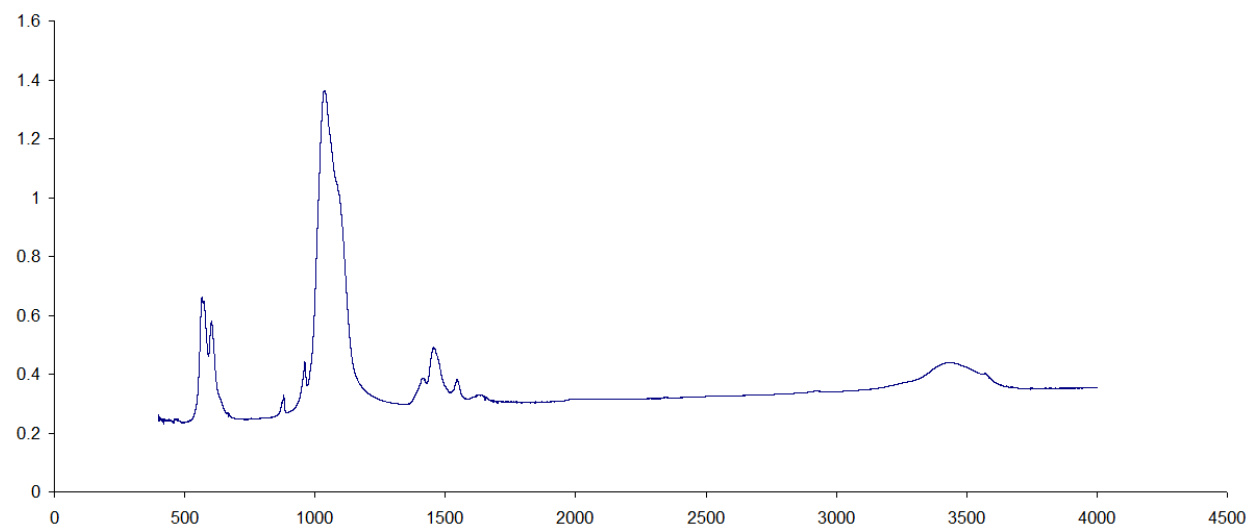


**Fig. S40** FT-IR spectrum of CAp (Table 1, Entry 1) , sintered at 850 °C.

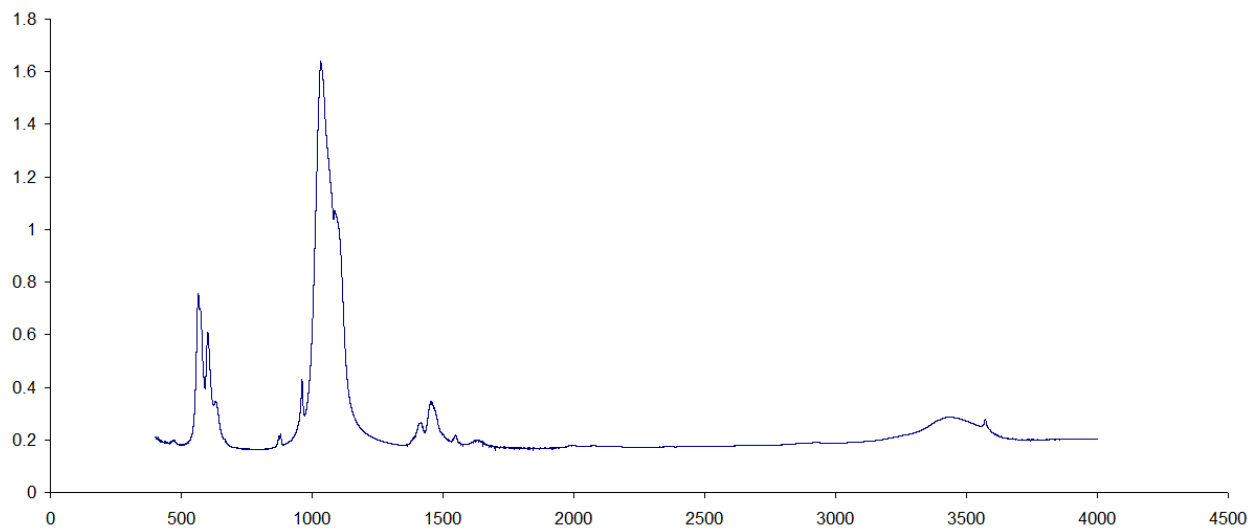


**Fig. S41** FT-IR spectrum of CAp (Table 1, Entry 1) , sintered at 1000 °C.

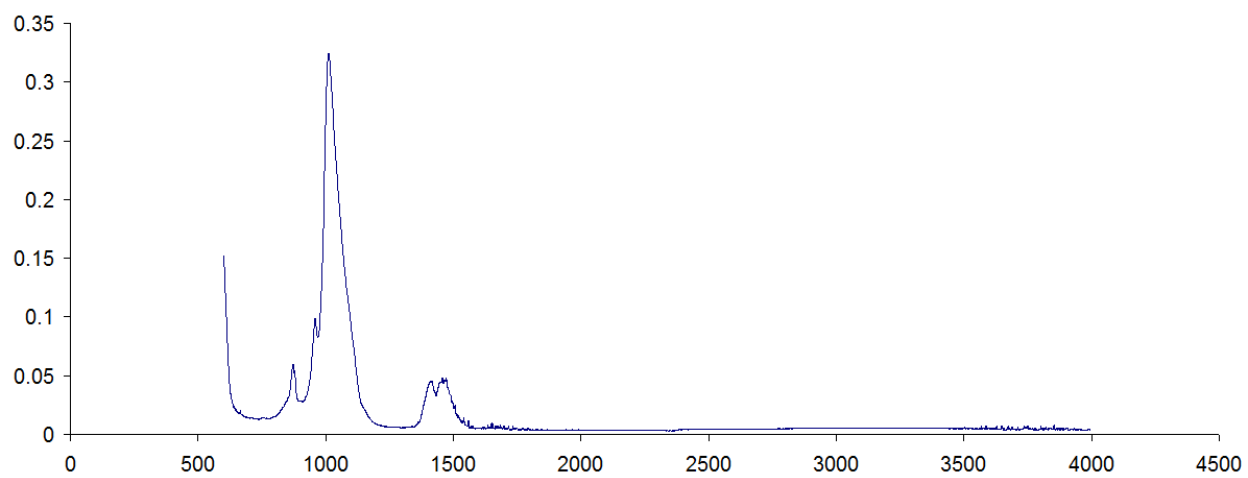


**Fig. S42** FT-IR spectrum of CAp (Table 1, Entry 2).

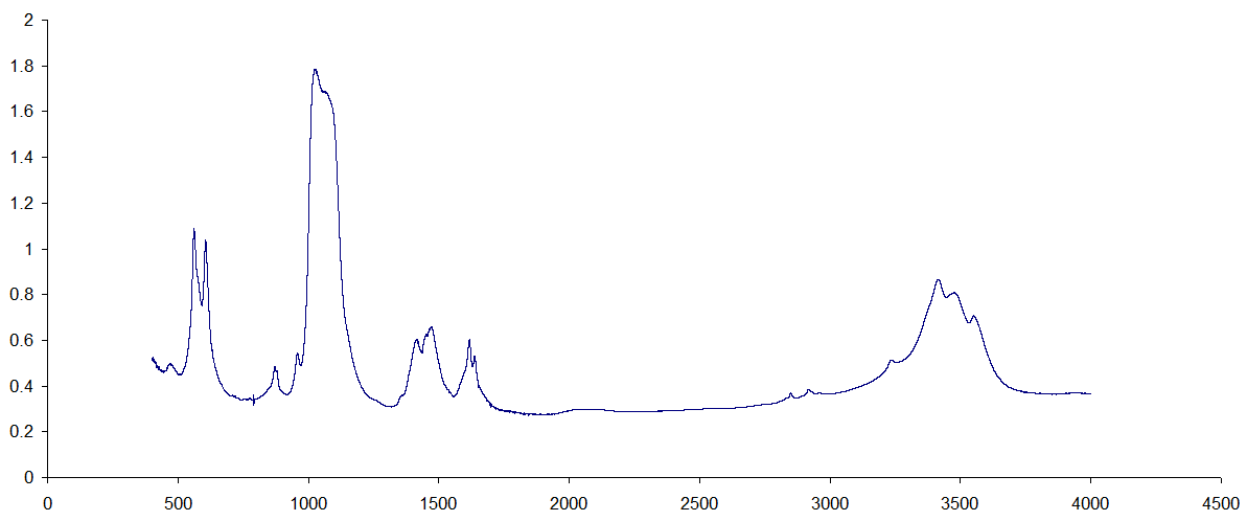


**Fig. S43** FT-IR spectrum of CAp (Table 1, Entry 3).

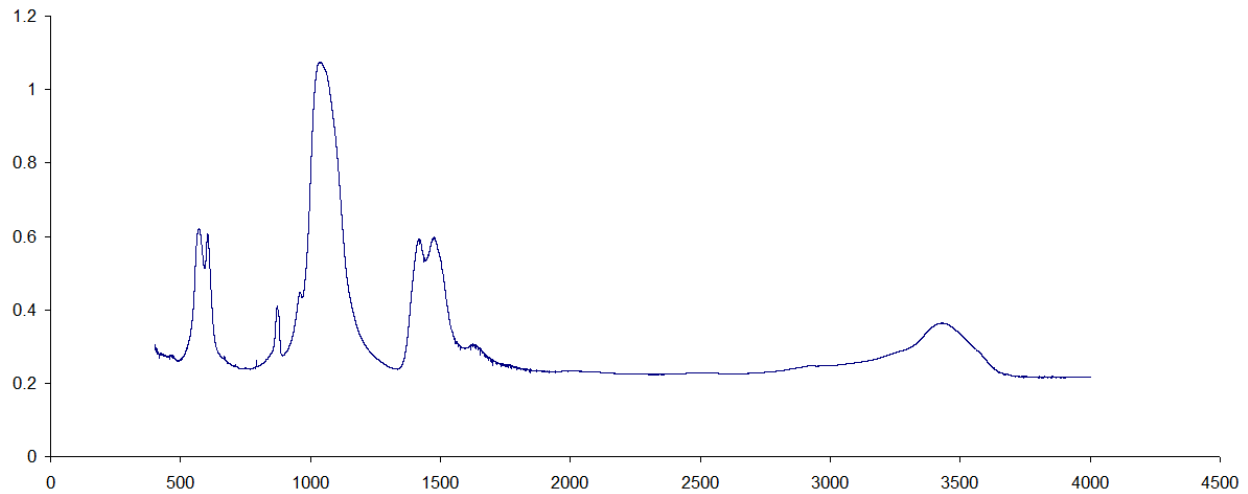


**Fig. S44** FT-IR spectrum of CAp (Table 1, Entry 4).

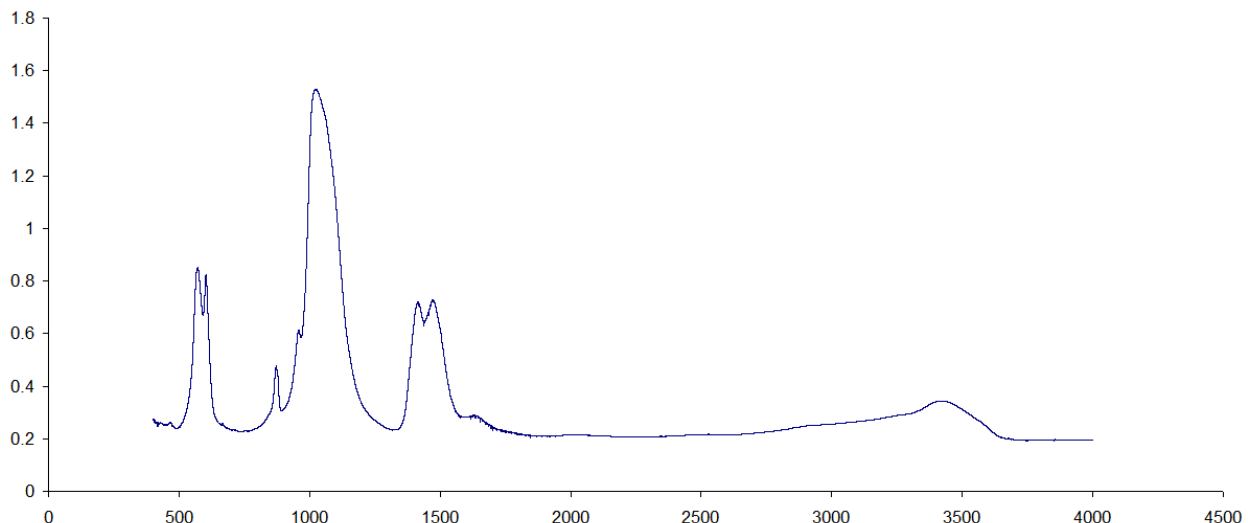


**Fig. S45** FT-IR spectrum of CAp (Table 1, Entry 5).

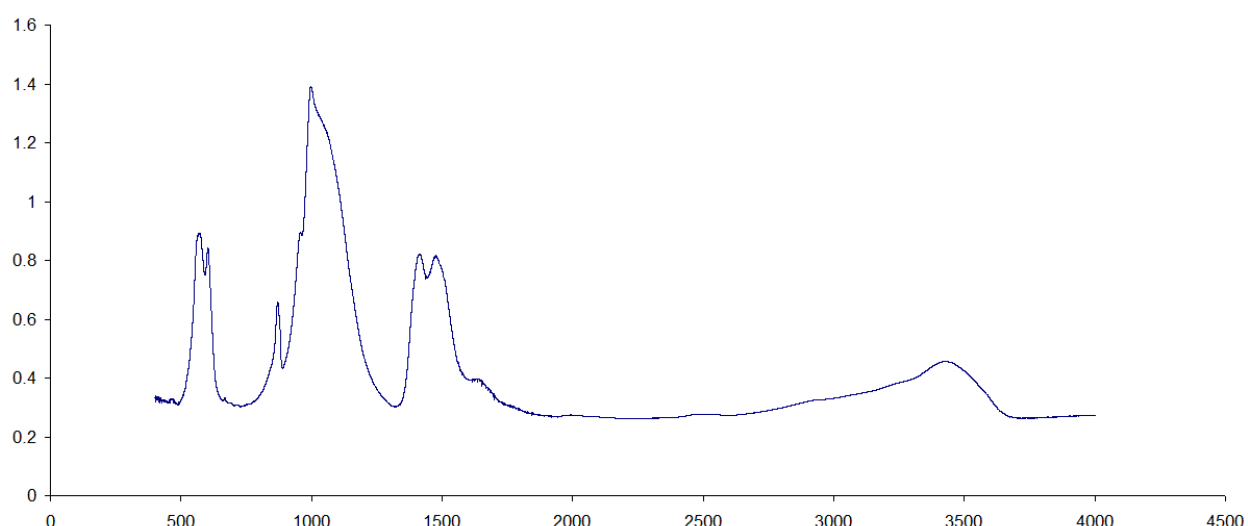


**Fig. S46** FT-IR spectrum of CAp (Table 1, Entry 7).

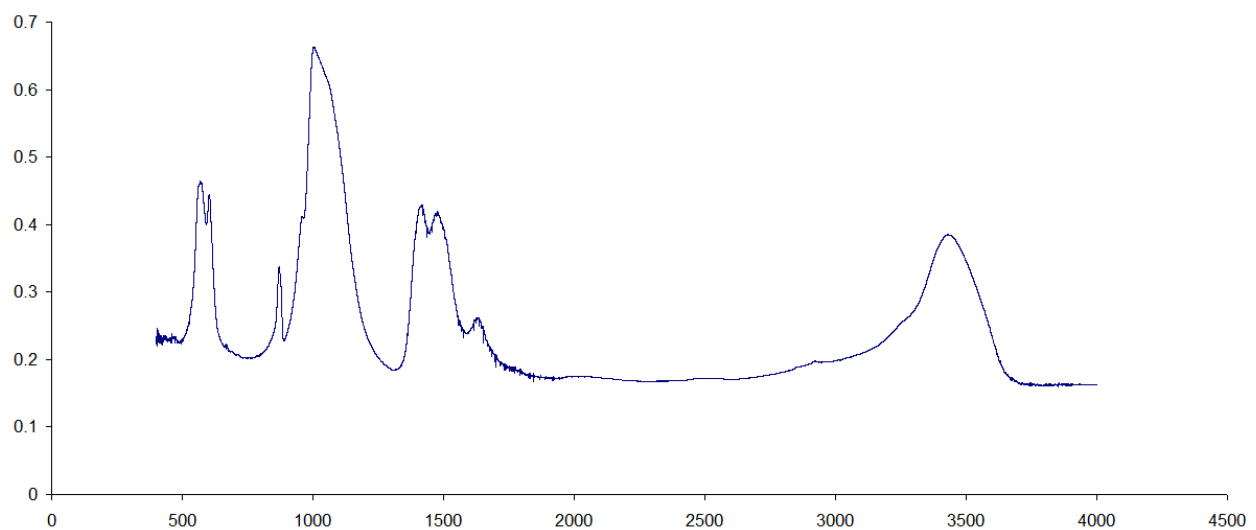


**Fig. S47** FT-IR spectrum of CAp (Table 1, Entry 8).

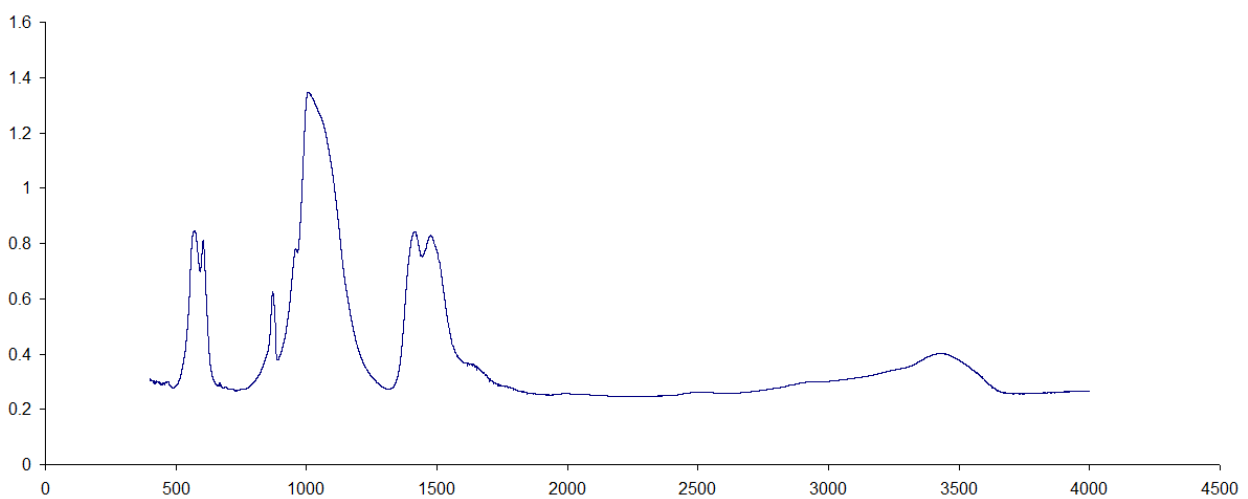


**Fig. S48** FT-IR spectrum of CAp (Table 1, Entry 9).

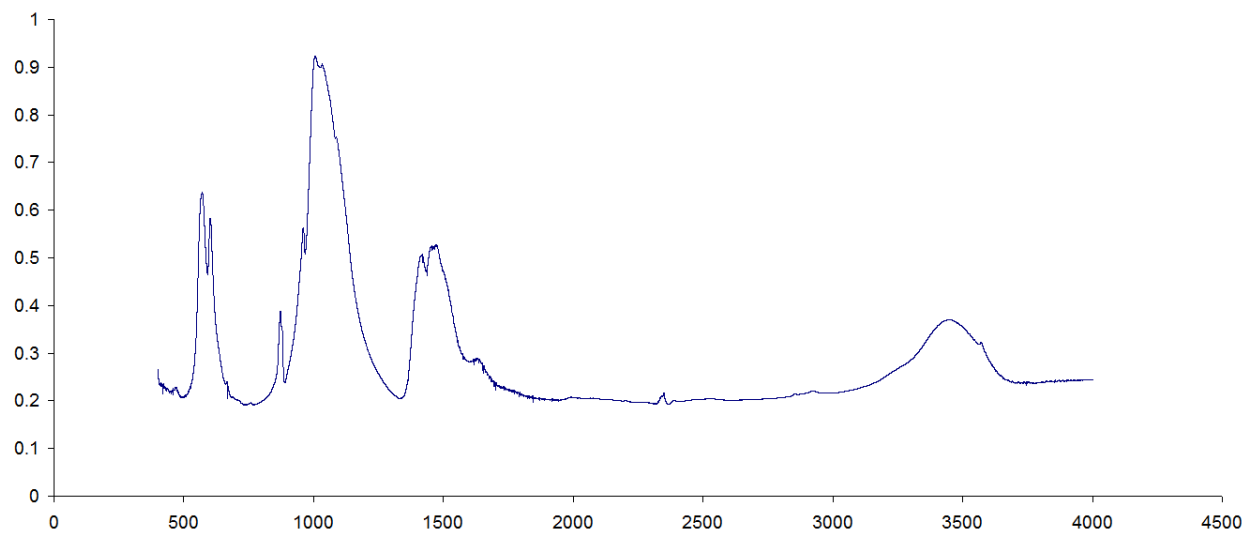


**Fig. S49** FT-IR spectrum of CAp (Table 1, Entry 9), sintered at 650 °C.

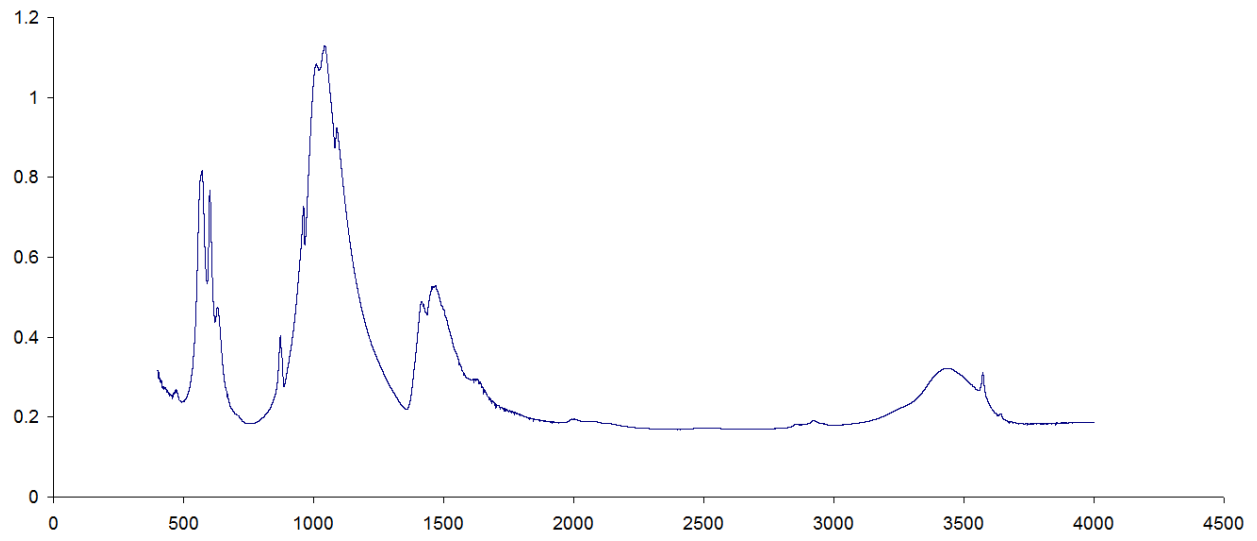


**Fig. S50** FT-IR spectrum of CAp (Table 1, Entry 9), sintered at 850 °C.

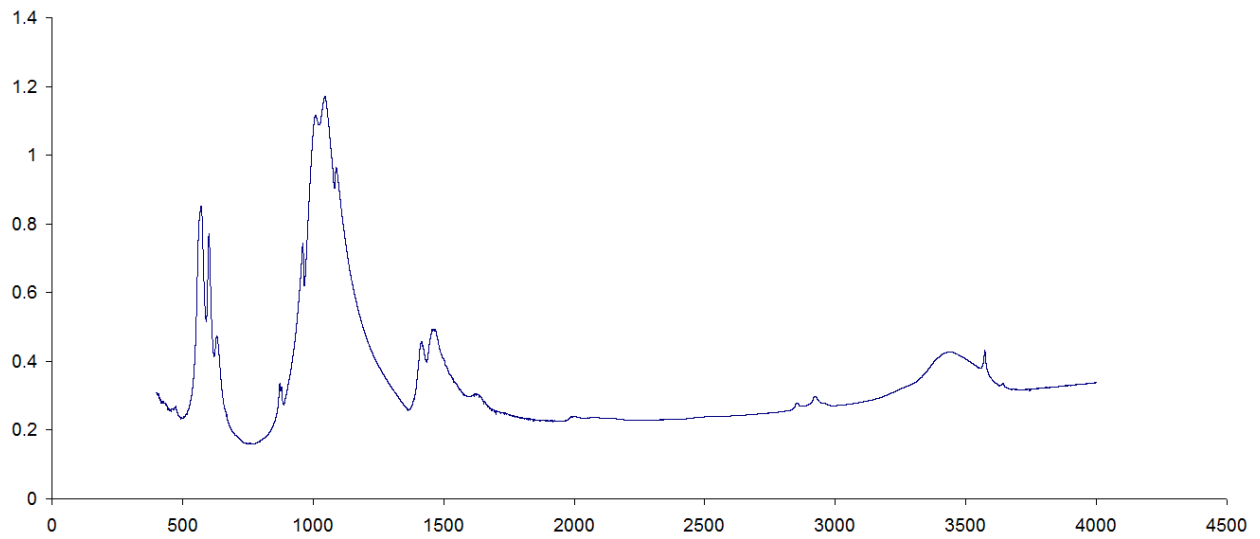


**Fig. S51** FT-IR spectrum of CAp (Table 1, Entry 9), sintered at 1000 °C.

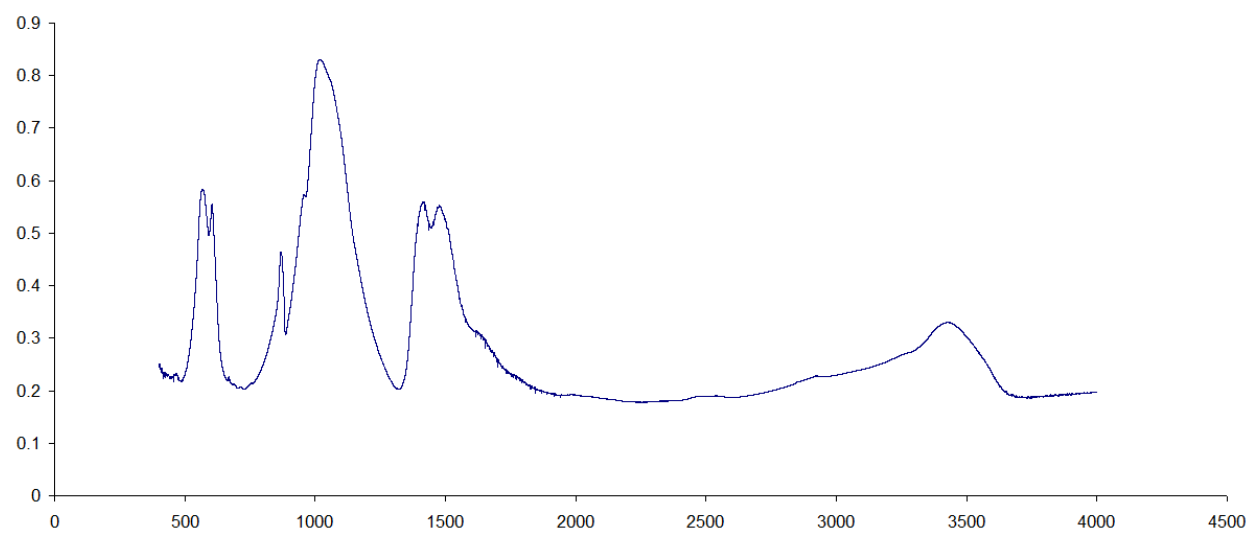


**Fig. S52** FT-IR spectrum of CAp (Table 1, Entry 10).

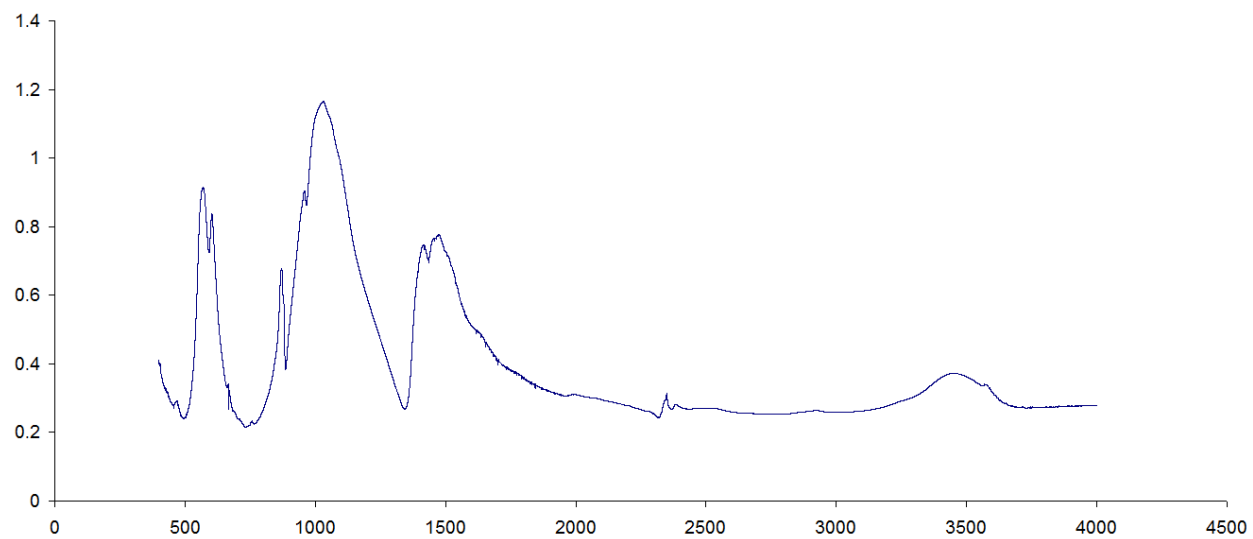


**Fig. S53** FT-IR spectrum of CAp (Table 1, Entry 10) , sintered at 650 °C.

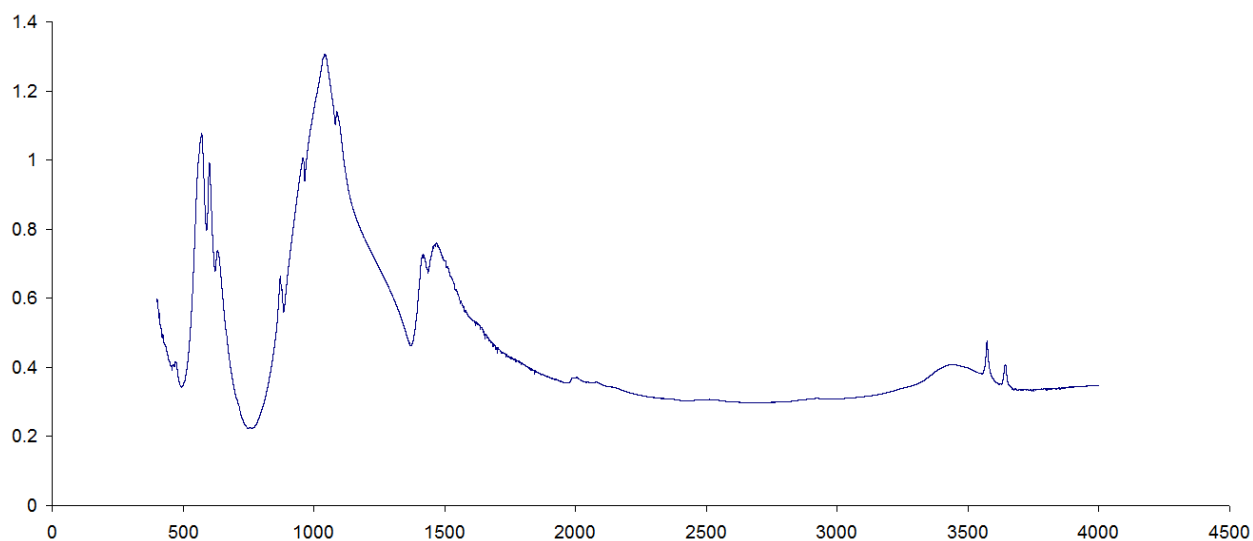


**Fig. S54** FT-IR spectrum of CAp (Table 1, Entry 10) , sintered at 850 °C.

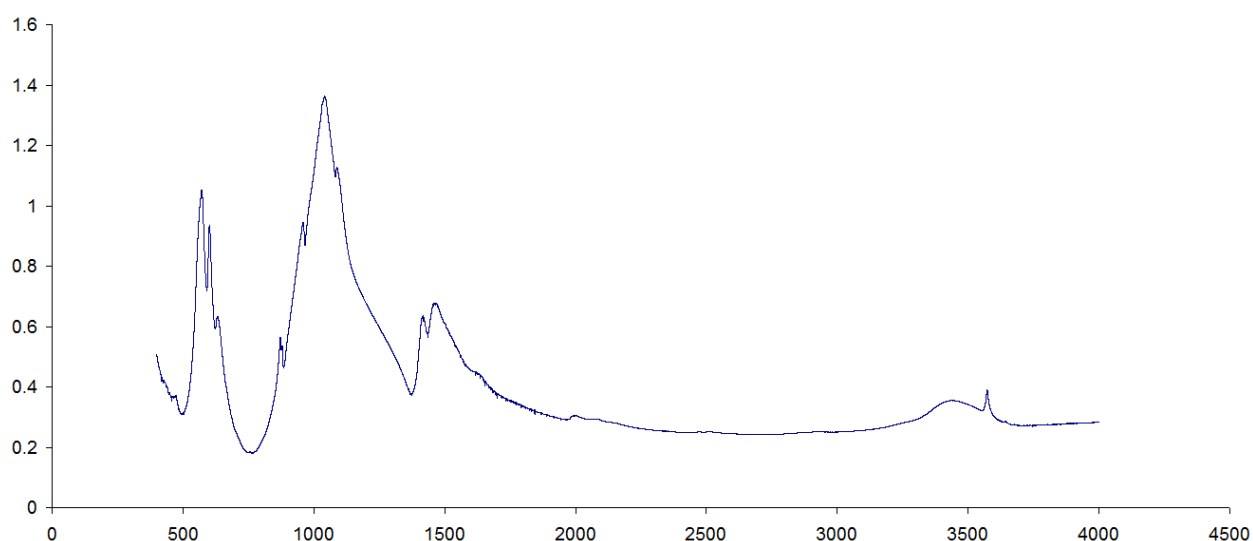


**Fig. S55** FT-IR spectrum of CAp (Table 1, Entry 10) , sintered at 1000 °C.

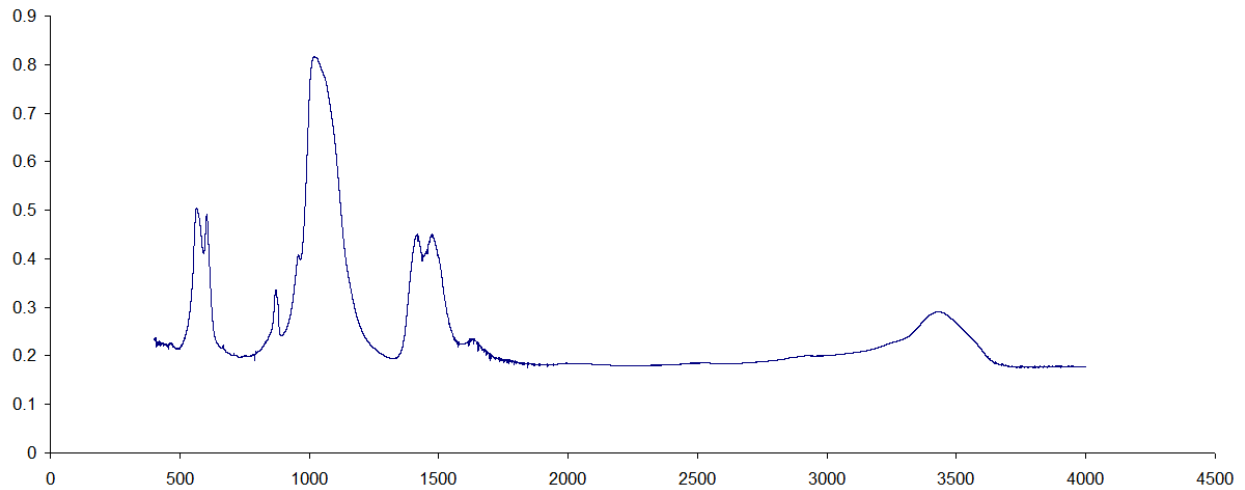


**Fig. S56** FT-IR spectrum of CAp (Table 1, Entry 11).

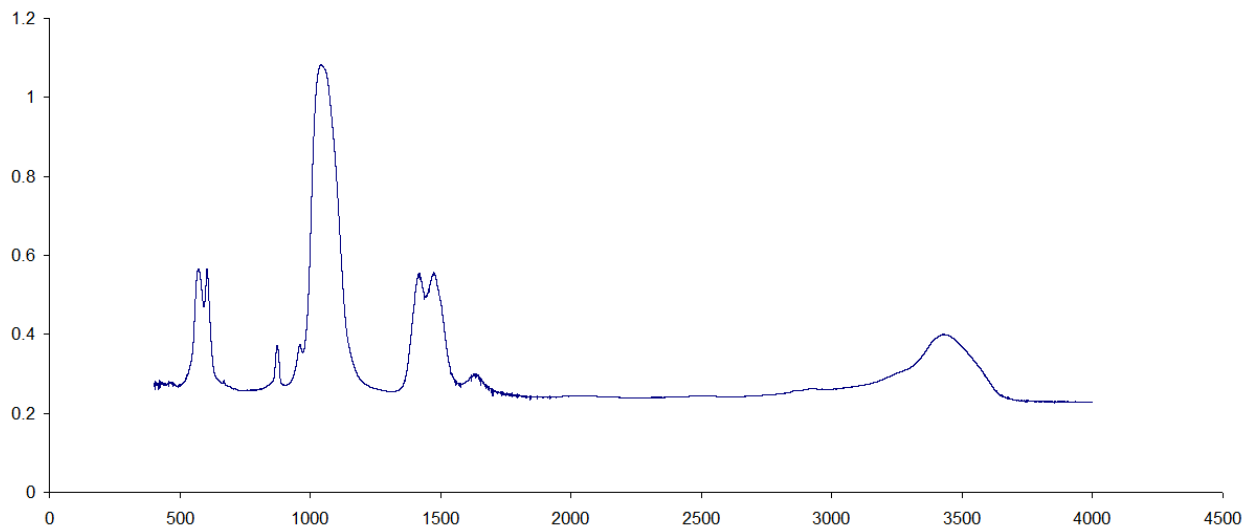


**Fig. S57** FT-IR spectrum of CAp (Table 1, Entry 12).

#### S4. Thermal studies of CAp samples

For CAp sample 1 in TGA curve (Fig. S58) we observe two marked areas of the mass loss. Two sharp peaks at DTG curve are matched to TGA plot. The peak at 425 °C correspond to dehydration process, and high temperature peak at 682 °C and less marked peak at 838 °C relate to CO<sub>2</sub> elimination.

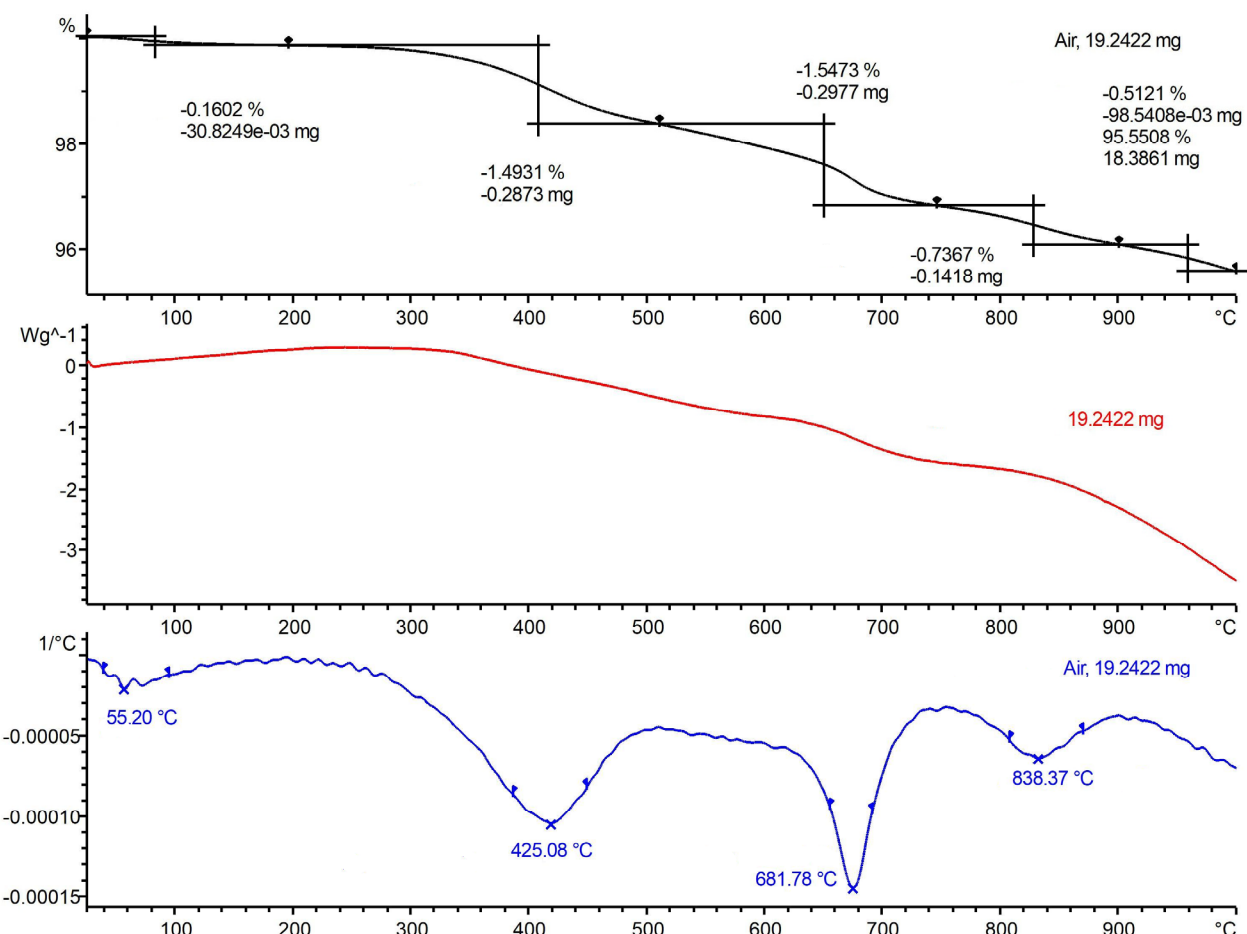
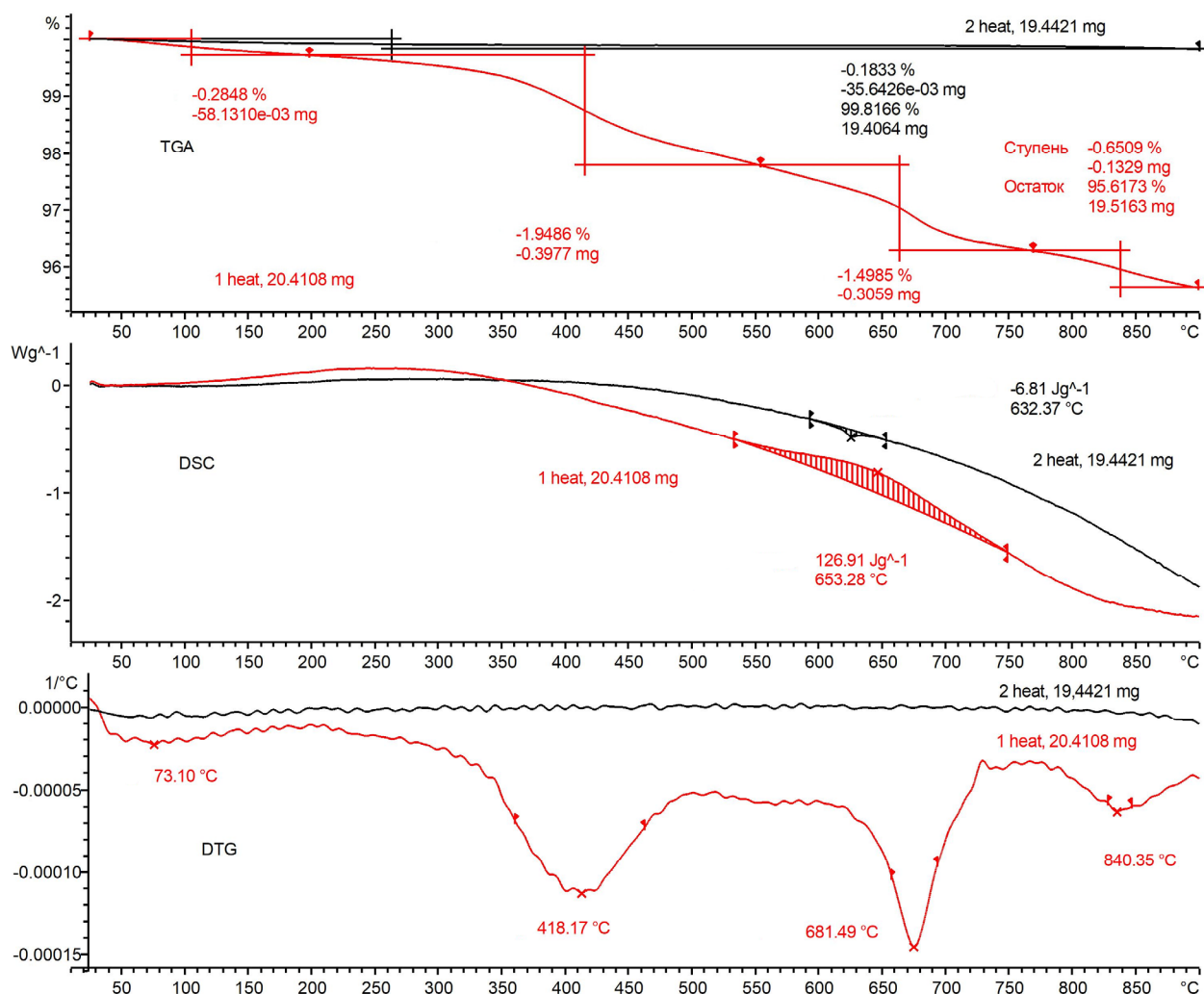


Fig. S58 TGA (black), DSC (red), and DTG (blue) plots of CAp (Table 1, Entry 1).

After the first heat and cooling in nitrogen atmosphere, CAp sample 1 has remained stable during the second heat (Fig. S59). Exotherm, detected in DSC plot (peak at 653 °C), may be attributed to the formation of new crystalline phase (buchwaldite?).



**Fig. S59** TGA (top), DSC (middle), and DTG (bottom) plots of CAp (Table 1, Entry 1), first and second heat.

After sintering at 650 °C and cooling in wet air atmosphere, CAp sample 1 demonstrates lower content of the absorbed water, high temperature peak in DTG plot (852 °C) is becoming a major (Fig. S60). The samples. sintered at 850 °C (Fig. S61) and at 1000 °C (Fig. S62), demonstrate similar behaviour.

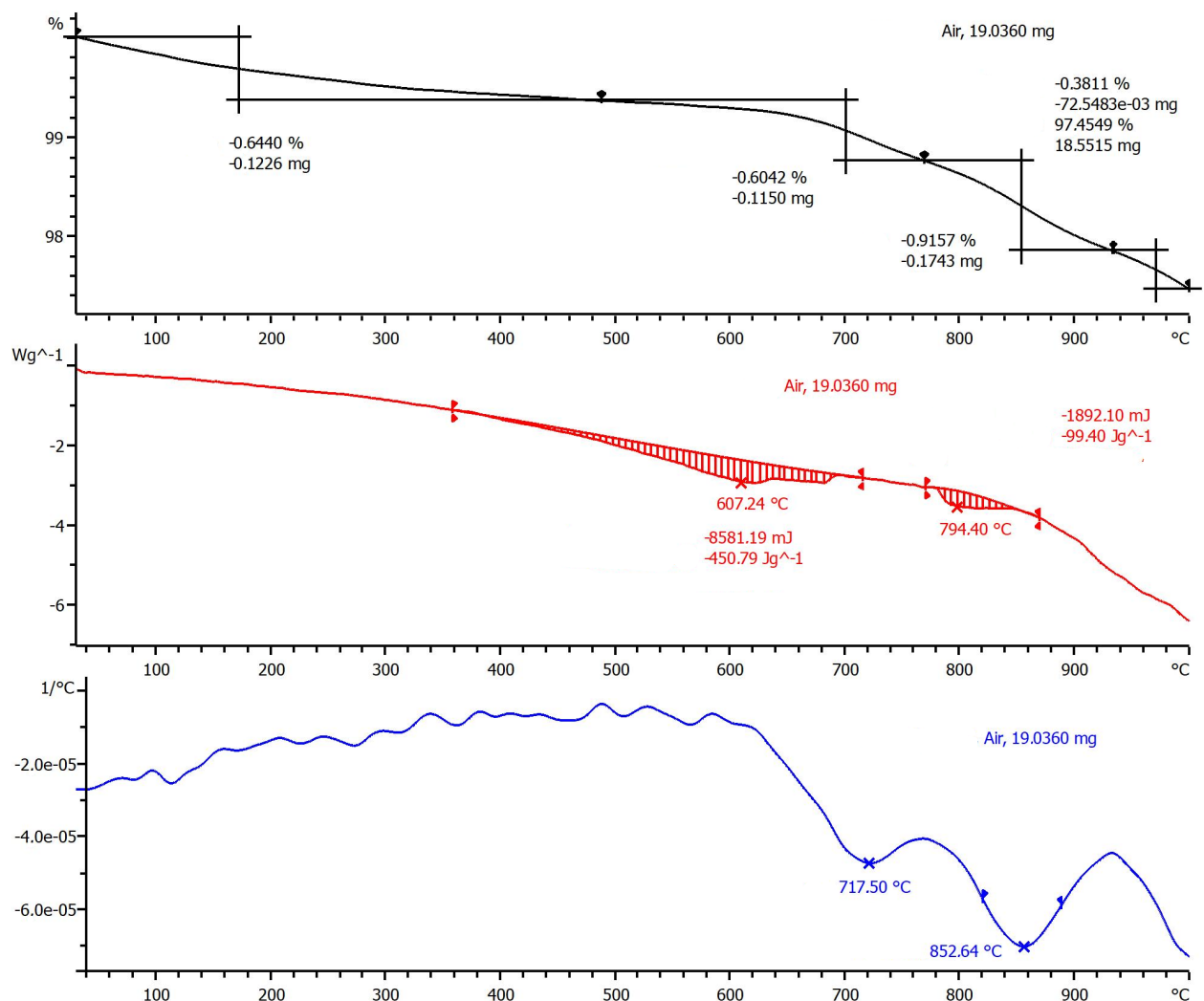


**Fig. S60** TGA (black), DSC (red), and DTG (blue) plots of CAp (Table 1, Entry 1), sintered at 650 °C.

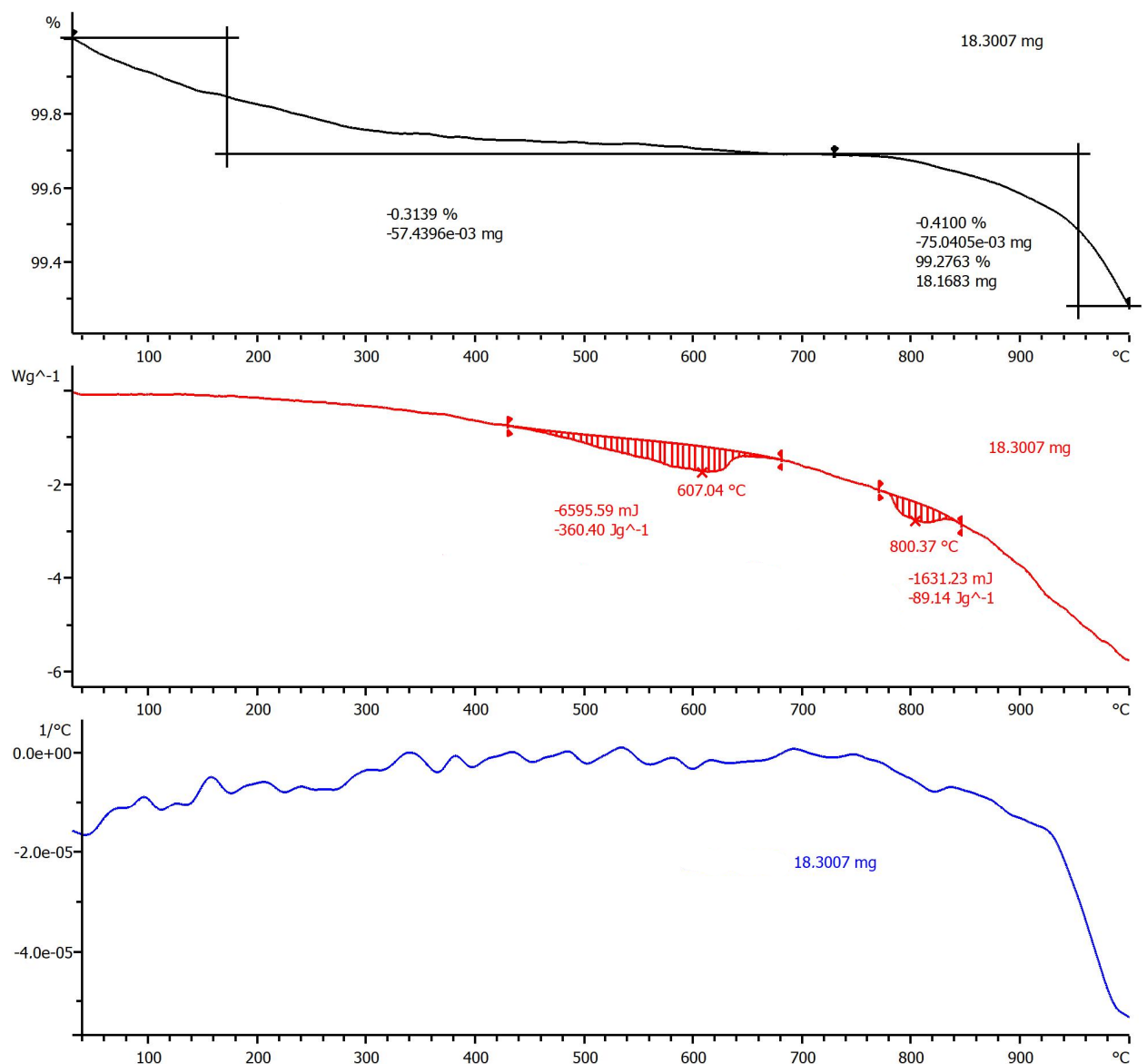


**Fig. S61** TGA (black), DSC (red), and DTG (blue) plots of CAp (Table 1, Entry 1), sintered at 850 °C.

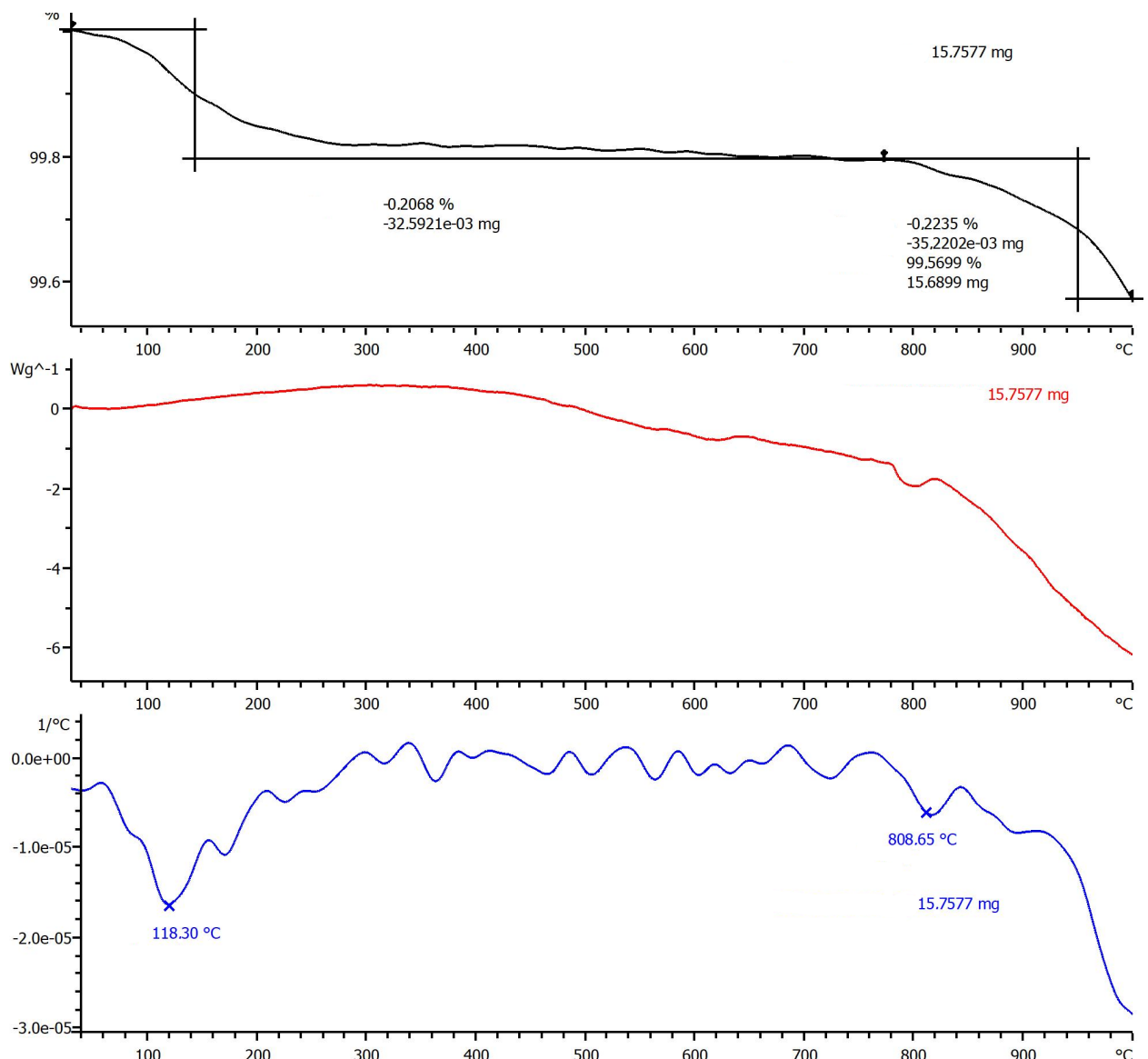


**Fig. S62** TGA (black), DSC (red), and DTG (blue) plots of CAp (Table 1, Entry 1), sintered at 1000 °C.

For perfectly shaped CAp sample with rod-like morphology we observe a series of dehydration peaks (Fig. S63).

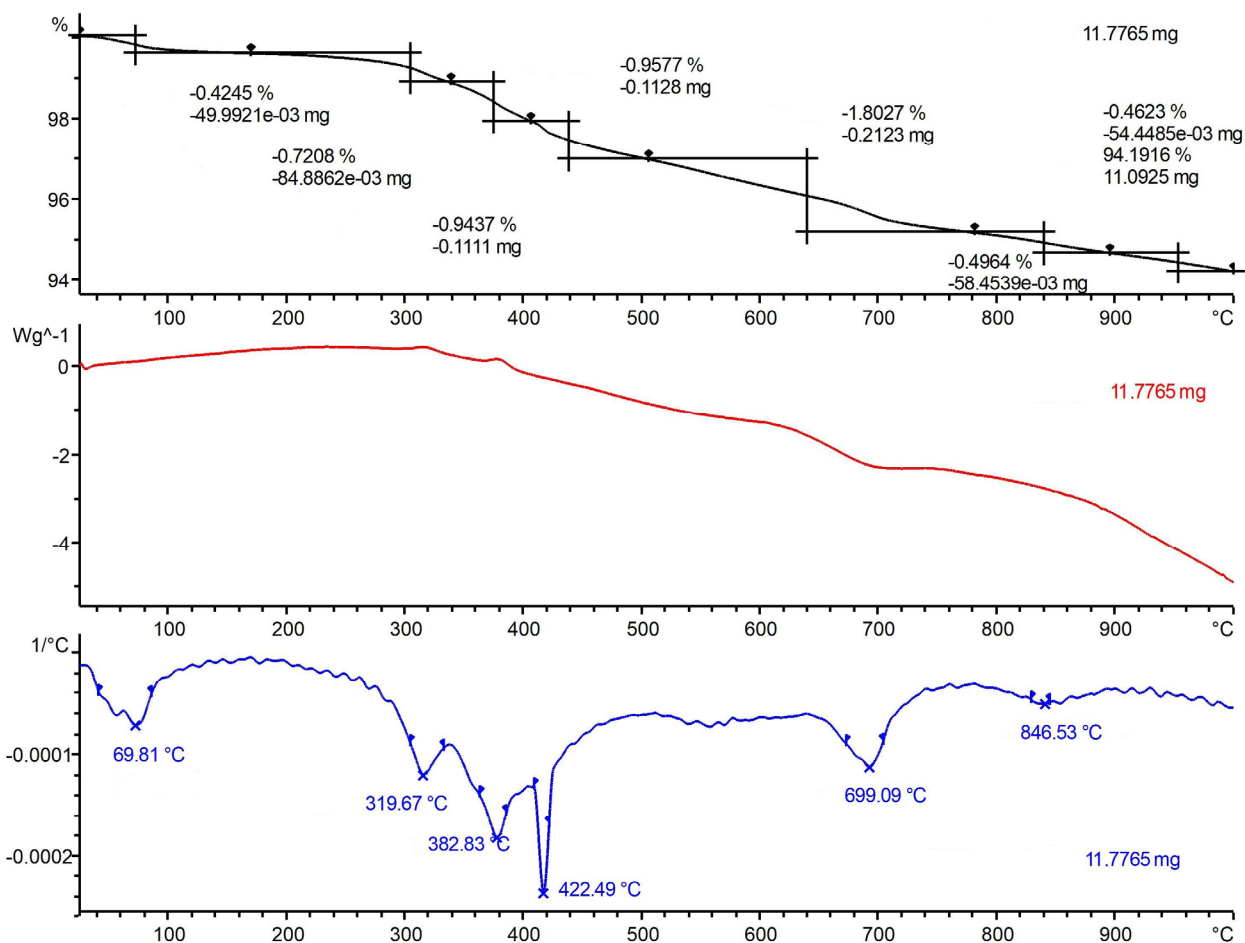


**Fig. S63** TGA (black), DSC (red), and DTG (blue) plots of CAp (Table 1, Entry 3).

For CAp sample with rod-like morphology and substantially lower crystallite size (~5  $\mu\text{m}$ ) dehydration is proceeding smoothly (Fig. S64).

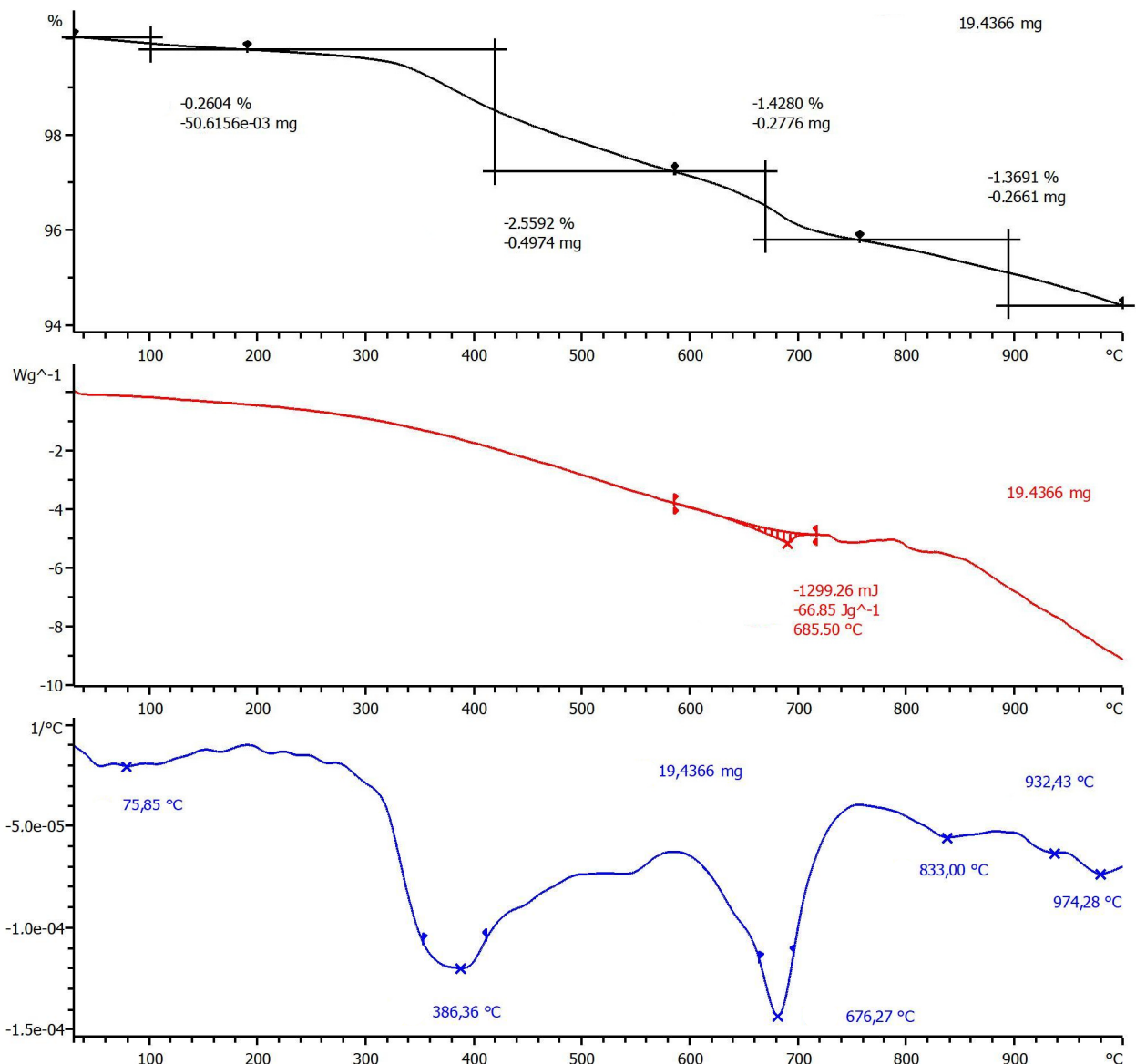


**Fig. S64** TGA (black), DSC (red), and DTG (blue) plots of CAp (Table 1, Entry 4).

For CAp sample 7 (perfectly shaped hexagonal prisms) dehydration occurs at higher temperatures (Fig. S65). Further CO<sub>2</sub> elimination is accompanied by phase transition. The view of DSC curve is in line with the data on partial melting of the CAp, obtained at pH~9 (was detected by SEM of the sintered samples 9 and 10).

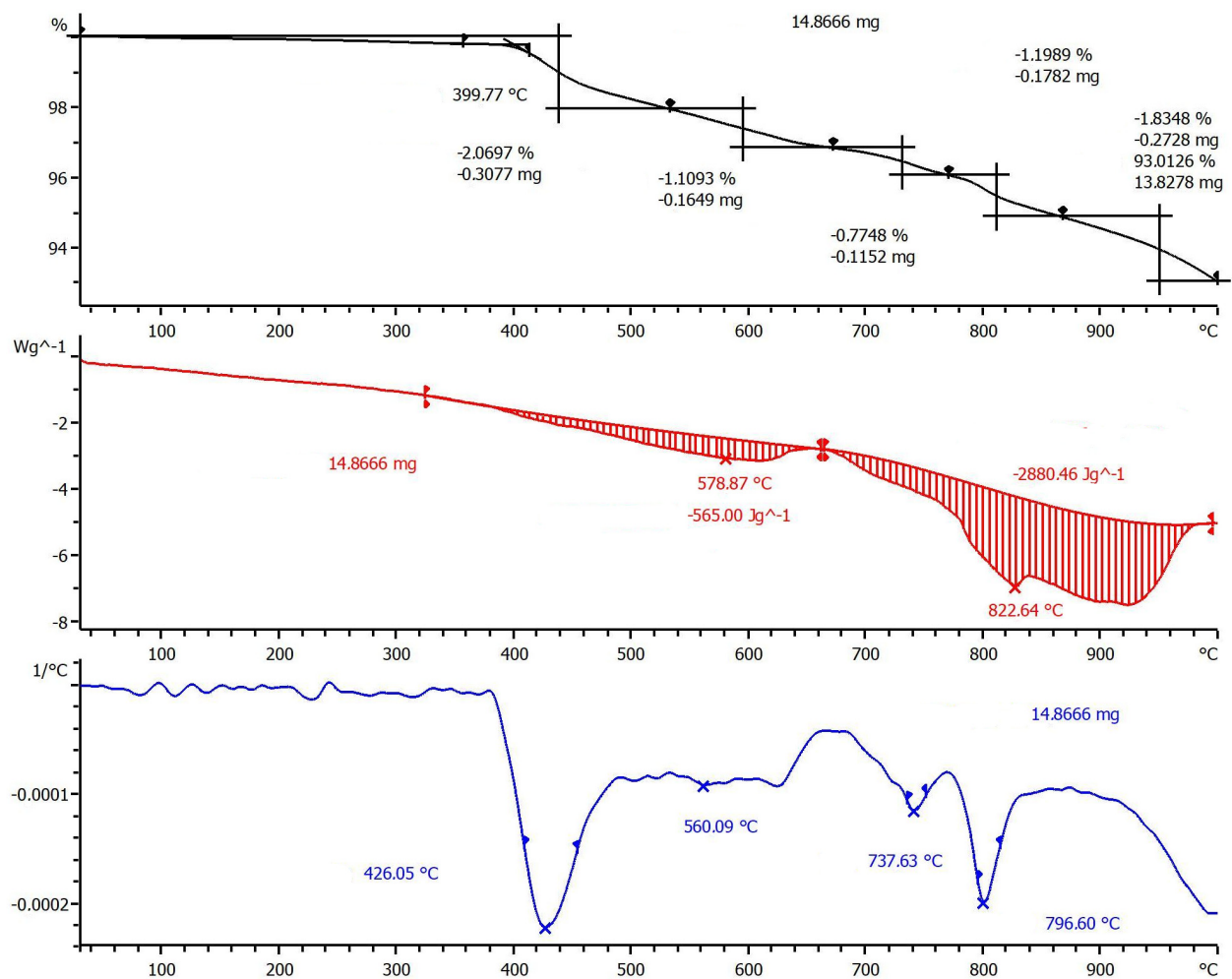


**Fig. S65** TGA (black), DSC (red), and DTG (blue) plots of CAp (Table 1, Entry 7).

For CAp sample 8 (mixture of prisms and amorphous species) CO<sub>2</sub> elimination occurs more easily (Fig. S66), due to higher starting carbonate content .

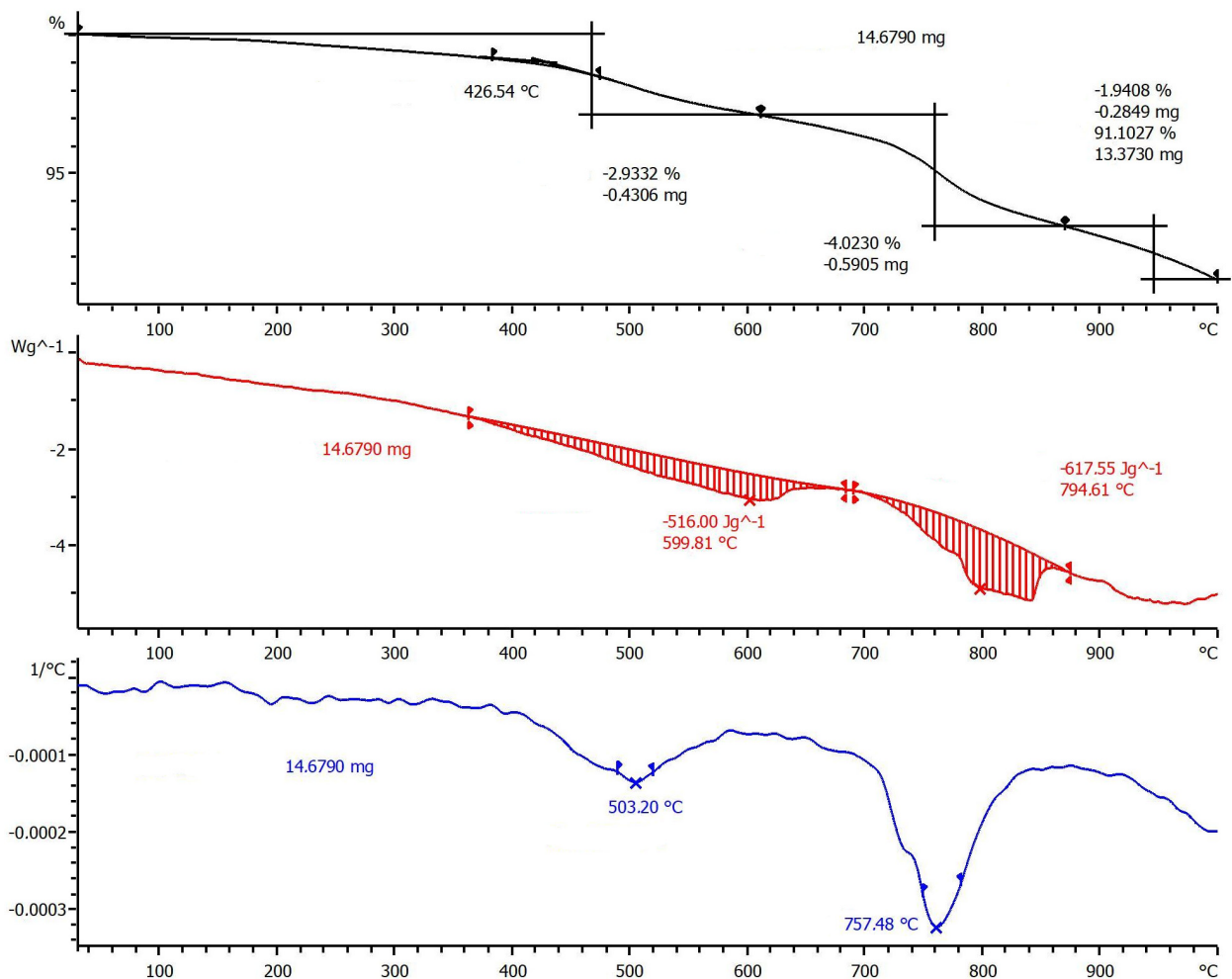


**Fig. S66** TGA (black), DSC (red), and DTG (blue) plots of CAp (Table 1, Entry 8).

TGA plots for CAp sample 8 (Fig. S66) and 10 (Fig. S67) are similar. DTG plot indicates more fluid dehydration, the main CO<sub>2</sub> loss at 700–850 °C is reflected in all graphs. A difference between DSC and DTG can be attributed to partial melting of the sample.

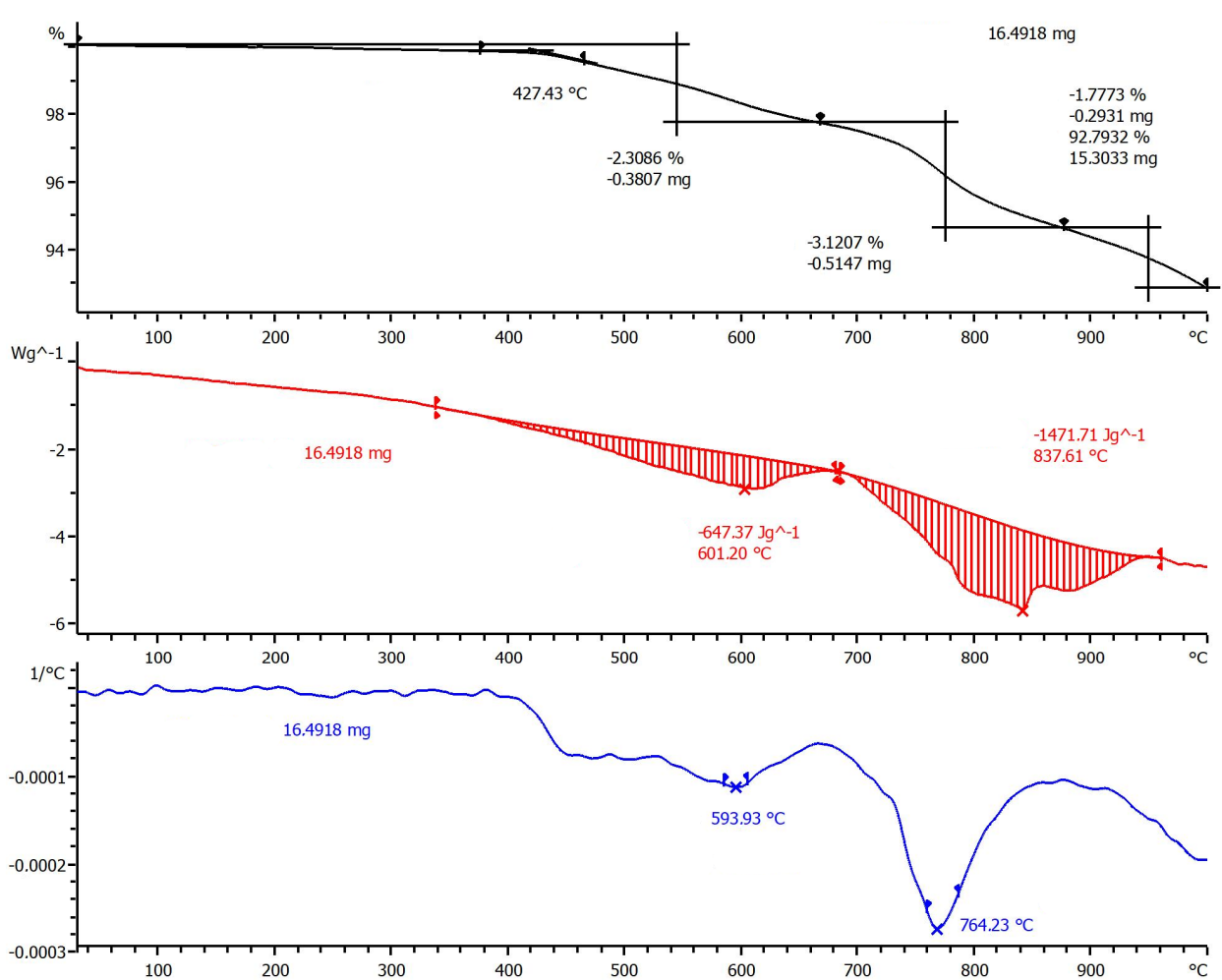


**Fig. S67** TGA (black), DSC (red), and DTG (blue) plots of CAp (Table 1, Entry 10).

After sintering at 850 °C, the sample 9 partially loses the ability of the water absorption (Fig. S68).

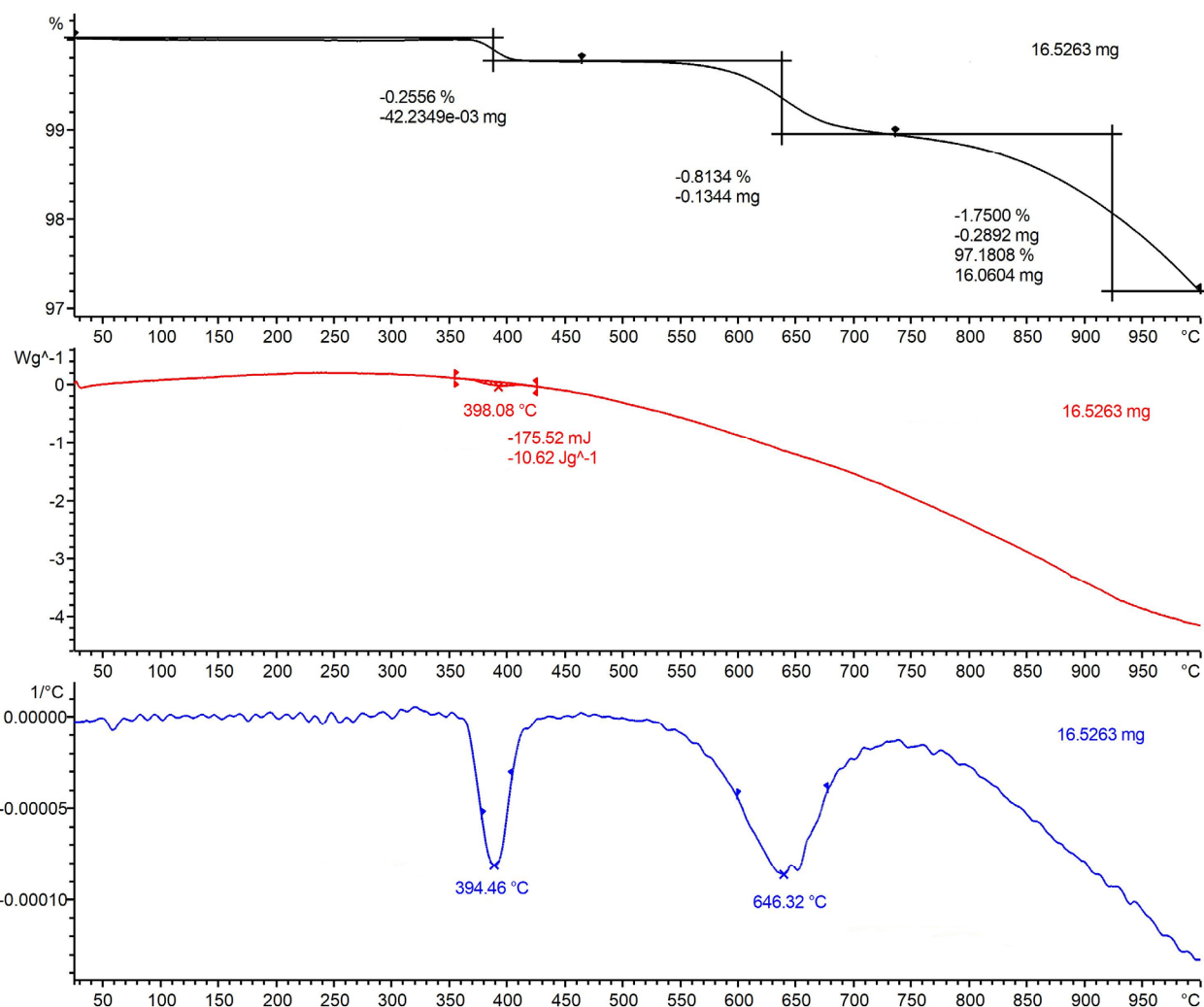


**Fig. S68** TGA (black), DSC (red), and DTG (blue) plots of CAp (Table 1, Entry 9), sintered at 850 °C.

The sintered sample 10 demonstrates similar behaviour (Figs. S69, S70). TGA curves of the sample 10, sintered at different temperatures, are presented in the main text of the article (Fig. 11).

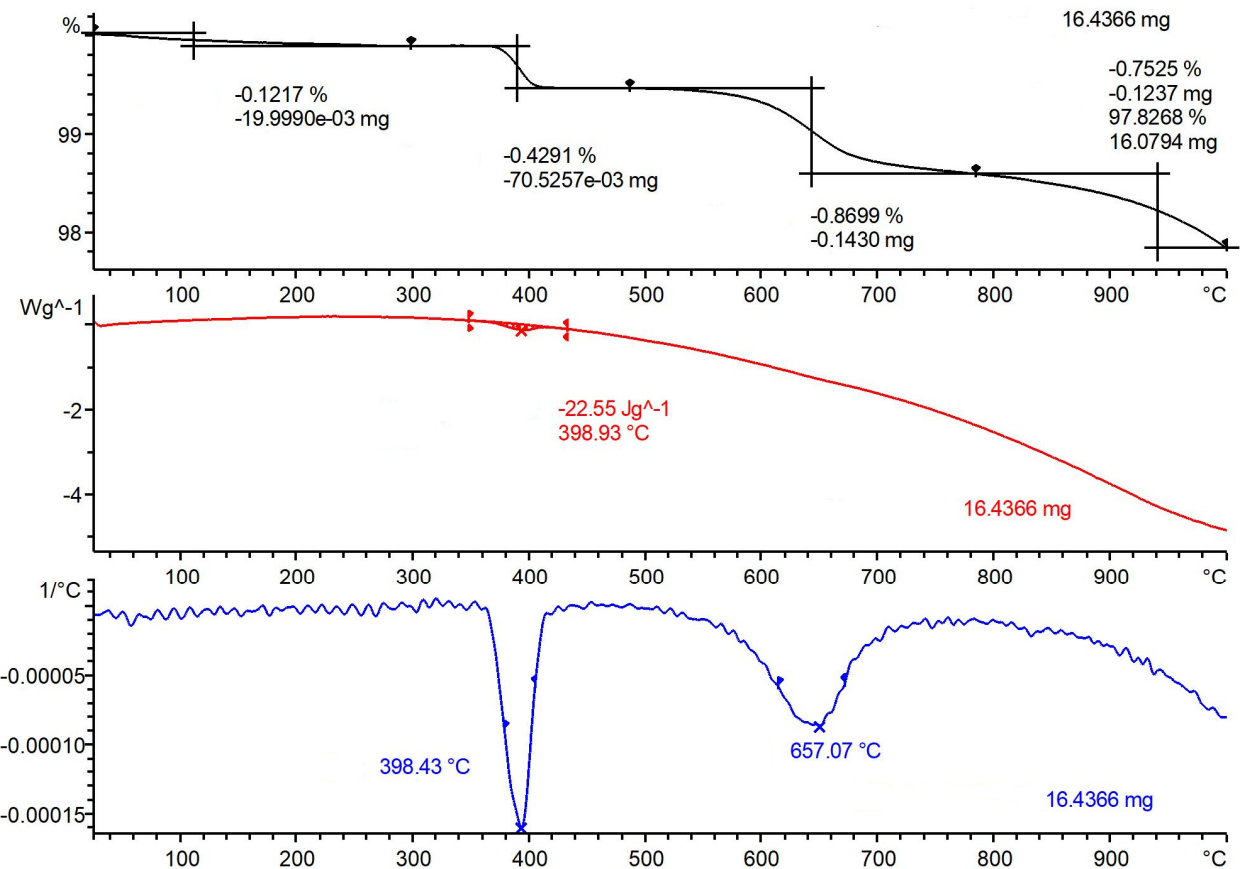


**Fig. S69** GA (black), DSC (red), and DTG (blue) plots of CAp (Table 1, Entry 10), sintered at 850 °C.

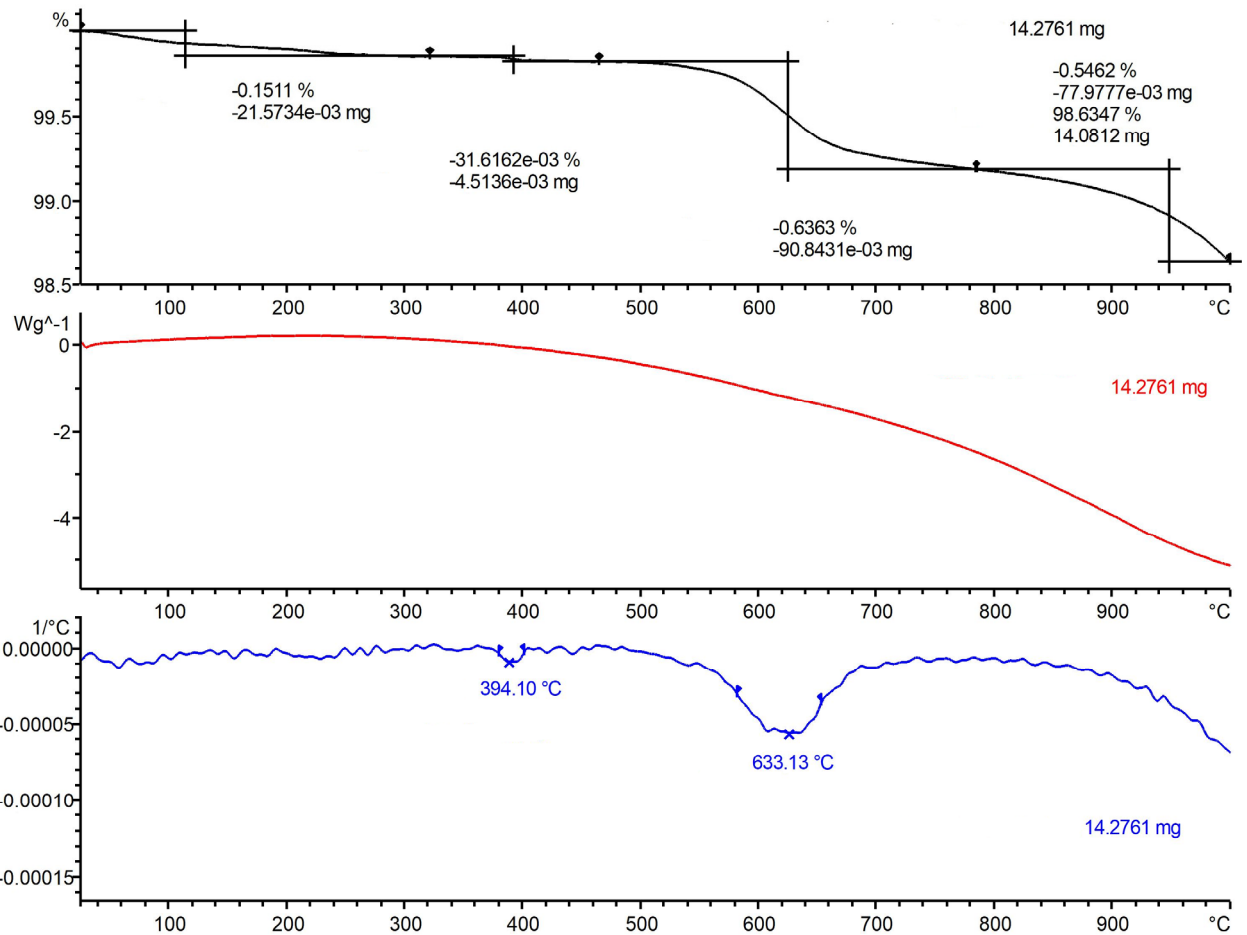


**Fig. S70** GA (black), DSC (red), and DTG (blue) plots of CAp (Table 1, Entry 10), sintered at 1000 °C.

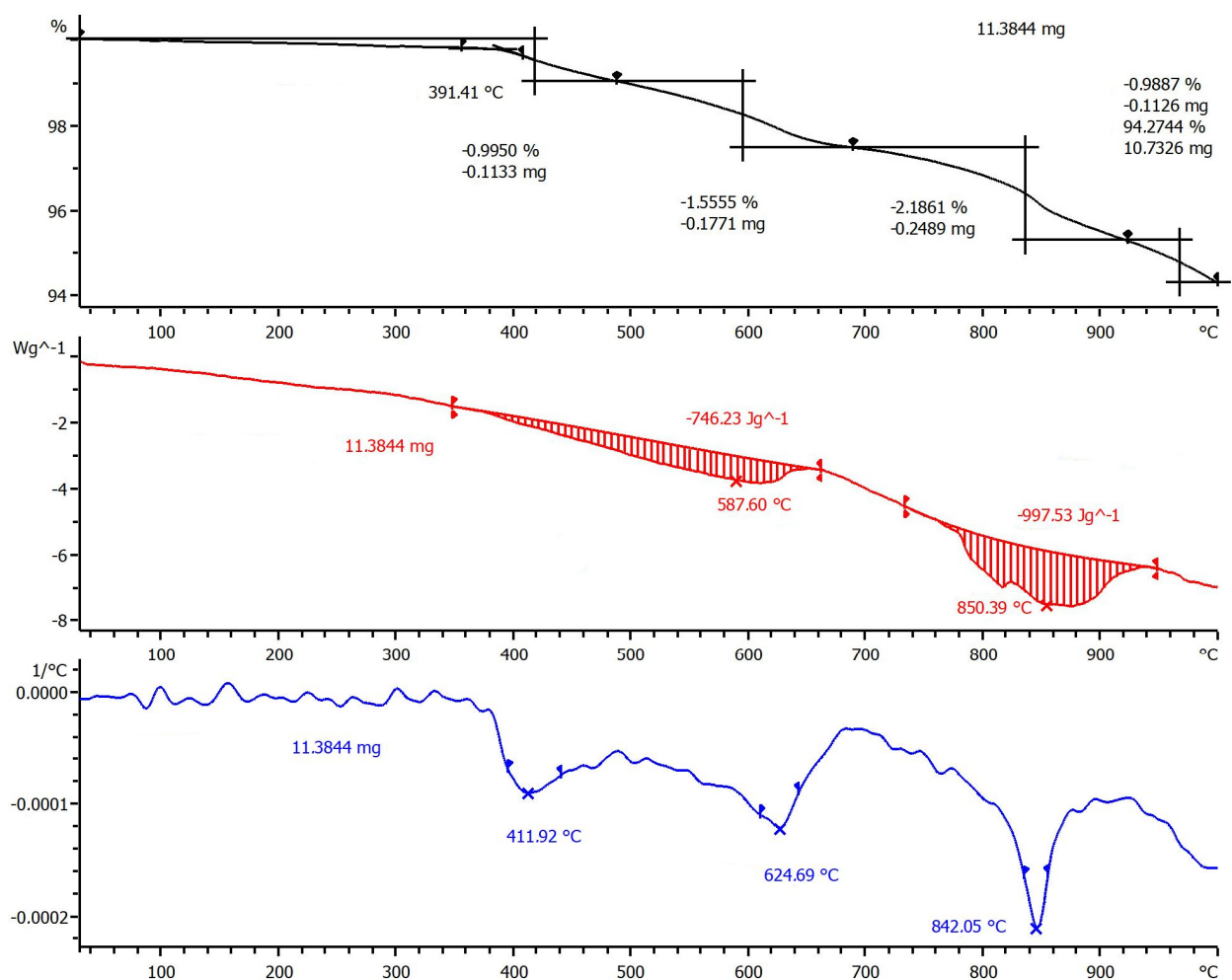


**Fig. S71** TGA (black), DSC (red), and DTG (blue) plots of CAp (Table 1, Entry 11).

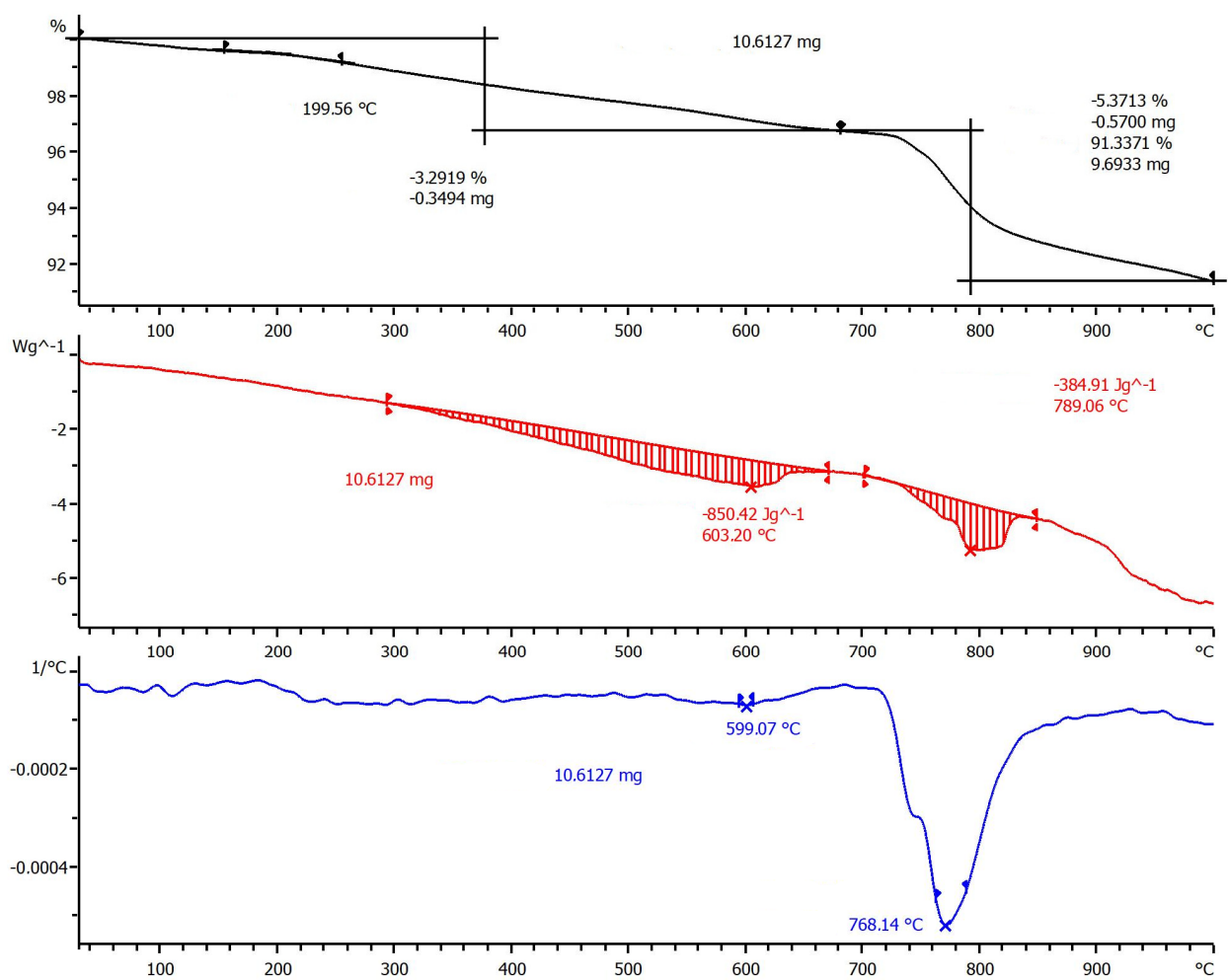


**Fig. S72** TGA (black), DSC (red), and DTG (blue) plots of CAp (Table 1, Entry 12).

## S5. UV calibration data for vancomycin solutions

Calibration was performed by recording of the UV spectra of Van·2HCl solutions in H<sub>2</sub>O and PBS with measuring of the absorption at 280 nm.

The results of the calibration are presented in Figs. S73 and S74.

For Van·2HCl aqueous solutions:  $y = 0.0044x + 0.0094$

$r^2 = 0.998$

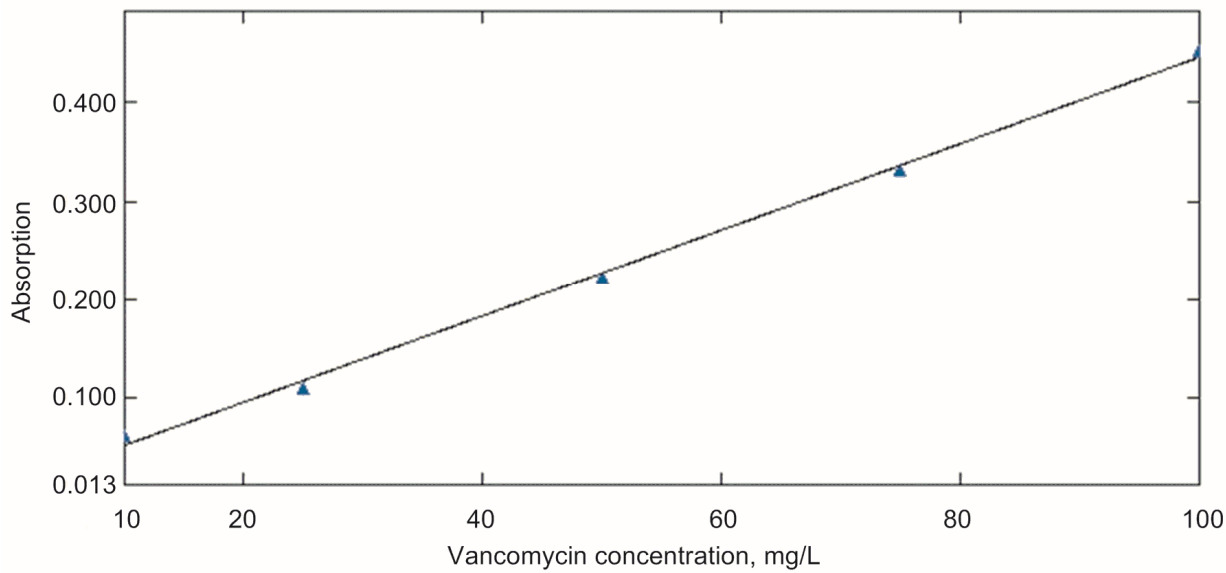


**Fig. S73** Calibration line for Van·2HCl solution in H<sub>2</sub>O.

For Van·2HCl solutions in PBS:  $y = 0.0043x + 0.0156$

$r^2 = 0.989$

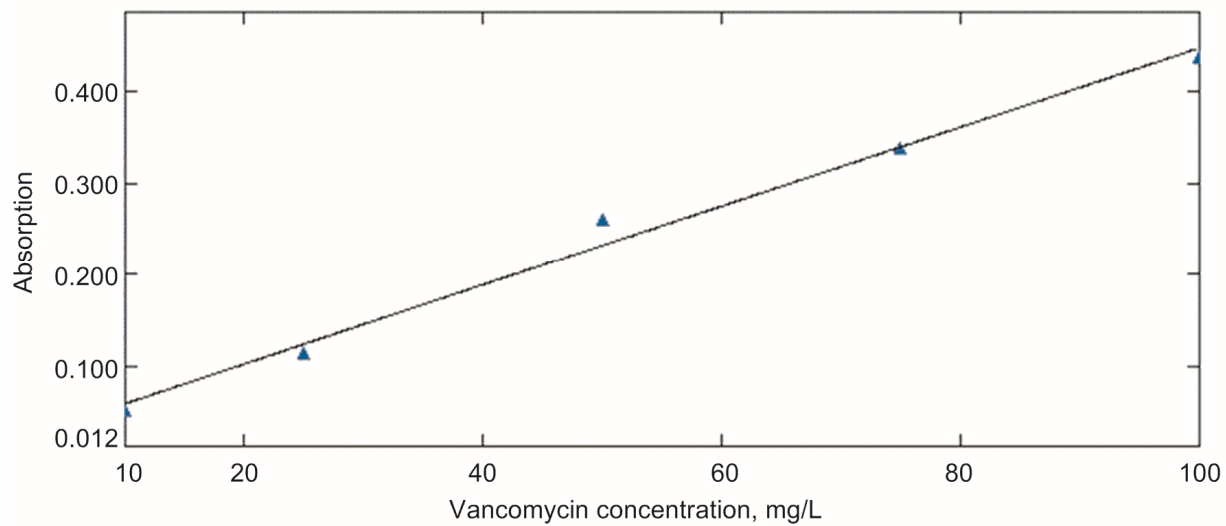


**Fig. S74** Calibration line for Van·2HCl solution in PBS.